

# POLITECNICO DI TORINO

*Master of science in Energy  
and Nuclear Engineering*

*Master of Science Thesis*



**POLITECNICO  
DI TORINO**



Agenzia Nazionale per le Nuove tecnologie,  
l'Energia e lo Sviluppo economico sostenibile

***Development of an energy simulation model of  
urban heating systems at the service of new  
residential districts.***

**Supervisor:**

Prof. Marco Masoero

**Co-supervisors:**

Prof. Sebastiano Caruso

Dr. Ing. Matteo Caldera

**Candidate:**

Nicolò Fabiani

Tesi ENEA nr. 2820, titolo originale “Sviluppo di un modello di simulazione energetica di sistemi di riscaldamento urbano al servizio di nuovi distretti residenziali”.

## Acknowledgements

Desidero ringraziare i supervisori che mi hanno seguito durante l'intenso percorso di tesi.

Innanzitutto ringrazio il Prof. Marco Carlo Masoero per l'infinita disponibilità e gentilezza e per aver deciso di seguire la tesi nel periodo complicato a cui siamo sottoposti. Un ringraziamento al Dott.Ing. Matteo Caldera per la sua disponibilità, per i preziosi consigli tecnici, per avermi spronato nei momenti adeguati del percorso, per aver fornito molte documentazioni utili allo sviluppo della tesi e per aver reso possibile un confronto costruttivo. Un ringraziamento al Prof. Sebastiano Caruso per l'aiuto, i preziosi consigli tecnici, all'evidenza frutto non solo della sua grande competenza ma anche del qualificato e lungo periodo di esperienza nel settore e per l'empatia e la simpatia con cui ha saputo innalzarmi il morale in qualche momento difficile. Un ringraziamento al signor Antonio Fratello per avere fornito preziose informazioni sull'infrastruttura oggetto del presente lavoro. Un ringraziamento a Iren S.p.A. per aver gentilmente fornito i dati di monitoraggio.

Ringrazio i miei genitori, Emanuela e Fabio, per il supporto morale ed economico durante l'intero percorso accademico. Inoltre ringrazio l'intera famiglia per essermi stata vicina sempre. Ringrazio la mia ragazza Edith per essere sempre al mio fianco ed aiutarmi sempre ed a qualunque costo.

Ringrazio i compagni di avventura al Politecnico con cui ho avuto l'onore di condividere bellissimi momenti formativi e non.

Ringrazio tutti i colleghi di lavoro per avermi sopportato e supportato fin dal primo periodo di stage.

Ringrazio gli amici del calcetto con cui spero di poter presto tornare a divertirmi.

Ringrazio i miei coinquilini torinesi Paolo e Lorenzo.

Infine un ringraziamento speciale va a mio fratello Lorenzo e sua moglie Chiara per avermi dato la gioia immensa di diventare zio. In un anno così travagliato l'emozione di vedere il proprio nipote crescere anche se solo attraverso uno schermo è stata una fonte di forza ulteriore.

## Contents

1.	Abstract .....	9
2.	Introduction.....	10
3.	State of art.....	11
3.1	Legislative framework of district heating.....	12
3.2	District heating layout .....	14
3.2.1	Thermal power plant.....	14
3.2.2.	Pumping system.....	17
3.2.3.	Distribution network.....	18
3.2.4.	Substation.....	20
3.3	Italian scenario.....	21
3.4	District heating models .....	24
4.	Methodology.....	27
4.1	Softwares .....	27
4.2	Logical approach to the model .....	28
5.	Case study.....	30
5.1	Data analysis.....	32
6.	Model.....	44
6.1	Pipe Model (Hydraulic analysis) .....	44
6.1.1	Validation of the model .....	46
6.2	Boundary conditions of the model.....	52
6.3	Boundary condition testing.....	58
6.4	Analysis of the heat exchange substation .....	61
6.5	Network Model.....	71
6.6	Thermal analysis .....	77
6.6.1	Validation of the model.....	79
6.6.2	Validation of the components and methodology used.....	80
6.6.3	Validation of pipe model (1) .....	83
6.6.4	Validation of new pipe model (2) .....	84
6.6.5	Validation of new pipe model (3) .....	86
6.7	Thermal model .....	90
7.	Results .....	98
7.1	Comparison with monitoring data .....	105
8.	Conclusion .....	110
	References .....	119

## List of figures

Figure 1 - Energy consumption met by different generation sources. [15] .....	15
Figure 2 - Projection to 2030 and 2050 of generation system used in District Heating in terms of energy supplied. [10].....	15
Figure 3 - Example of load curve for cogeneration plants. ....	16
Figure 4 - Different possible district heating distribution layout [34].....	19
Figure 5 - Example of district heating substation with DHW and heating need. [30] .....	20
Figure 6 - Example of district heating substation with only heating need. [30] .....	20
Figure 7 - Temperature at substation 1 vs time in Tannheim DH. [20].....	25
Figure 8 - Temperature at substation 2 vs time in Tannheim DH. [20].....	25
Figure 9 - Number of substations in the entire district heating network with nominal power in a specific range. [28] .....	30
Figure 10 - AutoCAD plan of the portion of the network under analysis.....	31
Figure 11 - Supply and return temperature at primary side for building located in Via Cotta 67. ....	33
Figure 12 - Supply, return temperature at secondary circuit and outside temperature for the building in Via Cotta 67. .....	34
Figure 13 - Supply, return temperature at secondary circuit and outside temperature for the building in Via De Andrè 1.....	34
Figure 14 - Gantt diagram of T supply availability for a building. ....	35
Figure 15 - Gantt diagram of return temperature at primary circuit for a building.....	36
Figure 16 - Gantt diagram of flow rate availability for a building. ....	36
Figure 17 - Building with very low data availability (Via Olmetto 14) .....	37
Figure 18 - Start and end time of measurement data for each building.....	37
Figure 19 - Poor data availability within the timespan (Via L. Da Vinci 13).....	38
Figure 20 - Heat Map for one building representing the median of temperature in °C for same hours in the same month.....	39
Figure 21 - Heat Map for a building with special setting imposed by plant manager (Via Bongiovanni 14)..	39
Figure 22 - Box Plot of supply primary temperature for every building in January. ....	41
Figure 23 - Box Plot of supply primary temperature for the different buildings from October to March.....	41
Figure 24 - Box Plot of supply primary temperature for every building in July.....	42
Figure 25 - Box Plot of return primary temperature for every building in January. ....	43
Figure 26 - User interface in OpenModelica of the created pipe.....	46
Figure 27 - DH network of the reference case. [29] .....	47
Figure 28 - Diagram view in OpenModelica of the reference exercise using the created pipe. ....	49
Figure 29 - Pressure vs node for the reference exercise calculated with the new pipe and from the reference. .....	50
Figure 30 - Mass flow-rate for each branch in the reference exercise and calculated with the new pipe....	50
Figure 31 - Pressure vs node for the reference case using created pipe and using static pipe. ....	51
Figure 32 - AutoCAD plan of the portion of the district heating under analysis.....	52
Figure 33 - Diagram view in OpenModelica of the supply network under analysis.....	54
Figure 34 - Pressure at the inlet of the network vs mass-flow entering in it. ....	55
Figure 35 - Diagram view in OpenModelica of the return network under analysis. ....	56
Figure 36 - Pressure exiting the lot vs mass flow. ....	57
Figure 37 - Diagram view in OpenModelica of the boundary conditions testing model. ....	58

Figure 38 - Measured and modelled pressure at measuring point vs time. ....	59
Figure 39 - Measured pressure vs mass flow-rate in the measure point from monitored data.....	60
Figure 40 - Regression curve, mass flow-rate vs power for a building.....	61
Figure 41 - Regression curve, mass flow-rate vs power for a building.....	62
Figure 42 - Regression mass flow-rate vs outside temperature for a building. ....	62
Figure 43 - Different types of substation adopted in the network under analysis. ....	63
Figure 44 - Climatic curve for one substation controller.....	64
Figure 45 - Graph explaining the return temperature control at primary side.....	64
Figure 46 - Interpolating surface for a building.....	66
Figure 47 - Icon view of valve model implemented in OpenModelica.....	67
Figure 48 - User view of valve model created in OpenModelica. ....	67
Figure 49 - Icon view of heat exchanger model implemented in OpenModelica. ....	68
Figure 50 - Icon view of substation model created in OpenModelica. ....	68
Figure 51 - User interface for substation model created in OpenModelica. ....	69
Figure 52 - Interpolating surface mass flow-rate vs power and secondary supply temperature. ....	69
Figure 53 - Diagram view in OpenModelica of the entire simulated network.....	72
Figure 54 - Mass flow-rate deviation between simulated and real values for each building. ....	73
Figure 55 - Outside temperature from real data for two adjacent buildings.....	74
Figure 56 - Deviation of outside temperature for two adjacent buildings.....	75
Figure 57 - Technical data sheet of Premant pipes (1) [31]. ....	77
Figure 58 - Technical data sheet of premant pipe (2). [31] .....	78
Figure 59 - Diagram view of the composed component. ....	79
Figure 60 - Icon view of the composed component.....	80
Figure 61 - Highlighting of the linear dissipation for the analyzed case. ....	81
Figure 62 - User interface in OpenModelica for the example analyzed.....	81
Figure 63 - Evolution of pipe state temperature for the example analyzed. ....	82
Figure 64 - Interpolation plane for the determination of outlet pipe temperature for one pipe.....	83
Figure 65 - Comparison of obtained results through finite volume and through the use of the interpolation plane. ....	83
Figure 66 - Deviation between finite volume method and used method. ....	84
Figure 67 - Comparison of outlet temperature obtained through finite volume and through new pipe model. ....	85
Figure 68 - Deviation between new implemented method and finite volume method. ....	85
Figure 69 - Outlet temperature for pipe zero using finite volume and using the new implemented pipe. ...	87
Figure 70 - Outlet temperature deviation between finite volume and new implemented method. ....	87
Figure 71 - User interface in OpenModelica of the new pipe. ....	88
Figure 72 - Thermal model for the supply in OpenModelica using finite volumes. ....	91
Figure 73 - Simulation time using dynamic pipe. ....	92
Figure 74 - Simulation time using new pipe. ....	92
Figure 75 - Deviation on inlet temperature using 1 minute time-step or 10 minutes time-step. ....	93
Figure 76 - Deviation of inlet temperature using 10 minutes time-step and 30 minutes time-step. ....	94
Figure 77 - Particular of the deviation. ....	94
Figure 78 - Simulation time using 30 minutes time-step. ....	95
Figure 79 - Simulation time using 10 minutes time-step. ....	95
Figure 80 - Complete model in OpenModelica. ....	96
Figure 81 - Inlet temperature at one substation using new pipe, dynamic pipe and monitored data. ....	98
Figure 82 - Particular of figure 81.....	99
Figure 83 - Inlet temperature vs datetime for the first pipe in the network. ....	99

Figure 84 - Simulated inlet temperature of pipe 9.....	100
Figure 85 - Delta inlet temperature between first pipe and pipe 9 .....	101
Figure 86 - Example of asymptote temperature reaching. ....	102
Figure 87 - Mass flow-rate vs date for the pipe analyzed. ....	102
Figure 88 - Evolution of inlet and outlet temperature at a substation. ....	103
Figure 89 - Mass flow-rate at substation.....	103
Figure 90 - Power exchanged at substation analyzed. ....	104
Figure 91 - Daily surface plot of inlet temperature for different pipes.....	104
Figure 92 - Monthly surface plot of inlet temperature for different pipes.....	105
Figure 93 - Inlet temperature at substation 10243 simulated and real....	106
Figure 94 - Particular of figure 93.....	107
Figure 95 - Inlet temperature at substation 10110 simulated and real.....	107
Figure 96 - Inlet temperature at substation 10552 simulated vs real.....	108
Figure 97 - Data availability for building 10552.....	108
Figure 98 - Inlet temperature at substation 10551 simulated vs real.....	109

## List of tables

Table 1 - Increase in length of the grid over the years. [38] .....	21
Table 2 - Increase in volume connected to the network over the years. [38] .....	21
Table 3 - Data of district heating network for different regions. [15].....	22
Table 4 - Data of district heating network in Italy for different climatic zones. [15] .....	23
Table 5 - Generation linked to district heating overview for different Italian regions. [15] .....	24
Table 6 - Substation typology, nominal power and number of user with same substation typology. ....	31
Table 7 - Availability of measured parameters for the building under analysis.....	33
Table 8 - Variables in the reference case. .....	47
Table 9 - Interpolation equation of substations control for all the different buildings. ....	66
Table 10 - Linear conductance for the different pipes present in the network under analysis.....	90

## List of symbols

$\dot{m}_a$	mass flow-rate entering port_a [ $\frac{kg}{s}$ ]
$\dot{m}_b$	mass flow-rate exiting port_b [ $\frac{kg}{s}$ ]
$I_s$	Momentum [ $kg * \frac{m}{s}$ ]
$I_{b\text{-flows}}$	Flow of momentum at boundaries [ $kg * \frac{m}{s^2}$ ]
$F_{s,p}$	Pressure forces [ $kg * \frac{m}{s^2}$ ]
$F_{s,fg}$	Friction and gravity forces [ $kg * \frac{m}{s^2}$ ]
$f$	Friction factor [-]
$\epsilon$	Roughness [mm]
$Re$	Reynolds number [-]
$\dot{m}$	mass flow-rate [ $\frac{kg}{s}$ ]
$g$	gravity acceleration [ $\frac{m}{s^2}$ ]
$c_p$	Specific heat capacity [ $\frac{J}{kg * K}$ ]
$T_s$	Supply temperature [°C]
$T_r$	Return temperature [°C]
$v$	Velocity [ $\frac{m}{s}$ ]
$D$	Diameter [m]
$k$	Thermal conductivity [ $\frac{W}{m * K}$ ]
$\tau_p$	Characteristic time [s]
$PP$	Power [W]
$\rho$	Density [ $\frac{kg}{m^3}$ ]
$T_{out}$	Outside temperature [°C]
$\Delta p_d$	Distributed pressure losses [Pa]
$\Delta p_l$	Localized pressure losses [Pa]
<b>DH</b>	District Heating
<b>EEC</b>	Energy efficiency certificate
<b>TOE</b>	Tonne of oil equivalent
<b>CAR</b>	High efficiency cogeneration
<b>RES</b>	Renewable energy sources
<b>CHP</b>	Cogenerative heat plant
<b>GG</b>	Degree day
<b>D.P.R</b>	Decree of the President of Republic
<b>MSL</b>	Modelica Standard Library

## 1. Abstract

The main objectives of the thesis is to develop an energy simulation model for the analysis of district heating networks using the object-oriented software *OpenModelica*. The software was chosen as it allows the dynamic study of complex multidomain systems. The modeling language *Modelica* allows to build complex mathematical models through an aggregation of the constituent models (modular modeling) thus making the construction of the model convenient as it is more manageable. Furthermore some studies demonstrate that *Modelica* simulation environments performs better in terms of multi-domain modelling, realistic control, modularity and flexibility with respect to other simulation environments.

A dynamic model of a district heating network has been developed starting from the analysis of a portion of the existing network located in Grugliasco (Turin) of which monitoring data have been provided by Iren S.p.A.

Before modelling a robust data analysis has been made using *MATLAB* environment to completely define the case study.

The major part of this work is the creation of a new pipe model in *Modelica* environment. The pipe models already available in *OpenModelica* are not computationally efficient in order to manage large networks they are based on finite volume approximation that is too much time consuming in order to run a district heating simulation.

Then the implementation of the consumer model including the heat-exchanger and flow-regulating valve controlled in accordance with the technical data sheet of the controller currently used in the district heating under analysis.

The results show that the different created pipes are able to handle both hydraulic variables using Haaland formula and thermal ones using one-dimensional energy balance analytical solution while consumer models are capable of governing both the flow-through and the heat exchange.

All the models created are reusable in other district heating case studies by only changing characteristic parameters of the network under analysis (e.g. diameter and length of the pipe, insulation thickness and thermal conductivity).

Furthermore the results obtained show that the models created make it possible to simulate a district heating network in reasonable time and with reliable results. The simulation of the entire portion of the network for a whole year with a timestep of 10 minutes is calculated in less than 6 hours while using a timestep of 30 minutes is calculated in 2.5 hours. Finally for a better results visualization a video with time evolving temperature in the supply portion of network for the entire year has been generated in AVI format.

The main limitation of the model are that just a portion of the network is analyzed, thus passing through the assumption that the flow-rate through the network portion is equal to the sum of the flow-rates of the buildings analyzed and that data for the secondary circuit are not available for the majority of building under analysis.

Pressure driven networks with loops, branches, several producers are possible to be simulated using the new components

## 2. Introduction

District heating systems are widely used in northern Europe where they cover a large part of thermal demand. As a practical example we can mention Sweden where district heating systems accounts for about 50% of the total heat demand, Danielewicz et al. (2016) [1]. The continuous growth of large cities has radically increased the number of district heating networks as this technology is particularly effective in the case of dense urban agglomerations.

The current energy context is requiring drastic changes in the management and construction of district heating networks. In fact, in recent years, the significant diversification of energy resources used caused by the progressive depletion of traditional energy sources has strongly encouraged the use of new sources, often based on other physical and chemical principles for energy generation. These new sources have different properties, not only from the point of view of the energy acquisition process but also from the point of view of its distribution reducing the importance of large, central energy sources in favor of the use of smaller, local but interconnected sources. [2]

The current energy scenario would therefore seem to discourage the use of centralized generations which are the basis of district heating systems. As a consequence there is a need for a continuous efficiency improvement of the district heating networks in order to make them competitive with other technologies. In order to analyze and optimize possible future changes in the operation of district heating networks new or modified methods must be developed and used to augment their efficiency and obtain significant energy savings.

Hence the need for reliable and easily replicable simulations of district heating networks both in thermal and hydraulic terms. Reliable simulations can actually provide indications on the advantages of possible variations in the network's management leading to energy savings.

In such a context, this work aim at providing aggregated models of typical components present in district heating networks (e.g. pipes, valves, heat exchangers) and easily reusable in different case study through a simple manipulation of the input data. The will of the work is also reflected in the software used which is open-source and so it encourages the various subjects in the scientific field to exchange models that are as reusable as possible.

These models must allow both thermal and hydraulic analysis of the network for a complete characterization of the district heating network.

### 3. State of art

Energy sector is important for the economic development and is crucial for the wealth of countries that should develop energy policies in order to use their own resources efficiently.

Moreover, an efficient use of energy leading to the maximization of energy saving is essential for reducing the greenhouse gases emission in the energy sector and meeting international goals for climate change mitigation.

The PNIEC defines national targets for renewable sources, energy efficiency and emission reduction. [3]

In detail:

- reduction of primary energy consumption compared to the PRIMES 2007 scenario by 43% against an EU target of 32.5%;
- reduction of greenhouse gas emissions compared to 2005 for all non-ETS sectors by 33%, "a target 3% higher than that set by the European Union";
- contribution of renewables to 2030 of 30% (2017 18.3%) differentiated between the different sectors:
  - 55.4% (2017 34.1%) of the share of renewables in the electricity sector;
  - 33% (2017 20.1%) in the thermal sector (uses for heating and cooling);
  - 21.6% renewables in transport.

The PNIEC therefore introduces the integration of energy efficiency into policies and measures with main purposes other than efficiency. The plan tends to incentivize the exploitation of the great potential in terms of efficiency in the construction sector with measures as energy requalification together with building, seismic, plant engineering and architectural renovation of buildings.

In addition, the European community has introduced rules on efficient district heating networks in the Clean Energy for all Europeans Package, which defines European policies on energy and climate up to 2030, establishing, for example, that the right to disconnect users of inefficient district heating is guaranteed (RED II Directive, art 24, paragraph 2 [4] ); efficient district heating can be counted for the verification of the achievement of the minimum RES quota obligations in buildings (RED II Directive, art 15, paragraph 4 [4]).

Moreover there are also incentives related to energy efficiency. A typical example for the Italian framework are the energy efficiency certificates. These certificates were created to set a mandatory primary energy saving target to the electricity or natural gas distributors with more than 50,000 end customers. Energy efficiency certificates are the instrument through which the implementation of the interventions to increase efficiency is certified on the basis of an equivalence of 1 EEC = 1TOE of primary energy saved. With the aim of effective control of the actual savings the latter must be measured. The energy efficiency certificates are traded on a specific market and have an average value of 260 euros / energy efficiency certificate. It is therefore evident that in this way the efficiency measures will present a shorter return time.

The use of a district heating system partly powered by cogeneration plants allows access to the mechanism. There are, in fact, types of energy efficiency certificates called CAR (high-efficiency cogeneration).

It can therefore be said that the use of district heating networks and their energy efficiency as well as the construction of new networks are coherent with the European and national framework.

### 3.1 Legislative framework of district heating

District heating is a technology mainly present in urban centers located in cold climatic areas, which allows the heat produced by centralized plants to reach consumers through a buried network of pipes. This network distributes hot or superheated water for the heating of buildings and for the production of sanitary hot water.

The idea behind district heating consists in the centralized generation of heat for all the thermal needs of the users. Through this type of energy distribution it is possible to achieve a high conversion efficiency (in case of use of cogeneration plants) as well as localize the generation in a few points thus ensuring simpler maintenance and plant management.

The thermal energy fed into the district heating networks can have different origins: it can be produced by a large conventional thermal power plant, it can be produced by cogeneration plant (higher average yields for the same fuel used than conventional plants), it can come from the incineration of solid urban waste, from industrial processes (low temperature waste heat), from low, medium and high temperature geothermal sources, from renewable sources (biomass, biogas from landfills, processing waste, etc.).

It is evident that a large variety of fuels can be used to generate heat, including natural gas, biomass, solar, geothermal and non-recyclable waste.

District heating has not a single definition. In fact, there are different definitions provided by various ministerial and legislative decrees:

- Ministerial Decree 24/10/2005 [5]: "Cogeneration plant combined with district heating is an integrated system, consisting of the sections of a combined production of electricity and heat that meet the criteria defined by the Authority for electricity and gas pursuant to article 2, paragraph 8, of legislative decree no. 79/99, , and from a district heating network for the distribution of heat, cogenerated by the cogeneration plant itself, to a plurality of buildings or environments for uses mainly connected with hygienic-sanitary uses and air conditioning, heating, cooling, conditioning of environments at residential destination, commercial, industrial and agricultural, with the exception, in the case of industrial environments, of uses in equipment and machines for industrial processes. The district heating network must simultaneously satisfy the following conditions:
  - supply, by means of a thermal energy transport network, a plurality of buildings or environments;
  - be an open system or, within the limits of the system's capacity, allow connection to the network of each potential customer according to principles of non-discrimination;
  - the sale of thermal energy to third parties must be governed by supply contracts, aimed at regulating the technical and economic conditions for supplying the service according to principles of non-discrimination and public interest, in the context of energy saving policies."
  
- Legislative Decree 28/2011 (art. 2 paragraph 1) [6]: "district heating" or "district cooling": the distribution of thermal energy in the form of steam, hot water or chilled liquids, from one or more production sources to a plurality of buildings o sites via a network, for space heating or cooling, for manufacturing processes and for the supply of domestic hot water."
  
- Ministerial Decree of 5 September 2011 [7] (Article 2, paragraph 1, letter f)): "[..] All the following conditions must be met: the network must develop on public land or on several private land, in any case not exclusively attributable to the operator as defined in letter e); b. the connection to the network must take place using devices equipped with specific measuring instruments that allow the accounting

and periodic invoicing to users of the service pursuant to ministerial decree no. 370 and subsequent amendments and additions; c. the sale of thermal energy must concern users of the service other than subjects or appliances attributable to the operator and must be regulated by supply contracts, aimed at regulating the technical and economic conditions of supply.”

- Legislative Decree 102/2014[8], transposing the EED Directive, provides the following definition of district heating and district cooling network (Article 2 paragraph 1), adopted to outline the phenomenon for the purposes of processing the official national statistics sent to Eurostat and detailed in this document: Thermal energy transport system, mainly built on public land, aimed at allowing anyone interested, within the limits allowed by the extension of the network, to connect to it for the supply of thermal energy for heating or cooling spaces, for the manufacturing processes and for covering the needs of domestic hot water.

The definition formulated by Legislative Decree 102 is consistent with the requirements that qualify a district heating network according to the instructions for completing the Eurostat questionnaire, that is the result of a synthesis and mediation between different national definitions.

The document shows the data for the first time, distinguishing them by systems that for the year 2017 fall within the definition of **efficient district heating** (Legislative Decree 102/2014, art 2 [8]):

- 50 per cent of energy from renewable sources;
- 50 percent waste heat;
- 75 per cent of cogenerated heat;
- 50 per cent of a combination of the above.

### 3.2 District heating layout

The main elements of a district heating system are:

- the thermal power plant;
- the pumping system;
- the control system;
- the distribution network ;
- the heat exchange substations.

#### 3.2.1 Thermal power plant

The configuration of the thermal plant depends both on the power and energy required and on the possible local availability of economically exploitable renewable sources (for example biomass). Small power plants (some tens of MW) are usually associated with a relatively low flow temperature (up to 90 °-C) and limited temperature differences between supply and return, while large power plants (hundreds of MW) can instead be associated with a higher flow temperature (120-140 °-C) and with greater temperature differences between supply and return.

Heat is mainly generated through:

- Cogeneration systems exploiting natural gas as primary fuel (fossil CHP);
- Cogeneration systems exploiting renewable sources (RES CHP);
- Geothermal heat pumps ;
- Residual heat from industrial processes;
- Standard boiler (exploiting natural gas, mainly used as integrative generation) ;
- Biomass boilers ;
- Reuse of the combustion heat of solid waste.

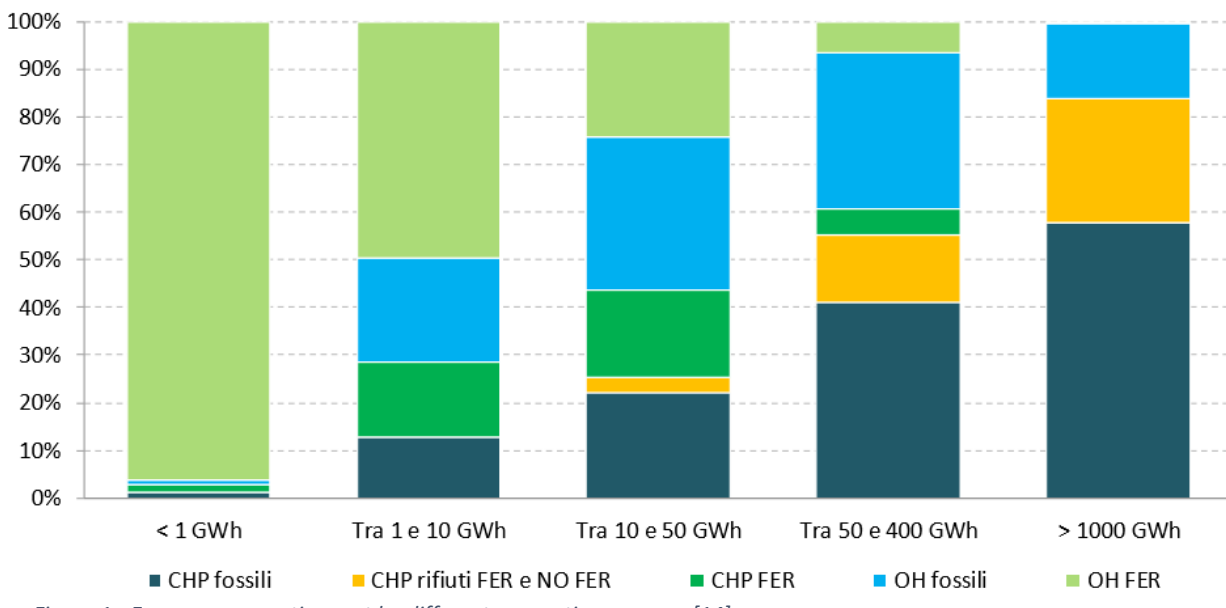


Figure 1 - Energy consumption met by different generation sources. [14]

As shown in figure 1 (for the Italian framework) the employment of renewable sources in simple boilers (FER OH) is concentrated in small networks while in cogeneration units (FER CHP) reach the maximum value in the class of thermal energy input 10-50 GWh and are mainly concentrated in medium-size systems.

Simple boilers fired with natural gas are concentrated in the intermediate classes, replaced in the smaller networks by RES, and in the larger ones by waste and gas CHP units. In the high and intermediate range boilers are used as integration in order to cover user demand at peak times demand and/or in cases of breakdowns or malfunctions of the main thermal production plant that supports the base load. Finally, waste is used almost exclusively in large plants.

The projections to 2030 and 2050 still see a predominant use of cogeneration, but at the same time a greater differentiation of resources with an increasingly important role entrusted to heat pumps, geothermal and solar thermal. The increase in the use of district heating will be partly favored by an increase in the percentage of the population living in urban areas (it is estimated that it will increase from 73% in 2010 to 84% in 2050), and partly by the increase in thermal needs. at low temperature which will make available a wider range of usable energy resources [9].

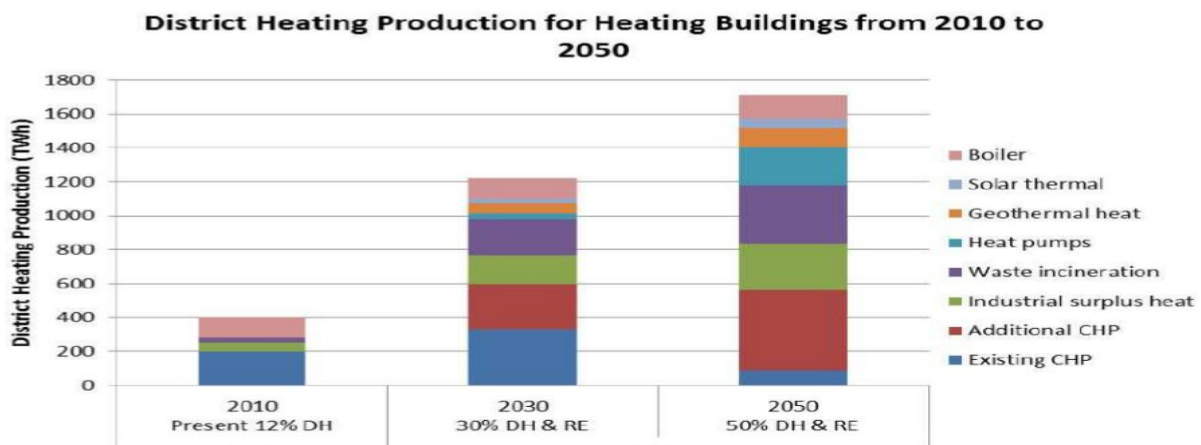


Figure 2 - Projection to 2030 and 2050 of generation system used in District Heating in terms of energy supplied. [9]

As regards the plants sizing, it is necessary to consider both the thermal demand of the users connected to the network and the losses in the network itself. The losses mainly depend on the operating temperature of the network, which is almost constant during the winter season, and increase if the heat energy demand of the users decreases. The heat requirement is calculated using the actual consumption data as initial step for constructing a load curve. The need the plant should meet will not be equal to the total load as large production plants lose much of their efficiency by working in high regulation.

For that reason, other supplementary systems are used. Among these, boilers are used in support of the thermal power plants to provide all the necessary heat when the request exceeds the availability of the power plant. Furthermore, they have a considerable use when the plant is under maintenance or there are failures. According to current legislation, these plants must meet very high efficiency requirements.

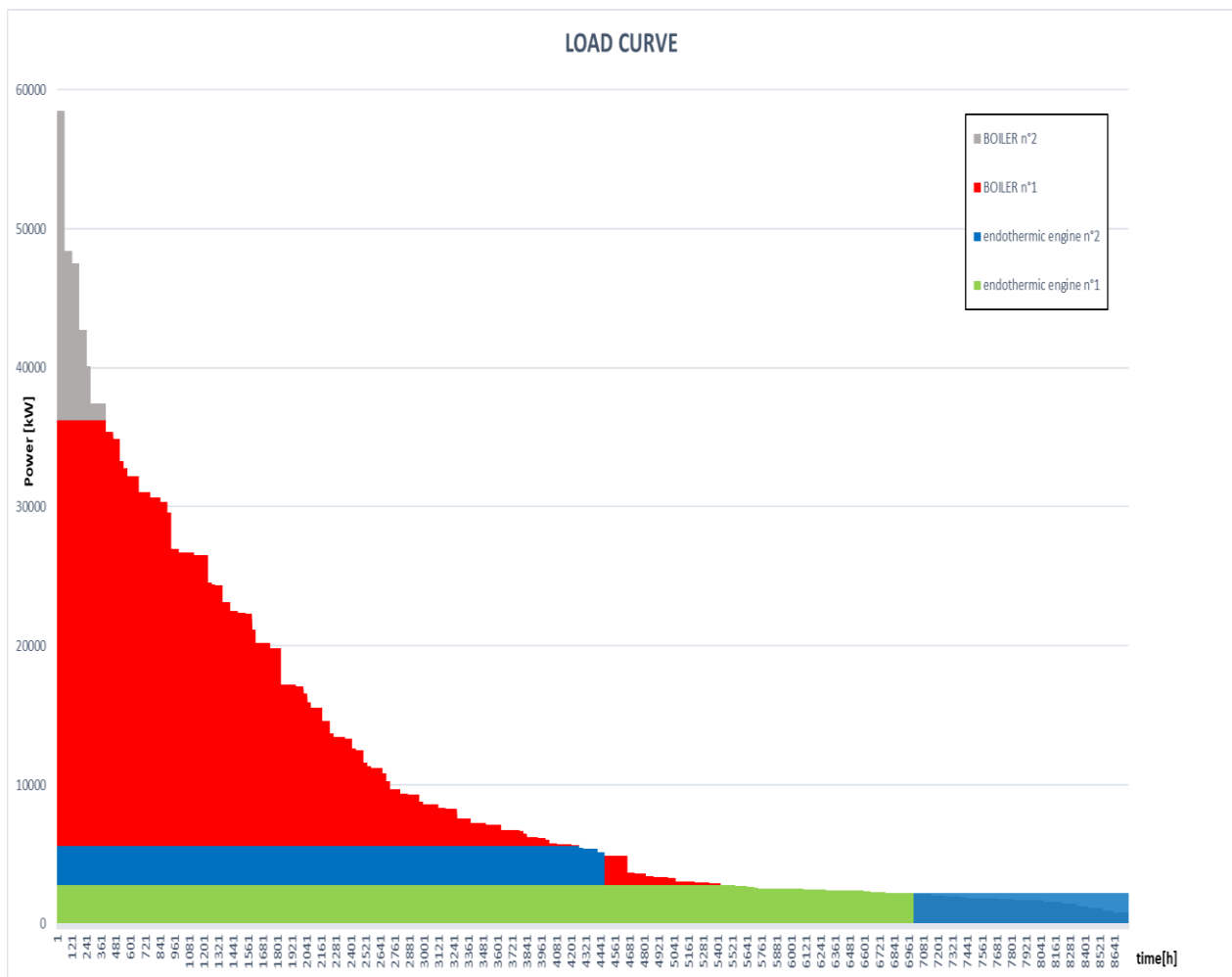


Figure 3 - Example of load curve for cogeneration plants.

The graph shows on the abscissa the hours per year the system is in operation and on the ordinate the thermal power required. It is evident that the system must satisfy a high thermal demand only for a few hours a year while for most of the time it must provide a quantity of energy much lower than the peak. If the power plant were dimensioned in relation to the peak, this would be oversized for most of its operation and this would affect the efficiency. It is therefore dimensioned by taking as a reference a lower than maximum requirement value and, in the hours of the year in which the plant must provide a greater amount of heat, integration boilers are used, as already mentioned.

### 3.2.2. Pumping system

Pumping systems allow to compensate for the pressure losses in the network. The operating pressure of the distribution network depends on the distributed and concentrated pressure losses that depend on the development of the network, on the length, on the branches and on the fluid velocities and on all the localized components (for example valves, heat exchanger).

The distributed head losses are generated by the viscous friction that is generated between the fluid and the surface of the pipe. These losses are described by the equation of Darcy-Weisbach, which has the following form:

$$\Delta p_d = f * \frac{L}{D} * \rho * \frac{v^2}{2} \quad (1)$$

Where:

- f: friction factor [-];
- L: pipe length [m];
- D: pipe diameter [m];
- ρ: density of the fluid [ $\frac{kg}{m^3}$ ];
- v: fluid velocity inside the pipe [ $\frac{m}{s}$ ].

The friction factor depends on the Reynold number (hence the flow rate) and the roughness of the pipeline. It can be determined by semi-empirical correlations or through the Moody diagram.

Localized leaks are those that locally hinder the regular flow of the heat transfer fluid. These losses are expressed through:

$$\Delta p_l = \beta * \frac{1}{2} * \rho * v^2 \quad (2)$$

Where β it is determined through experimental analyzes.

The choice of circulator size is made in such a way that the working point of each circuit (Q, Δp) calculated with the previously described method, falls on the characteristic working curve of the circulator, avoiding the extreme points of the curve itself in order to guarantee greater work flexibility.

The main components of a pumping station are the pumps, the filters, the expansion tank, the automatic control system and the reserve tank.

The pumps must be properly chosen as they are often exposed to intense working conditions, namely high pressures, extreme temperatures and continuous running. These conditions require a durable pump constructed from strong materials and with quality parts. The system works in automatic control in order to be able to compensate for the pressure losses of the network. Pump speed regulation systems have often been successfully adopted on inverter (VSD), to reduce the considerable electrical consumption of pumping.

It is necessary that even the users furthest away from the power plant and therefore hydraulically disadvantaged are able to receive the demanded heat. For the sizing of the substation pumping the most disadvantaged users are those under consideration. Numerous control valves will be arranged to cope with the different levels of pressure throughout the network.

The velocity of the heat carrier fluid in the pipes is usually set in the range of 1.5 ÷ 3 m / s. High fluid velocities lead to smaller pipe diameter but, on the other side, to high pressure losses that must be compensated by pumps with higher operating point (lead to higher costs), while low velocities involve the use of larger diameter pipes with a consequent increase in installation costs and heat losses. Finally, the optimal fluid velocity value is a trade-off between installation and operating costs.

### 3.2.3. Distribution network

The transfer of the heat carrier fluid from the production plant to the user takes place through a network of underground pipes.

It is possible to distinguish between two types of district heating distribution:

- Direct distribution;
- Indirect distribution;

In the latter case, the heat carrier fluid is distributed to the heat exchange substations of the buildings. The substations have a heat exchanger through which the heat transfer fluid of the primary circuit transfers heat to the water present in the secondary circuit (that of the user), and then returns to the plants to heat up again and repeat the cycle.

This configuration presents several advantages like more effective maintenance, possibility of a relatively easy identification of leaks and easier regulation, management and accounting of the thermal flow. On the other hand, the system is rather expensive and the energy losses in the network are greater than in the direct system which instead consists of a single distribution network where the heat transfer fluid directly feeds the emission terminals into the environment.

The distribution network is divided into primary and secondary networks. The primary network is the main backbone while the secondary is made up of the branches at the substations / users

The main components of the primary [10]:

- Steel pipes suitable for transporting superheated water. They present a maximum pressure of 16 bar and a limit temperature of 130 °C;
- Localized devices (such as valves) must also be made of steel. The valves will be of the sphere type and must be installed in such a way as to be easy to control and reach for people in charge;
- Filters with the function of intercepting the impurities that would cause damage to the other equipment available to the network;
- Vent and drain valves of the same sphere technology.

Furthermore a proper insulation, in terms of insulator material and its thickness, reduce the heat losses to the ground [11].

This is due to the fact that distribution heat loss is determined by multiple factors such as geometrical condition (network dimension, length and ground conditions), pipes (type of pipes, insulation materials and thickness) and district heating operation (e.g. temperature level, bypass operation and leakages).

The choice of insulation thickness takes into account the average ambient temperature, the thermal conductivity of the insulation material and its price. The increase of the insulating thickness coinciding with the decrease of the thermal losses and therefore to an energy saving, will decrease emissions. However, an insulation thickness that allows zero heat loss does not exist and very high levels of insulation are achieved at high costs. A balance must be established between the cost of the insulating material and the energy savings obtained. The equilibrium point indicates the optimal thickness of the insulation [12].

The main components present in the secondary network are [10]:

- Externally insulated steel pipes (or cast iron, fiberglass or plastic material);
- Flanged ball or butterfly shut-off valves;
- Filter;
- Vent and drain valves, equivalent to those used in the primary circuit;
- High efficiency heat exchangers, generally with corrugated plates. The arrangement of the plates is parallel.

The pipes must withstand mechanical stresses related to the pressure and velocity of the fluid, as well as thermal stresses due to the temperature differences of the network.

The topography of the distribution network differs in relation to the distribution of the users in the area, to the size and to any and possible future expansions of the network itself. The different configurations are tree-network, ring network and multi-ring network.

The **branched network** has a main backbone from which the various supply lines to the various buildings are detached. This configuration does not have closed delivery and return circuits, thus increasing the risk of interruption of a large part of the supply line

The **ring network** has a closed main supply and return lines from which the various supply lines to the various buildings are disconnected. This configuration reduces the risk of interruption of a large part of the supply line and also reduces the pressure losses of the network. On the other hand, the costs related to the purchase and installation increase.

The **multi-ring network** has more than one closed supply and return lines. This is the least risky configuration as a fault in a specific area of the network still allows the reach of all users but the most expensive one. In this type of network the direction of flow cannot be pointed out a priori.

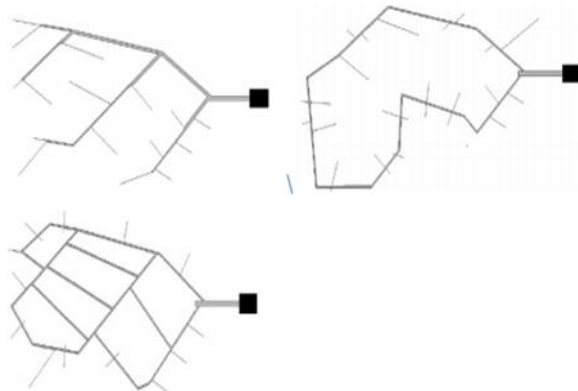


Figure 4 - Different possible district heating distribution layout [34].

Finally network distribution can be also classified according to the different parameters as the fluid vector (hot water or superheated water or steam), the maximum operating temperature and the number of pipes (up 4 pipes).

### 3.2.4. Substation

The heat exchange substation has the task of separating the primary circuit of the district heating network from the user circuit in the indirect system. It consists of a heat exchanger and other components such as regulation valve, electronic flow temperature regulator and thermal energy meter [13]. In the case of users characterized by high demands, multiple heat exchangers in series or in parallel are used.

The substations can be equipped with electronics with different settings and levels of detail. For example the setting varies if the building requires only heat for space heating purposes or for both space heating and domestic hot water production.

To ensure high safety and energy saving standards, the different configurations can:

- Limit the flow rate of the primary through a motorized modulating regulating valve on the primary side if the controller requires modulation.
- Modulate the speed of the secondary pump.

The controller modulates when:

- The return temperature is greater than a predetermined range;
- The flow temperature cannot reach the set-point in secondary supply circuit based only on climatic curve;
- Domestic hot water boiler temperature is not at set-point plus-minus delta.

In addition, the measured data is used for heat accounting purposes through remote reading of the heat meter.

The following figures show the functional diagrams of the substations in the case of users served only by heating and users with both heating and domestic hot water services

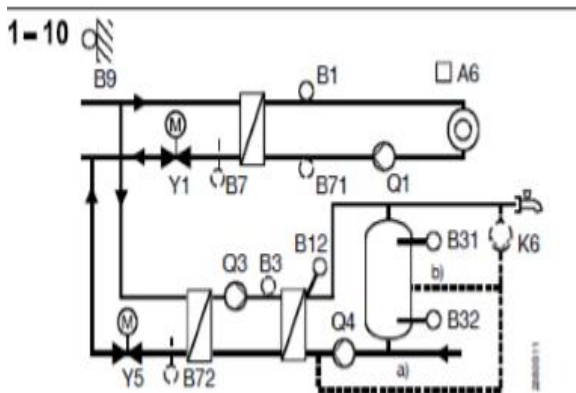


Figure 5 - Example of district heating substation with DHW and heating need. [29]

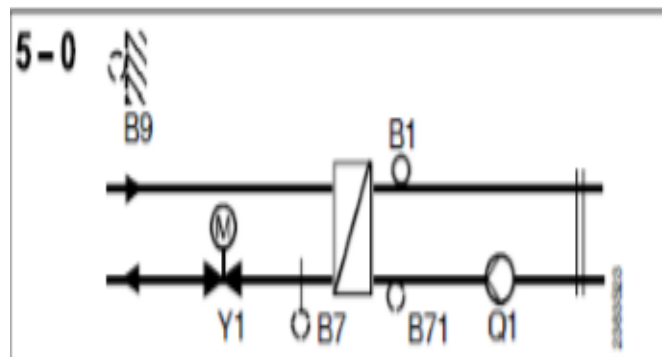


Figure 6 - Example of district heating substation with only heating need. [29]

### 3.3 Italian scenario

In Italy, some factors such as the milder climatic conditions compared to northern European countries and the methanisation program launched in the 1950s in northern Italy delayed the use of the heating networks compared to the rest of Europe.

In particular, the first district heating networks in Italy were installed in the 1970s. Between 1971 and 1979 the networks of Modena, Brescia, Mantova, Verona and Reggio Emilia were built [13].

Although Italy ranks among the Countries with a lower diffusion of the service At European level and despite the fact that the share of heat served by district heating is still marginal, from “AIRU data processing, 2015 Yearbook”, it can be seen how, between 1999 and 2014 the trend of diffusion of district heating is positive. Actually, as can be seen from table 2, the volume connected went from 117.3 (Mm<sup>3</sup>) to 316.2 (Mm<sup>3</sup>) with an increase of 7.3%. Moreover, table 1 shows, in the same time frame (1999-2014), the increase in the DH networks which in 2014 reached almost 4000 Km.

*Table 2 - Increase in volume connected to the network over the years. [38]*

Year	Connected volume (Mm <sup>3</sup> )		
	In the year	To 31 December	Increase
	Mm <sup>3</sup>	Index	%
1999	9,1	109,8	9,0%
2000	7,5	117,3	1,00
2001	8,6	125,9	1,07
2002	6,4	132,3	1,13
2003	7,8	140,1	1,19
2004	4,2	144,4	1,23
2005	11,2	155,6	1,33
2006	21,7	177,3	1,51
2007	21,3	198,7	1,69
2008	13,2	211,9	1,81
2009	14,6	226,5	1,93
2010	17,9	244,4	2,06
2011	19,0	263,4	2,25
2012	16,1	279,4	2,38
2013	22,7	302,1	2,58
2014	14,1	316,2	2,70
<b>Average 2000-2014</b>	<b>13,8</b>		<b>7,3%</b>
<b>Average 2009-2013</b>	<b>18,0</b>		<b>7,4%</b>

*Table 1 - Increase in length of the grid over the years. [38]*

Year	Network extensions	
	Increase over the year (km)	Extension to 31 December (km)
1999	115	996
2000	95	1.091
2001	151	1.242
2002	121	1.363
2003	108	1.471
2004	38	1.509
2005	158	1.667
2006	286	1.953
2007	218	2.171
2008	85	2.256
2009	148	2.404
2010	368	2.772
2011	105	2.877
2012	284	3.161
2013	646	3.807
2014	167	3.974

The most recent data analysis available, from “GSE elaboration on AIRU, GSE, Regions data 2018”, indicates that a volume of 363,9 Mm<sup>3</sup> is currently heated with an increase of 47,7 Mm<sup>3</sup> compared to the data referred to 2014. The same can be said for the extension of the network which from 3974 Km (in 2014) reached 4835 km of extension with an increase of 861 Km in just four years. In Italy, at the end of 2018 there were a total of 314 DH networks in operation, with 255 municipalities in which there is at least one network, distributed in 13 regions. Another interesting data (table 3) is that this technology is basically limited to the central-northern area in which about 80% of the district heated volume is covered by 4 regions (Lombardia, Piemonte, Emilia Romagna, Trentino Alto Adige).

Table 3 - Data of district heating network for different regions. [14]

Regions	Number of district heating municipalities	Number of district heating networks	Installed thermal power (MW)	Overall extension of the network (km)	Number of substations	Heated volume (Mm <sup>3</sup> )
Piemonte	51	54	2.857	1.082	12.939	98,2
Valle d'Aosta	7	8	137	69	969	3,4
Lombardia	43	51	3.275	1.356	35.536	156,1
Prov.Aut.Bolzano	53	76	737	1.058	19.689	22,7
Prov.Aut.Trento	25	28	304	192	3.317	9,6
Veneto	11	11	349	143	2.114	16,5
Friuli Venezia Giulia	8	8	77	27	319	1,5
Liguria	4	5	94	18	91	4,2
Emilia Romagna	20	31	1.233	659	8.312	44,1
Toscana	30	39	141	178	6.021	2,7
Umbria	1	1	18	11	73	0,6
Marche	1	1	15	15	411	0,7
Lazio	1	1	83	26	550	3,6
Italy	255	314	9.32	4.835	90.342	363,9

Finally, it is important to highlight how the spread of district heating networks also in Italy is strongly dependent to the climate zone and to the demographic dimension of the municipality served (table 4):

- In colder climate zones the number of district heating municipalities and DH networks cover 94% and 92% respectively;
- 63% of district heating municipalities have less than 10000 inhabitants, while large municipalities (over 250000 inhabitants) have the lowest percentage (3%);
- The highest percentage (97%) of the heated volume is located in the colder climatic zones (zones E and F);

The definition of the zones is done through degree-days. They correspond to the sum, on all days of the year, of the difference (only the positive one) between the internal ambient temperature (fixed by convention at 20 ° C) and the average daily external temperature.

$$GG = \sum_{e=1}^n (20 - T_{out}) \quad (3)$$

The D.P.R. n. 412 of 26 August 1993 introduced, based on the calculation of degree-days, six climatic zones on the Italian territory:

- Zone A: municipalities with degree-days below 600;
- Zone B: municipalities with degree-days between 600 and 900;
- Zone C: municipalities with degree days between 901 and 1400;
- Zone D: municipalities with degree days between 1401 and 2100;
- Zone E: municipalities with degree days between 2101 and 3000;
- Zone F: municipalities with degree-days above 3000.

Table 4 - Data of district heating network in Italy for different climatic zones. [14]

Climatic zone	Demographic size of municipalities	Number of district heating municipalities	Number of district heatings	Installed thermal power (MW)	Overall extension of networks (km)	Number of substations	Heated volume (Mm <sup>3</sup> )
<b>Climate zone D</b>		15	24	309	174	3.882	10,9
less than 10.000 inhabitants		7	14	64	88	2.713	1,0
Between 10.000 and 60.000 inhabitants		4	4	35	29	457	1,3
Between 60.000 and 250.000 inhabitants		2	3	45	20	120	1,2
More than 250.000 inhabitants		2	3	164	37	592	7,4
<b>Climatic zone E</b>		132	155	7.823	3.265	57.475	314,6
less than 10.000 inhabitants		53	55	248	200	6.516	7,4
Between 10.000 and 60.000 inhabitants		53	58	2.095	900	11.178	73,3
Between 60.000 and 250.000 inhabitants		21	29	2.301	1.199	28.546	105,7
More than 250.000 inhabitants		5	13	3.178	966	11.234	128,2
<b>Climatic zone F</b>		108	135	1.189	1.395	28.985	38,5
less than 10.000 inhabitants		101	126	920	1.082	21.744	25,8
Between 10.000 and 60.000 inhabitants		6	8	254	311	7.221	12,4
Between 60.000 and 250.000 inhabitants		1	1	15	2	20	0,3
More than 250.000 inhabitants		-	-	-	-	-	-
<b>Total</b>		255	314	9.320	4.835	90.342	364
less than 10.000 inhabitants		161	195	1.233	1.370	30.973	34
Between 10.000 and 60.000 inhabitants		63	70	2.384	1.241	18.856	87
Between 60.000 and 250.000 inhabitants		24	33	2.361	1.221	28.686	107
More than 250.000 inhabitants		7	16	3.342	1.004	11.826	136

At the end of 2018, the total installed thermal power to service the DH network was 9328 MW. This is mainly produced by plants of thermal production only fueled by fossil fuels (5669 MW) while plants powered by renewable sources covered only 6% of the power produced.

Regarding the power produced from cogeneration plants is about 26 % of the total produced and the most of this power (71 %) is produced by using fossil fuels (mainly natural gas). Overall the percentage of power produced by fossil fuel is around 84%.

Looking more specifically at the region level, Lombardia presents the highest percentage (35%) of the total thermal power and about 62 % of this power is produced by plants of thermal production only fueled by fossil sources. Cogeneration plants fueled by fossil fuel cover about 19% of the thermal power produced. Overall, only 5% of the thermal power produced in Lombardia is produced through renewable sources.

The second region that produces more MW of thermal power (2857 MW) is Piemonte and 97% of this power is produced by plants fueled by fossil fuels.

Unlike, Toscana covers most of its DH production (only 1,5% of the total) through renewable sources with a percentage of 90 %. This is due to the strong presence of geothermal energy sources locally available.

*Table 5 - Generation linked to district heating overview for different Italian regions. [14]*

Regions	Cogeneration plants			Thermal production only plants			<u>Total thermal power</u>
	powered by RES	powered by fossil sources	powered by waste	powered by RES	Powered by fossil fuels	Powered by recovery heat	
<b>Piemonte</b>	37	1.059	-	41	1.719	-	<b>2.857</b>
<b>Valle d'Aosta</b>	5	8	-	22	85	17	<b>137</b>
<b>Lombardia</b>	79	611	449	93	2.026	18	<b>3.275</b>
<b>Prov.Aut.Bolzano</b>	72	41	30	216	380	-	<b>737</b>
<b>Prov.Aut.Trento</b>	14	54	-	55	181	1	<b>304</b>
<b>Veneto</b>	17	66	25	19	218	4	<b>349</b>
<b>Friuli Venezia Giulia</b>	3	10	-	6	58	-	<b>77</b>
<b>Liguria</b>	-	36	-	1	56	-	<b>94</b>
<b>Emilia Romagna</b>	11	242	118	19	843	-	<b>1.233</b>
<b>Toscana</b>	5	8	-	122	7	-	<b>141</b>
<b>Umbria</b>	-	4	-	-	13	-	<b>18</b>
<b>Marche</b>	-	1	-	-	13	-	<b>15</b>
<b>Lazio</b>	-	14	-	-	69	-	<b>83</b>
<b>Italy</b>	241	2.154	622	594	5.669	40	<b>9.320</b>

### 3.4 District heating models

District heating systems modelling is computationally demanding. The simulation of energy transfer through the system is a cornerstone of every DH model analysis [15]. The energy transfer depends both on the mass-flow rate and on the carrier fluid temperature. There is a strong difference between mass-flow and temperature dynamics as mass flow changes are transmitted in the order of seconds along the distribution network while temperature changes are transmitted significantly slower as they are linked to the water flow in the pipes [16].

The transport delay in the pipes is the key aspect of the dynamics in a district heating simulation. It is defined as the time the fluid takes to flow from pipe inlet to outlet. Many studies focusing on temperature dynamics in DH have been made. Some authors [17] made a model of the Vilnius DH grid in Lithuania using two different modeling tools for comparing temperature variations and heat loss in the system.

They evaluate the supply circuit of a DH network with 27 heat exchanger substations (consumers) that are located within an area of  $3.6 \text{ km}^2$ . In the analysis the flow-rate to the substations is known and therefore considered as boundary conditions. Furthermore specific heat, density and fluid viscosity are considered constant. They found a finite element code in ANSYS that is capable of simultaneously modelling fluid flow and heat transfer in a DH network. In addition the code is independent of network geometry and standard discretisation methodology.

Stevanovic et al. [18] studied the Zemun DH grid (Serbia) thermal transients and fluid dynamics propagation time delays from the thermal power plant to the consumers. The thermal transients are caused by a rapid increase and decrease of the heat power plant load. They applied a numerical scheme of the third order in space for the solution of energy equation founding that the calculated and measured temperatures at three substations shows good agreement. The three consumer substation used as benchmark are at different distances from the heat plant. A similar type study that presents a fully dynamic model for transport delays in pipes was conducted by Grosswindhager et al. [19] treating the Tannheim DH grid in Austria. They compared the temperature at two consumer with real data for a one-day analysis finding following results:

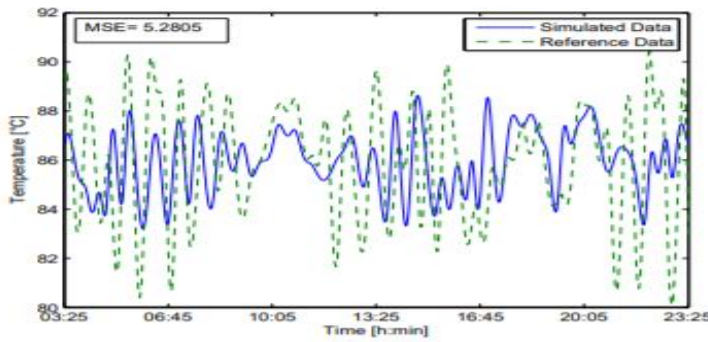


Figure 7 - Temperature at substation 1 vs time in Tannheim DH. [19]

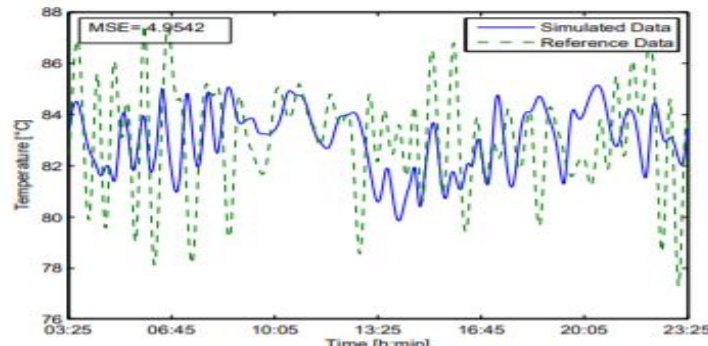


Figure 8 - Temperature at substation 2 vs time in Tannheim DH. [19]

The cited studies deal with physical models based on advection exchange formulated through a finite difference analysis. On the other hand, the propagation of water can be modelled by only considering the inlet and outlet of the pipe where the output calculation is based on the propagation delay. This method is the so-called node method that was described by Benonysson [20].

An overview of different modelling approaches for district heating pipes was presented by Pálsson et al. [21]. They found that the number of floating point operations per time step using finite element method varies linearly with the number of discretization elements while the number of floating point using the node method remains the same for every pipe.

Finally more recent simulation involves plug-flow approach using spatialDistribution operator used to cope for zero flow and flow reversal. [22]

Some studies demonstrate that plug-flow approach is faster compared to finite volume method implemented in dynamic pipe present in Modelica Standard Library.

Van der Heijde and others made a comparison of the two different approaches simulating a reference case study a small initial portion of Pongau DH network (Austria). The portion interests 3 consumer and the power plant. They found that dynamic pipe model with a discretization of one meter is 68 times slower than the plug-flow approach. [23]

The plug-flow approach is applied in DisHeatLib library in Modelica that is supported by Dymola and other commercial softwares. In Openmodelica no library makes it possible to simulate complex district heating network without using dynamic pipe component.

## 4. Methodology

This section describes the softwares used, underlining the reasons that led to their choice and illustrates the methodology adopted for the creation of reliable models for the simulation of district heating networks. Finally, solution methods in *OpenModelica* are briefly discussed.

### 4.1 Softwares

The models have been developed in the equation-based, object-oriented language *Modelica*, which is an open source, equation based programming language to model complex systems such as thermo-hydraulic systems. In *Modelica* the equations are not assignments like in most programming language but they describe equality and there is not a geographical order for equation and definition. The language is therefore called acausal. This permits better reuse of models because equation do not specify flow variable direction.

For example we can have  $y = x^3$  and *Modelica* can also solve x from this equation if y is known.

Other advantages of *Modelica* are its multidisciplinarity and the complete definition of parameters. In *Modelica* model, different domains can be connected and contemporary described and the parameters appear as physical quantities (making dimensional analysis possible). *Modelica* has four built-in types: Real, Integer, Boolean, String. Typically, user-defined types are derived, to associate physical quantity, unit, nominal values, and other attributes.

The existence of different validated components libraries is a further advantage. Using modifications is possible to reuse the component. By using *Modelica*, it is therefore possible to create standardized libraries of district heating components. These components can be used by drag-and-drop to easily replicate an existing district heating network. The objects created in the district heating library can only interact with parameters and data available internally and at its boundaries. Thanks to this drag-and-drop technique a user could reuse already defined and validated components and manage the components through a convenient graphic interface of the physical variables of interest. It is now clear that the user interface must be developed with looking to simplicity in order to make the created component accessible to more subjects. Furthermore it is possible to create documentation about the component itself explaining its functioning.

The connector are instances of connector classes, which describe the variables of the communication interface specified by the connector. The variables in the connector could be flow, potential and stream variable where: flow represents a flow of conserved quantity(mass, energy, momentum etc.), stream variables are associated and transported with the only flow variable and potential variables are those who cause component reaction. Potential variables can be used to determine flow variables. The stream variable is strongly used in fluid libraries as models need to be able to handle bi-directional flows, closed circuits and the transients. [24]

All of the objects used in the library can be connected using the designated connector. When three or more connectors are used at a single point, a mixing/splitting is automatically made by *Modelica*.

A simulation environment is needed to translate and execute *Modelica* models. In this study, models have been developed, simulated and validated in *Modelica* modelling and in *OpenModelica* simulation environment version 1.16.0. Like *Modelica*, *OpenModelica* simulation environment is open-source. The goal with the OpenModelica effort is to create a comprehensive Open Source Modelica modeling, compilation and simulation environment based on free software distributed in binary and source code form for research, teaching, and industrial usage. [25] [26]

As regards the simulation of district heating systems, a validated library exists in *Modelica*. The *DisHeatLib* library contains models for pipes, substations, thermal power plants, users and boundary conditions. An in-depth analysis of the library led to the choice of not using it for, mainly, 2 reasons:

- The pipe model present in the library uses a plug-flow approach with the use of the spatial distribution operator which is not yet supported in *OpenModelica*. This has meant that even the validated examples of the library cannot be simulated in *OpenModelica* but only in commercial software such as *Dymola*.
- Substation models require the presence of the secondary circuit. Since the secondary circuit data was not available for most of the buildings in the case study, the different substation models were not usable.

Methods for handling data and for the visualization of results has been developed using *MATLAB*.

As the data sets grow in size and complexity, it becomes more and more difficult to work with them, particularly when the data does not fit in memory. During the work it was noted that some data to be used as input to the model were out of memory using software such as *Excel* while *MATLAB* environment makes easier and convenient the analysis and displaying of big data.

## 4.2 Logical approach to the model

The approach used in order to correctly implement the model according to the prefixed aim of the work followed the following working time logic:

- First of all, an analysis of the monitoring data was carried out in order to define the functioning of the network of the case study analyzed. The analysis allowed to understand the approach to be used to define the network as well as to make decisions regarding the complexity of the model in relation to the data provided;
- Subsequently a hydraulic analysis of the network was carried out. The decision to start from the hydraulic analysis is clear from what is underlined in paragraph 4.1. The flow variable, flow rate in mass, is in fact determined on the basis of variations in the potential pressure variable. The hydraulic analysis therefore allows to define the flows circulating in the network under analysis. In this phase, the pipe models were defined from which the boundary conditions under pressure were determined through a back-modeling technique (see chapter 6.2). Subsequently, the components concerning the substation were modeled such as, for example, the control valves and heat exchangers.
- The last modeling step involved thermal analysis. As described in chapter 4.1, the pipe model in the DisHeatLib library is not usable in *OpenModelica* and, therefore, the only other model already present in validated libraries that can be used for the purposes of the work is the dynamicpipe present in Modelica standard library. This model uses a finite volume analysis which makes the simulation of the district heating network particularly expensive computationally. For this reason it was decided to model a new component that would allow the thermal analysis through the solution of equation (15) and at the same time the hydraulic analysis defined in the second modeling step.
- Finally, the results of the simulations were compared with the monitoring data, showing the reliability of the models implemented.



## 5. Case study

The case study is a portion of the Grugliasco district heating network. This portion belongs to the district heating system serving the municipalities of Rivoli, Collegno and Grugliasco that is an interconnected system managed by the company Iren S.p.A. The coverage of the base load is guaranteed by the cogeneration plant located in the production plant C.E.N.T.O. located in “via Genova 66”(Rivoli). This cogeneration plant consists of two gas turbines and a counter-pressure steam turbine with nominal thermal power equal to 82 MWth. The integration and backup systems are present both in the aforementioned plant and in the plant in Via Leonardo Da Vinci 44 (Grugliasco) characterized by total nominal power equal to 41.4 MWth. The boilers of the Grugliasco thermal power plant constitute a heat generation substation to increase the temperature of the network. These boilers also allow the Collegno users that are located far from C.E.N.T.O. plant to be district heating . This solution is optimal in terms of energy saving because it allows to reduce the thermal losses of the network.

It is consequently evident that the regulation adopted is load tracking: the boilers modulate the thermal power generated on the basis of the thermal needs and the measured return temperatures that varies according to the power required by the substations. The network is provided with a single pumping station at the Rivoli power plant. The station includes 9 pumps equipped with inverters, for an installed power of approximately 0.5 MWel, which have the task of regulating the flow rate and keeping the network under pressure.

The substations are of various sizes in terms of nominal power, ranging from about 8 kWt for smaller substations, up to over 4000 kW nominal. The substations can be divided by intervals of rated power according to Figure 9 [27]:

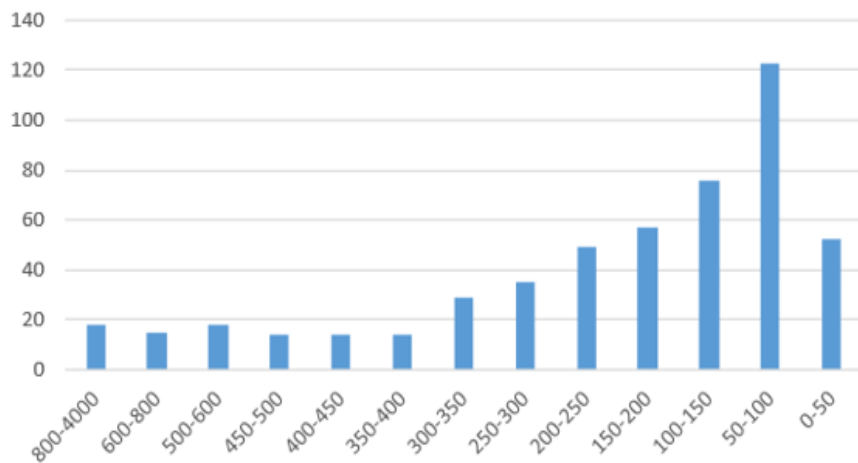


Figure 9 - Number of substations in the entire district heating network with nominal power in a specific range. [27]

The portion of the network under analysis supplies new buildings through an indirect system. The buildings served generally have high thermal performance both as regards the masonry package and the emissions systems used as they are of recent construction.

Twenty-three users in the lot will be analyzed as the buildings for which there is no remote reading were not considered. The buildings analyzed have mixed operation (heating plus domestic hot water) with the exception of a single building which works only in heating. Furthermore, the gross volume of the buildings under analysis is equal to 103961 cubic meters.

The figure shows the detail of the analyzed network portion.

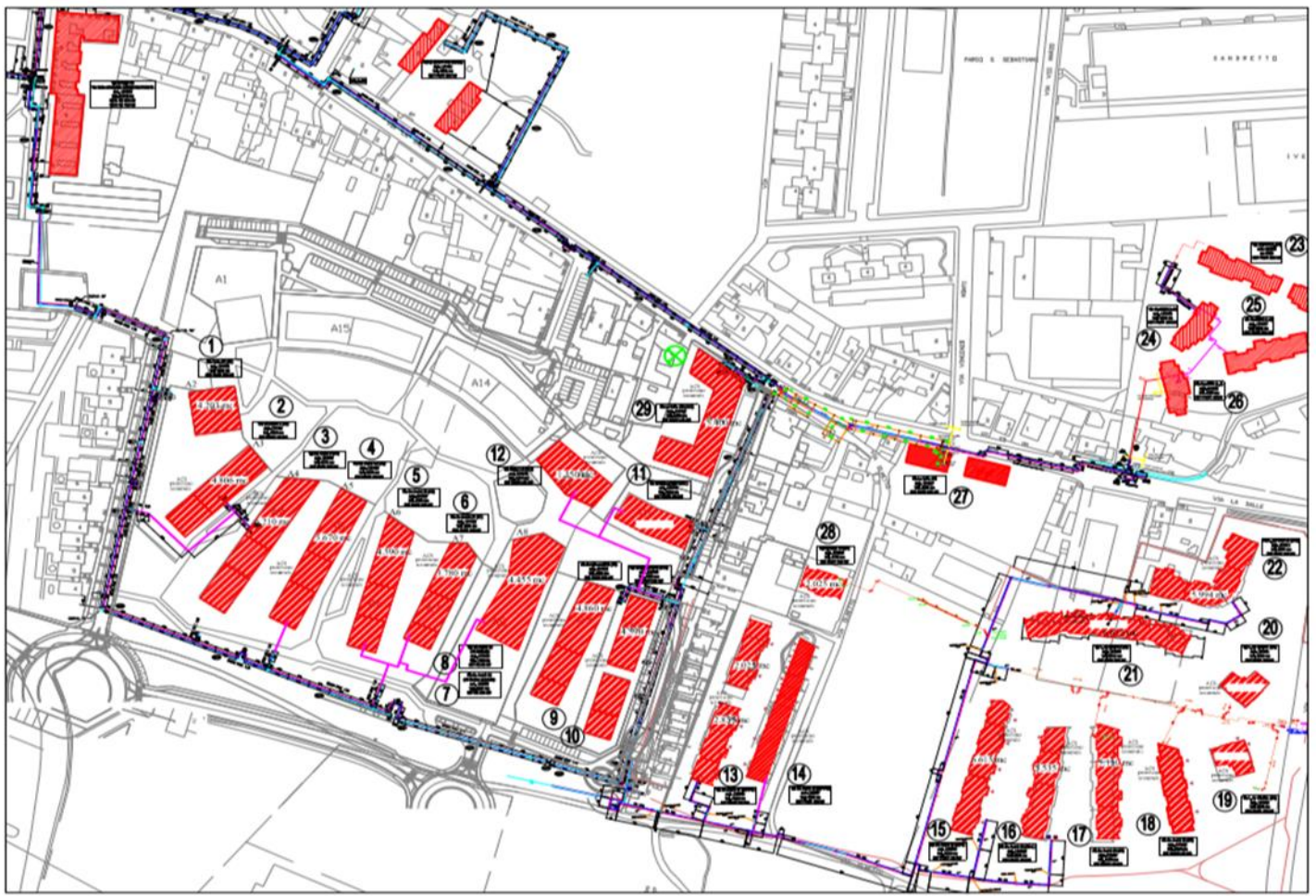


Figure 10 - AutoCAD plan of the portion of the network under analysis

The substations present differ in nominal power, specifically:

Table 6 - Substation typology, nominal power and number of user with same substation typology.

Substation tipology	Nominal Power [kW]	N° of users
1	250	2
2	200	3
3	150	7
4	120	1
5	100	10

The substations of the lot are therefore divided into 5 different types based on the rated power. The most used types are those with nominal power of 100 kW and 120 kW for a total of seventeen substations. Comparing these data with those of the entire network (figure 9), we note that all the substations belong to the two power ranges with the greatest presence of substations in the network (100 to 150 kW and 150 to 250 kW).

## 5.1 Data analysis

The analysis of the district heating network focuses on the "IL BORGO" lot in Grugliasco (Turin) for a total of 23 buildings. The data is recorded through a data logger with different codes based on the measured quantity, in particular:

- *SIE230\_01\_02\_05*: Measures the return temperature to the secondary;
- *SIE230\_01\_01\_05*: Measures the delivery temperature to the secondary;
- *SIE230\_01\_02\_01*: Measures the outside temperature;
- *UH50SI\_01\_00\_07*: Measures the primary flow temperature;
- *UH50SI\_01\_00\_08*: Measures the return temperature to primary;
- *UH50SI\_01\_00\_06*: Measures the instantaneous flow to primary;
- *UH50SI\_01\_00\_05*: Measures the heat exchanger power;
- *ROSVAL\_02\_00\_03*: Measures the supply pressure;
- *ROSVAL\_01\_00\_03*: Measures the return pressure.

The first step of the analysis takes into consideration the different physical parameters for each building. This is done to provide a specific framework on the buildings and subsequently set up final reasoning to be implemented in the model. The data is analyzed in *MATLAB* by importing *Excel* files. The sensors record data on the basis of clocks which must be reported to calendar dates. In *MATLAB*, the clock is reset to a specific date through the *datetime* function. Datetime is initialized at 00:00:00 on 01-01-1970.

Data are usually available from September 2018 to the end of July 2019. It should be noted that not all measured values are present for all buildings, as depicted in Table 7:

Table 7 - Availability of measured parameters for the building under analysis.

BUILDING	CODE	Tprim_S	Tprim_R	Tsecond_S	Tsecond_R	M_FLOW_P	POWER	PRESSURE
Via Cotta 67	10243							N
Via de André 1	10165							N
Via de André 9	10162							N
Via de André 13	10161							N
Via de André 23	10158			N	N			N
Via de André 27	10157			N	N			N
Via de André 35	10110							N
Via Bongiovanni 26 A9	10264				N			N
Via Bongiovanni 26 A10	10241				N			N
Via Bongiovanni 14 A11	10263				N			N
Via Gaber 14 A13	10245				N			N
Via de André 47	10552			N	N			N
Via de André 49	10551			N	N			N
Via Olmetto 14	10544			N	N			N
Via de André 55 B5-2	10160	N	N			N	N	N
Via de André 55 B5-1	10159	N	N			N	N	N
Via de André 69	10164			N	N			N
Via de André 73	10549			N	N			N
Via L.Da Vinci 11 (B1)	10545			N	N			N
Via L.Da Vinci 13 (B9)	10521				N			N
Via L.Da Vinci 9 (B2)	10163			N	N			N
Via La Salle 130(A12)	10246			N	N			
Via L.Da Vinci 15 (B10)	10224				N			N

From this table it is evident that the secondary parameters are not available for the majority of buildings and that the pressure measure is available in only one specific point. So, starting from the monitoring data, it was decided to focus attention on the primary, as data in the secondary (user) circuit were not available for the majority of buildings.

From a first plot of the quantities over the entire time span of measurement it is possible to obtain various information on the buildings in the lot:

- The first figure shows the primary side supply and return temperature for the first building analyzed (Via Cotta 67). It is evident that the supply temperature increases in winter and then decreases in summer, while the return temperature maintains a more constant behavior;

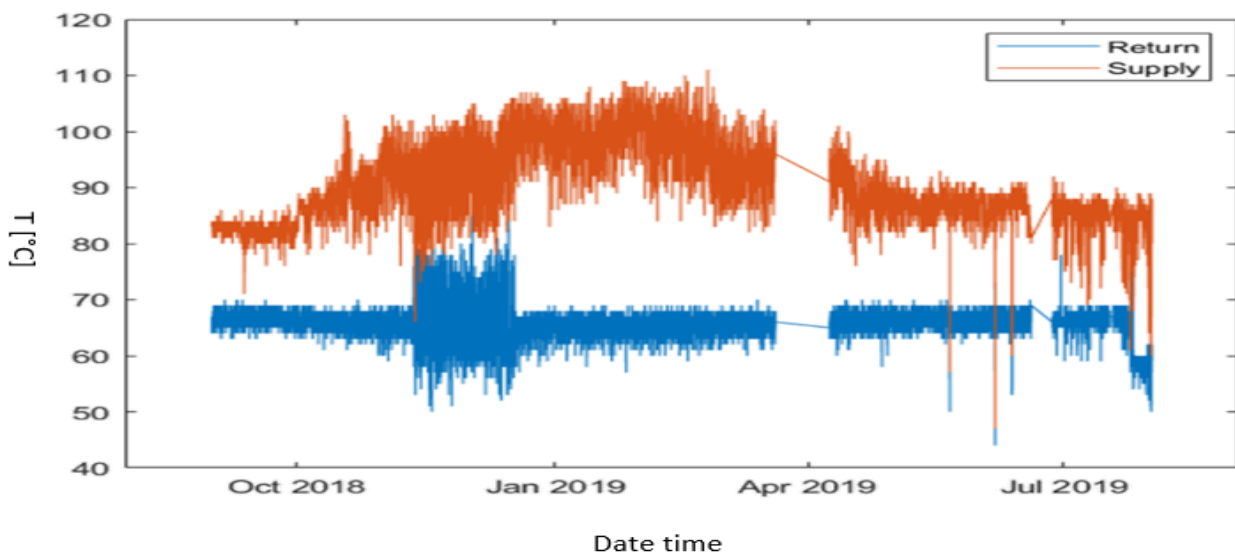


Figure 11 - Supply and return temperature at primary side for building located in Via Cotta 67.

- The following figures shows the temperatures at secondary side for two buildings where the above measurements are available. The graph shows that the deliver temperature at secondary side remains practically constant during the entire analysis period while the return temperature decreases when the outside temperature decreases (heat load is higher). This information will be of fundamental importance in subsequent analyzes regarding substations.

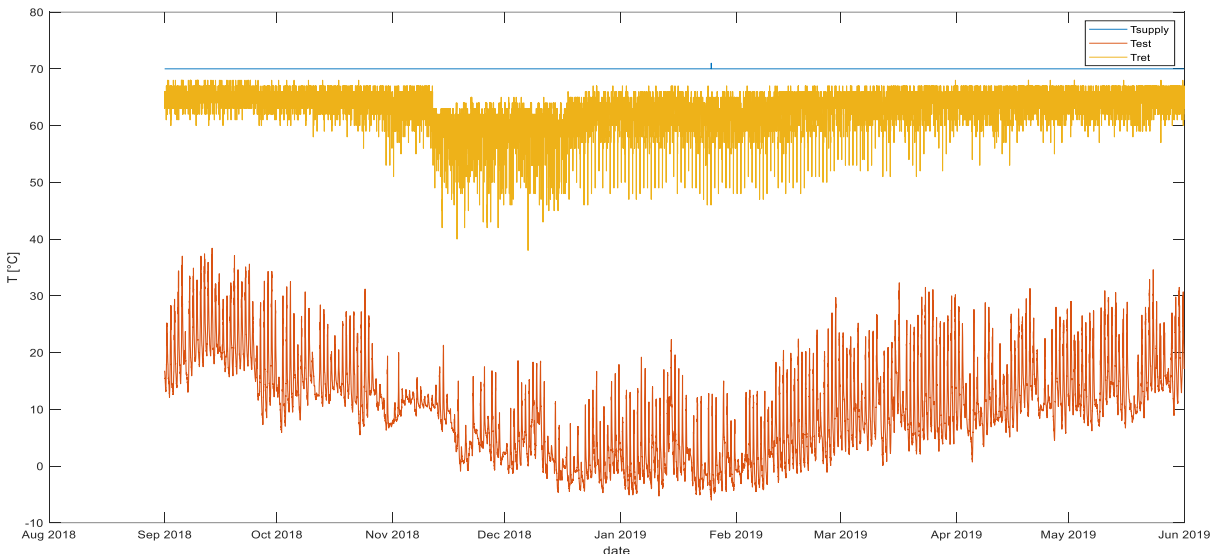


Figure 12 - Supply, return temperature at secondary circuit and outside temperature for the building in Via Cotta 67.

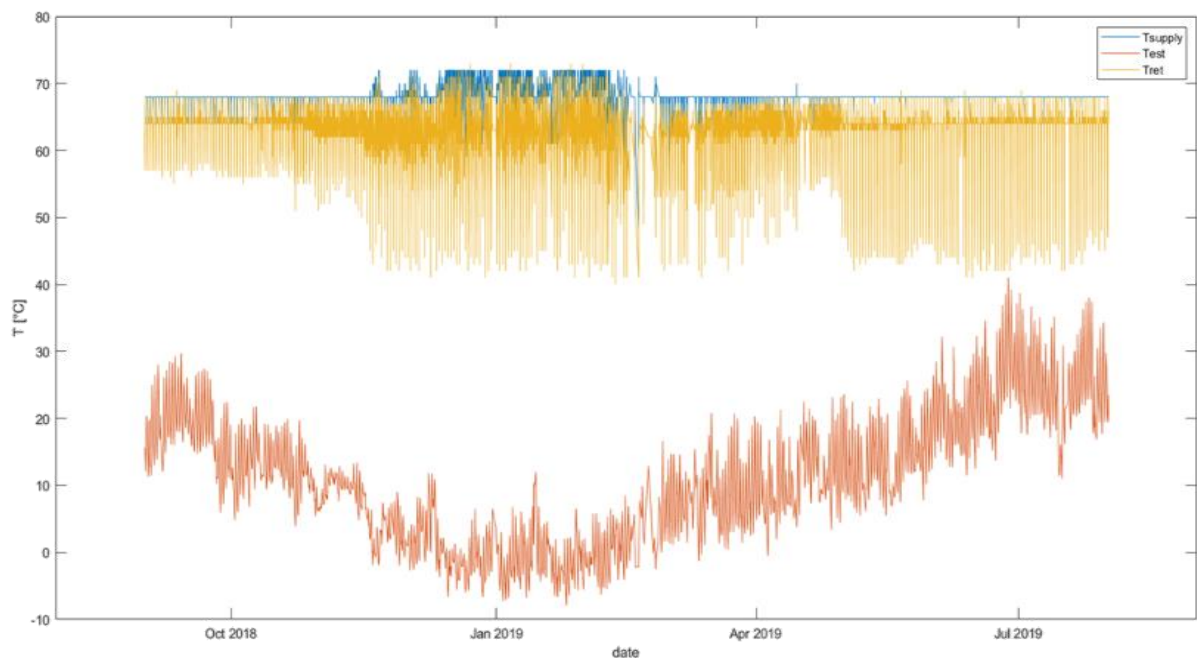


Figure 13 - Supply, return temperature at secondary circuit and outside temperature for the building in Via De Andrè 1.

Specific charts were generated in order to more accurately assess the availability of data for the different buildings during the time period under analysis.

This chart typology was developed for each building concerning three variables:

- 1) Supply temperature at primary side;
- 2) Return temperature at primary side;
- 3) Actual flow-rate at primary side.

The diagram shows for each day and for each month the amount of data available at different hours for a maximum of 24 per day. In the following plots an example of one building availability of data:

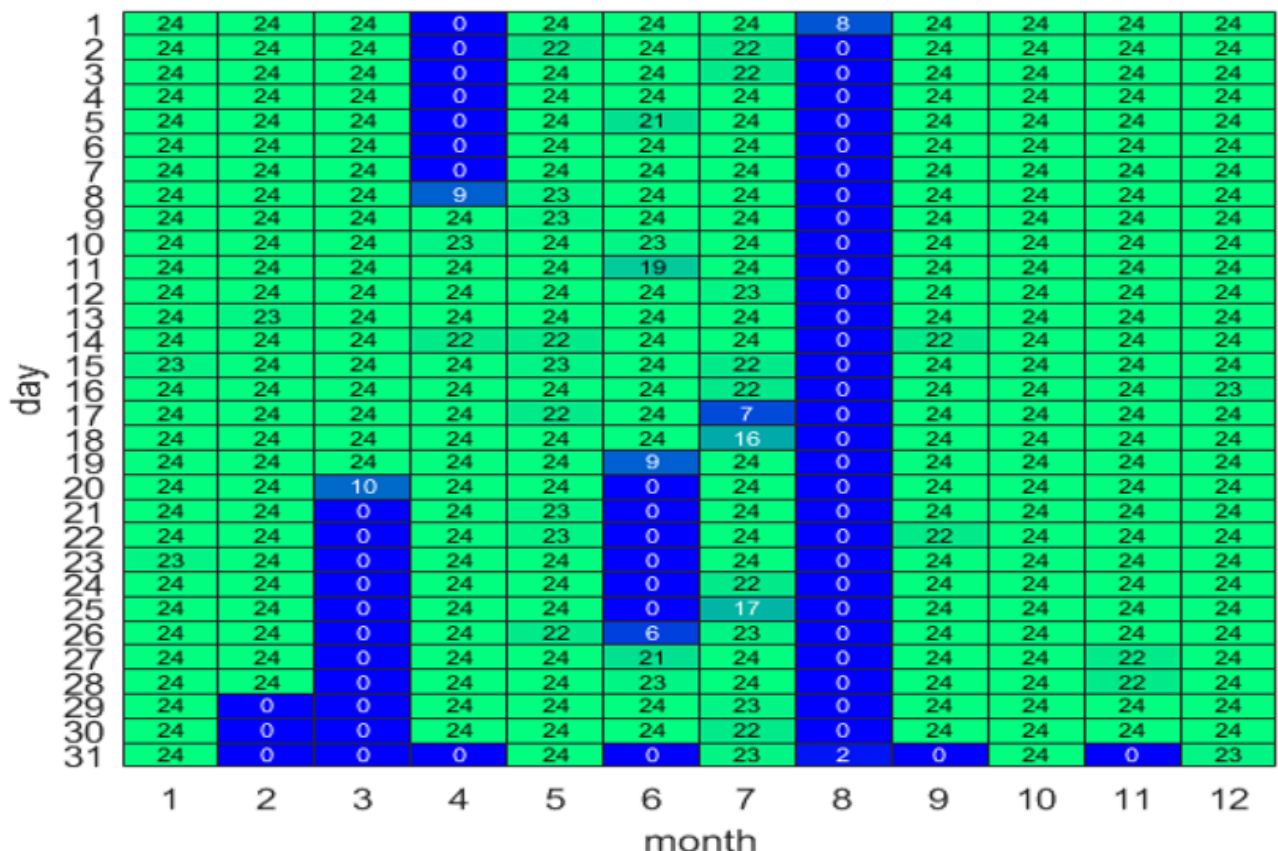


Figure 14 - Gantt diagram of T supply availability for a building.

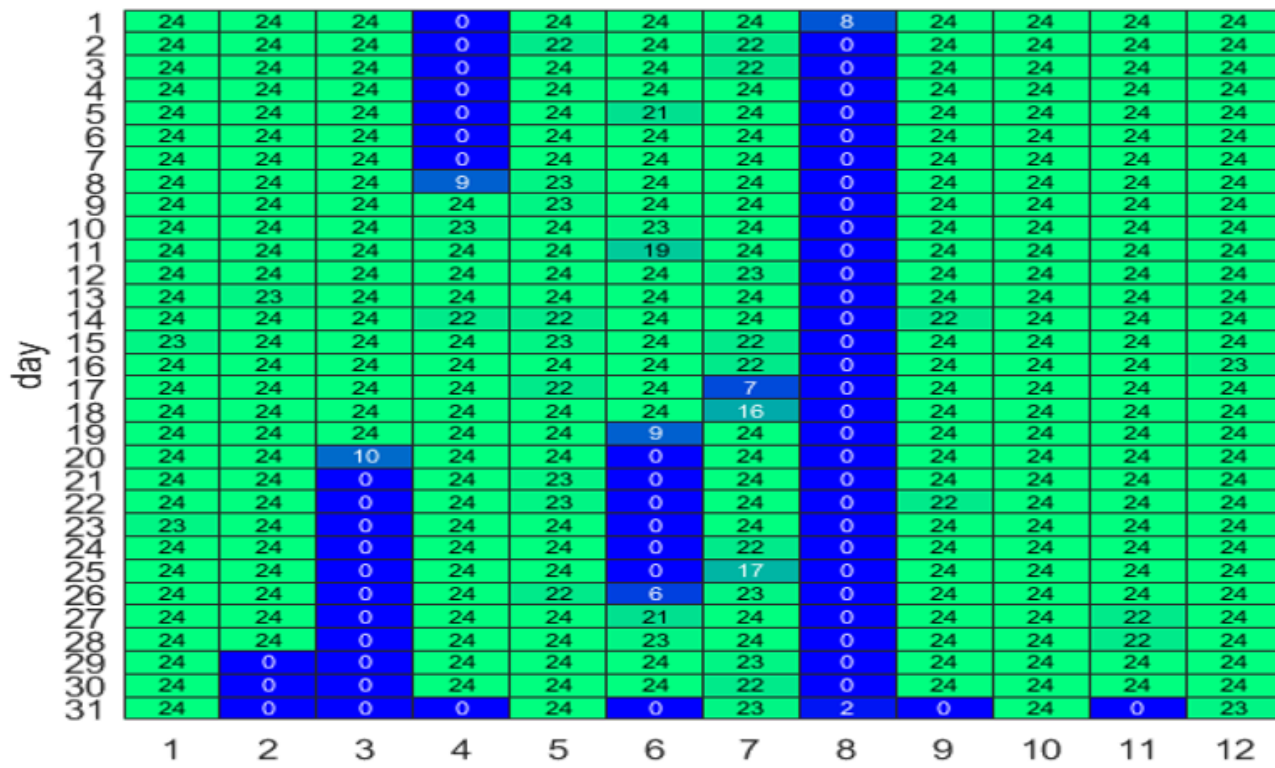


Figure 15 - Gantt diagram of return temperature at primary circuit for a building.

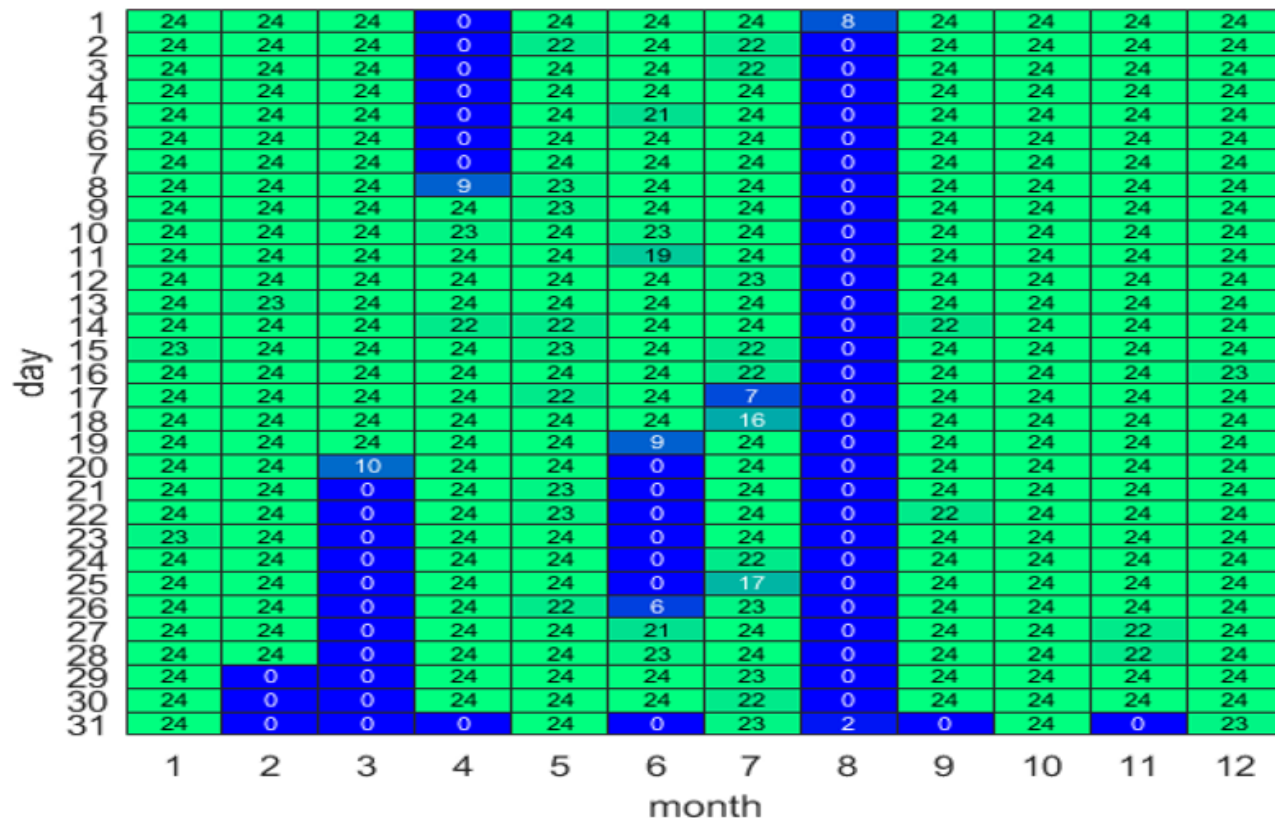


Figure 16 - Gantt diagram of flow rate availability for a building.

The results show excellent availability of primary circuit data for the majority of buildings. For buildings with very small amounts of data (see figure 17), it was decided to use data from the nearest buildings of the same heated volume size.

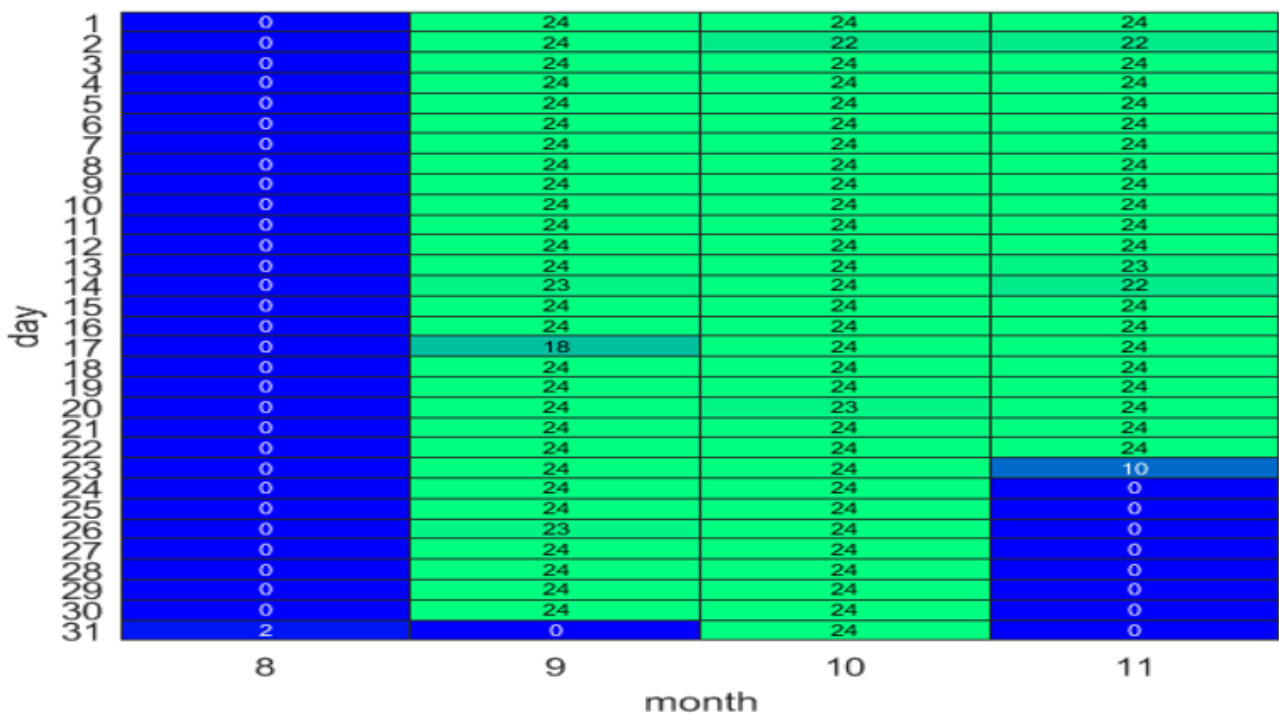


Figure 17 - Building with very low data availability (Via Olmetto 14)

Summarizing the availability of data at the primary side, a diagram was produced with the start and end of the measurement data for each building:

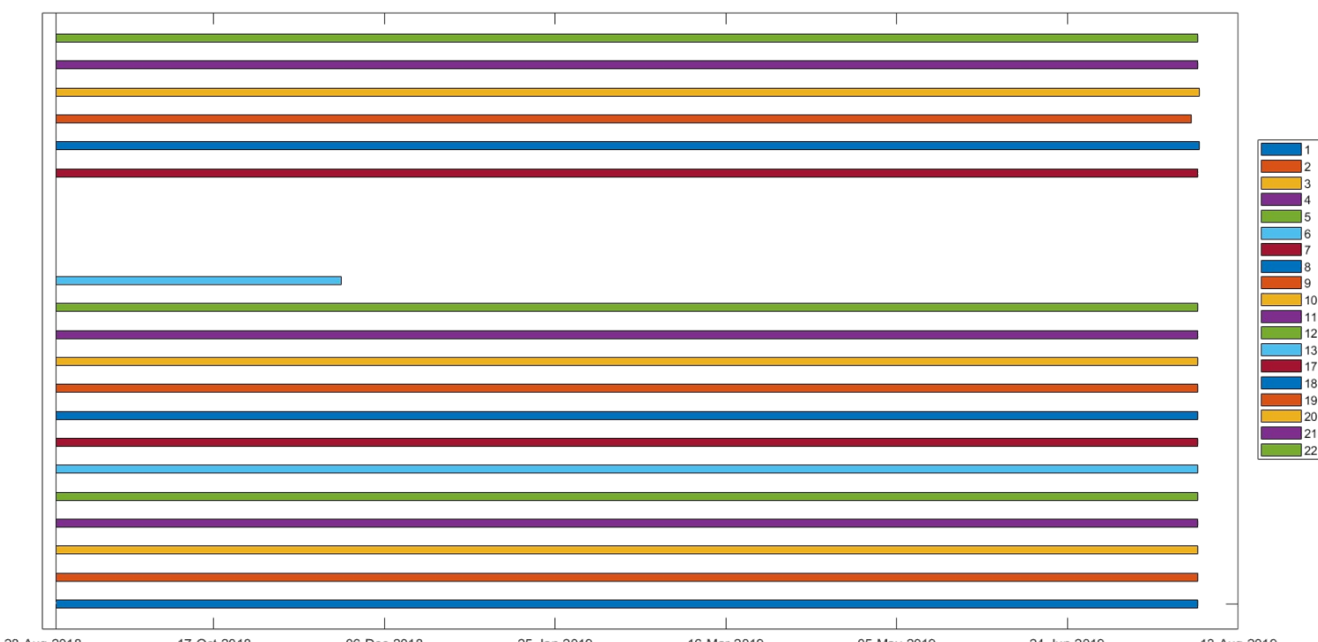


Figure 18 - Start and end time of measurement data for each building.

Figure 18 confirms that for almost all the buildings the data are available for a period of time from the end of August 2018 to the end of July 2019.

It should be noted that this figure could be misinterpreted. In fact, it shows the time span in which the data are present based on the beginning and end of them. This means that there could be months with partial missing data. An example is reported in the following figure:

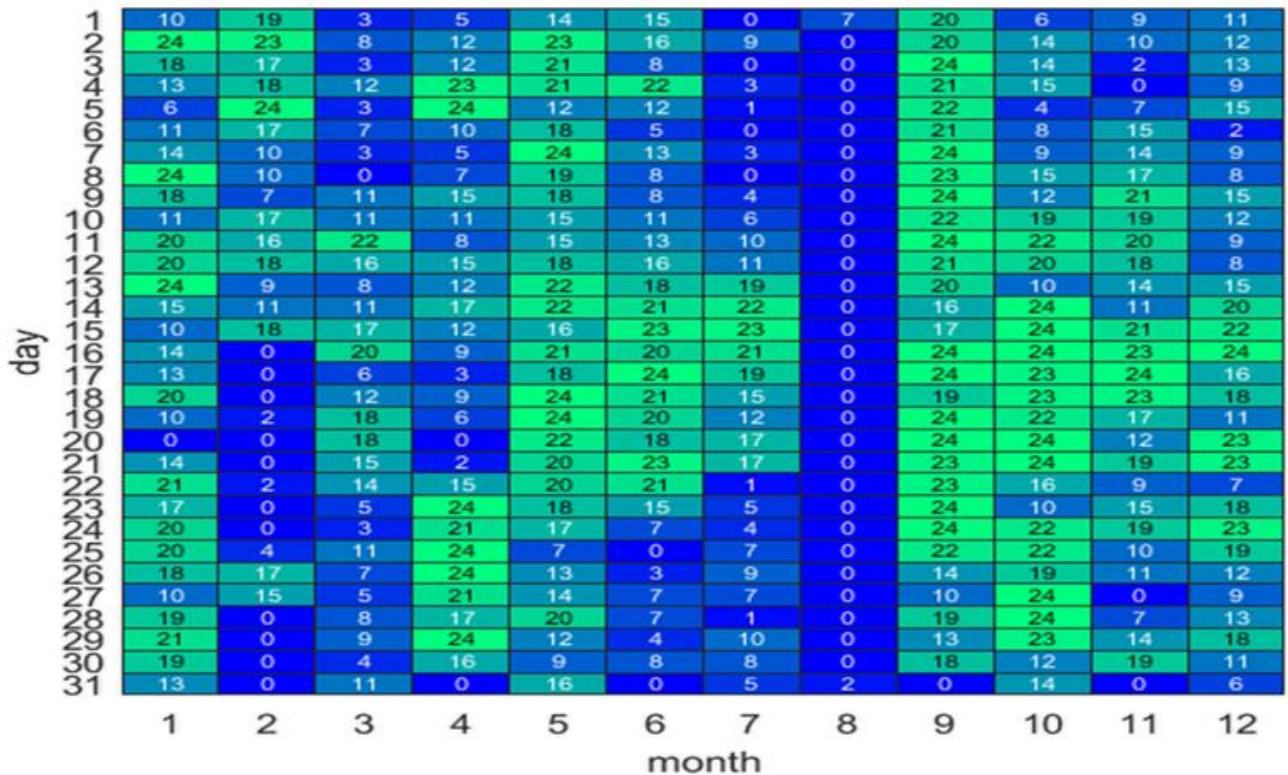


Figure 19 - Poor data availability within the timespan (Via L. Da Vinci 13).

A heat map is a data visualization technique that shows magnitude of a phenomenon as color in two dimensions. The variation in color may be by hue or intensity, giving obvious visual cues to the reader about how the phenomenon is clustered. There are two fundamentally different categories of heat maps: the cluster heat map and the spatial heat map. In a cluster heat map, magnitudes are laid out into a matrix of fixed cell size whose rows and columns are discrete phenomena and categories, and the sorting of rows and columns is intentional, with the goal of suggesting clusters or portraying them as discovered via statistical analysis. In this particular case the intensity is dependent on the median of temperature at same hour for different month. Heat maps have been generated that show the variation in the flow temperature based on the hour and month for each building. From the figures it can be seen that the higher temperatures occur in the morning and in the winter months as the need for heat increases.

Furthermore, for some buildings in the night hours the temperatures are very low as the plant manager can vary the activation times of the system and so the system could be off in that specific period of time (see figure 21):

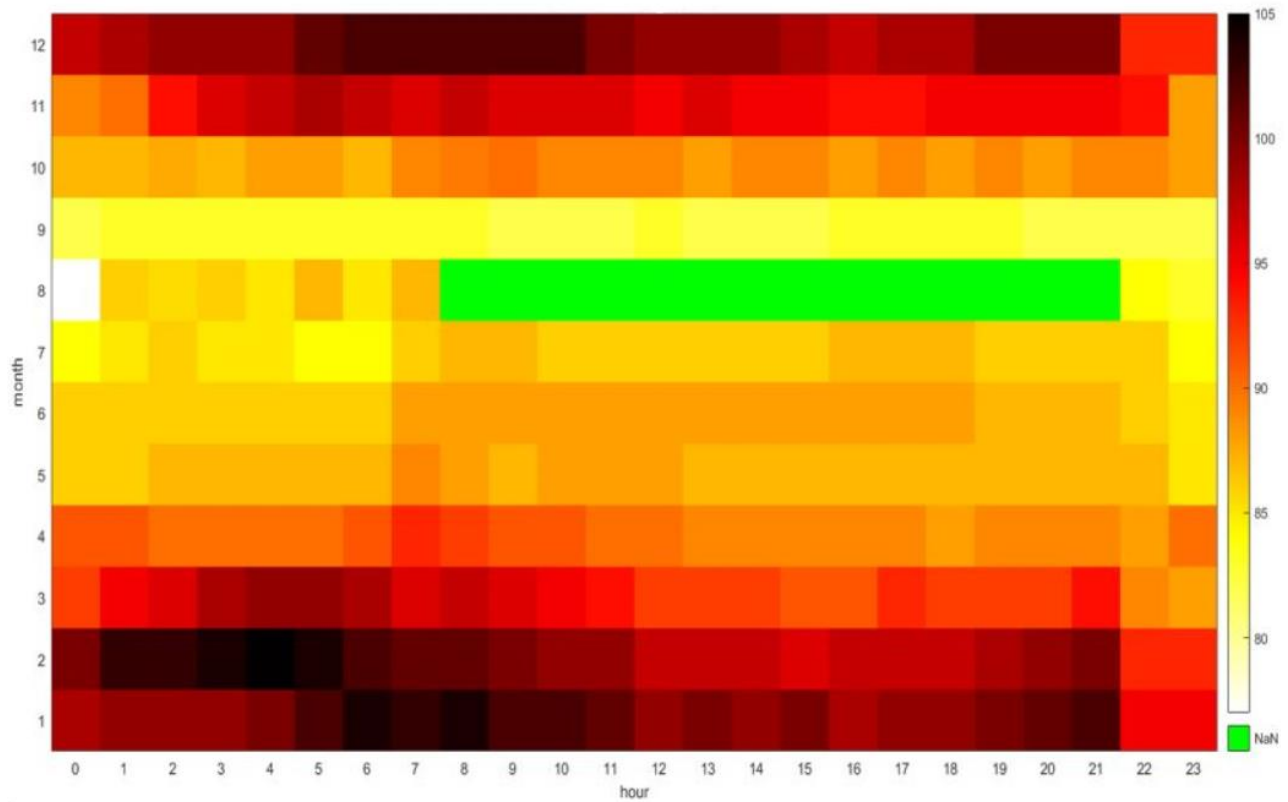


Figure 20 - Heat Map for one building representing the median of temperature in °C for same hours in the same month.

We can see two peak temperature periods during the day: one occurs early in the morning (from 5 to 10 am) and the other in the evening. Furthermore, while in the winter months the temperature reaches peaks of about 105 °C, in the summer months the peak is around 88 °C.

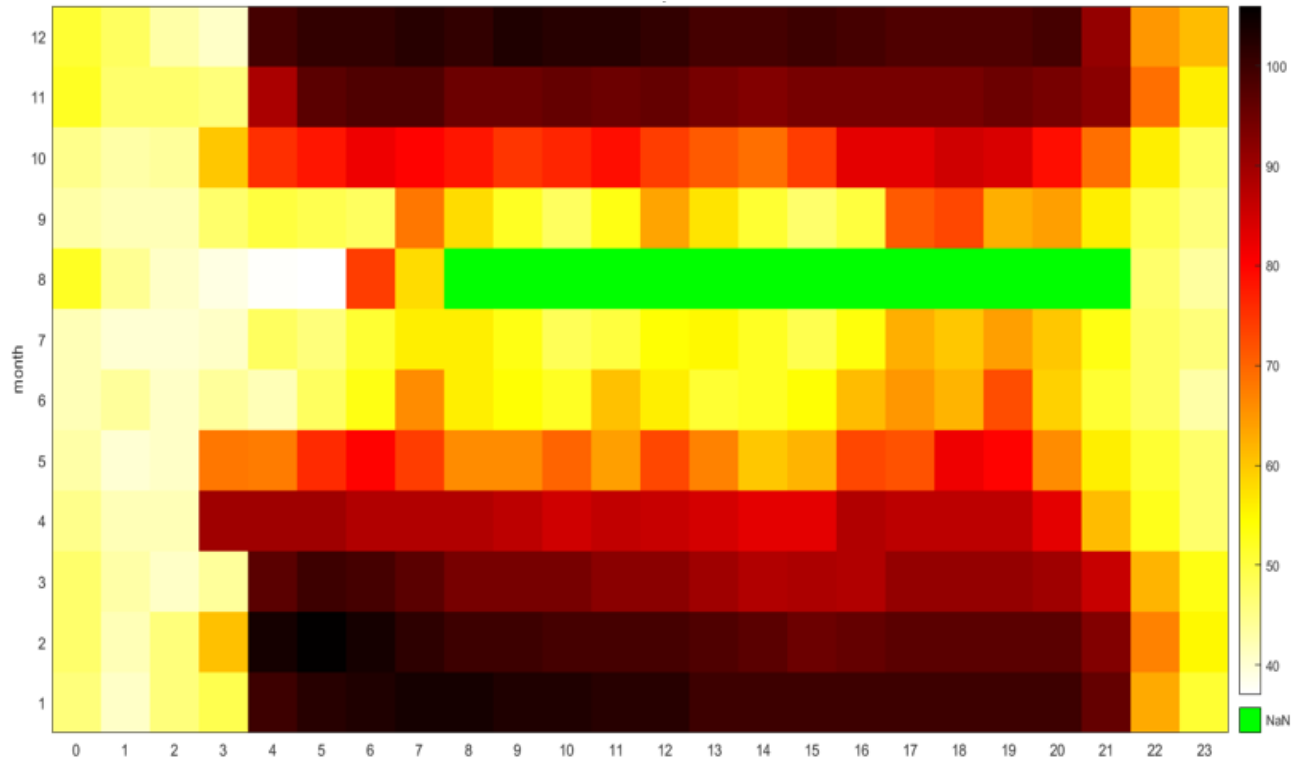


Figure 21 - Heat Map for a building with special setting imposed by plant manager (Via Bongiovanni 14).

The figure above is a classic example of substation management. We can see how at night time the substation is deactivated bringing the temperature to a rapid decrease while during daytime the temperature is kept in a fairly constant range.

Box plot is a method for graphically depicting groups of numerical data through their quartiles. Box plots may also have lines extending from the boxes (*whiskers*) indicating variability outside the upper and lower quartiles. A boxplot is a standardized way of displaying the dataset based on a five-number summary: the minimum, the maximum, the sample median, and the first and third quartiles.

Minimum : the lowest data point excluding any outliers.

Maximum : the largest data point excluding any outliers.

Median (Q2 / 50th percentile) : the middle value of the dataset.

First quartile (Q1 / 25th percentile) : also known as the *lower quartile*  $q_n(0.25)$ , is the median of the lower half of the dataset.

Third quartile (Q3 / 75th percentile) : also known as the *upper quartile*  $q_n(0.75)$ , is the median of the upper half of the dataset.

An important element used to construct the box plot by determining the minimum and maximum data values feasible is the interquartile range or IQR denoted below:

Interquartile range (IQR) : is the distance between the upper and lower quartiles.

A boxplot is constructed of two parts, a box and a set of whiskers. The lowest point is the minimum of the data set and the highest point is the maximum of the data set. The box is drawn from  $Q_1$  to  $Q_3$  with a horizontal line drawn in the middle to denote the median.

In order to make correct assumptions regarding the primary flow temperature for the various buildings, a boxplot has been generated for the flow temperature of the different buildings in different time frames:

- January to March;
- October to March;
- Month by month;
- Single boxplot for all building month by month.

The figures show the lower temperature in the summer months and that the median for buildings in succession is not always decreasing due to hydraulic transmissivity and storage effects. Furthermore, the buildings for which the interquartile range is greater are those for which the plant managers set an attenuation and / or night shutdown as already highlighted by the analysis carried out through the heatmap (see building 4,10,14,16,19 in figure 23). Finally, it is possible to note that for building 18 the data present is decidedly scarce (as already underlined by the Gantt chart, see figure 17).

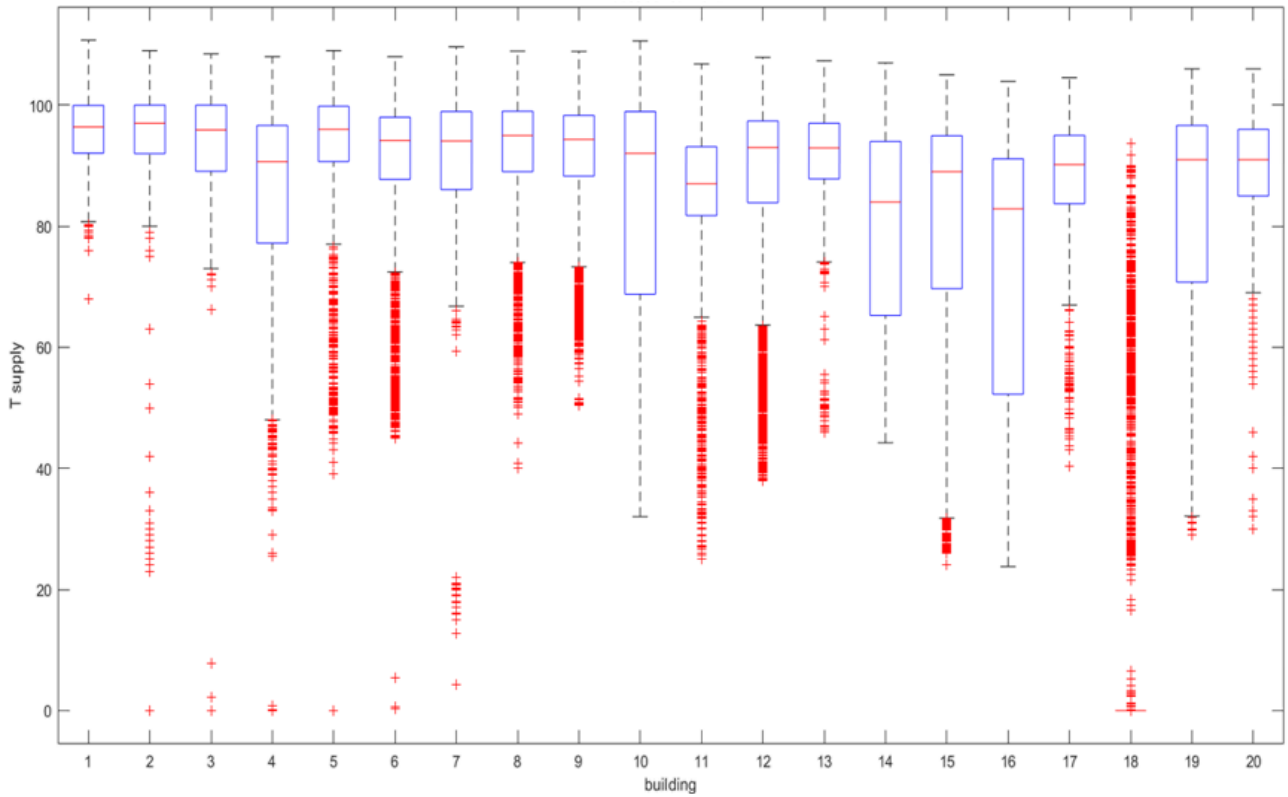


Figure 23 - Box Plot of supply primary temperature for the different buildings from October to March.

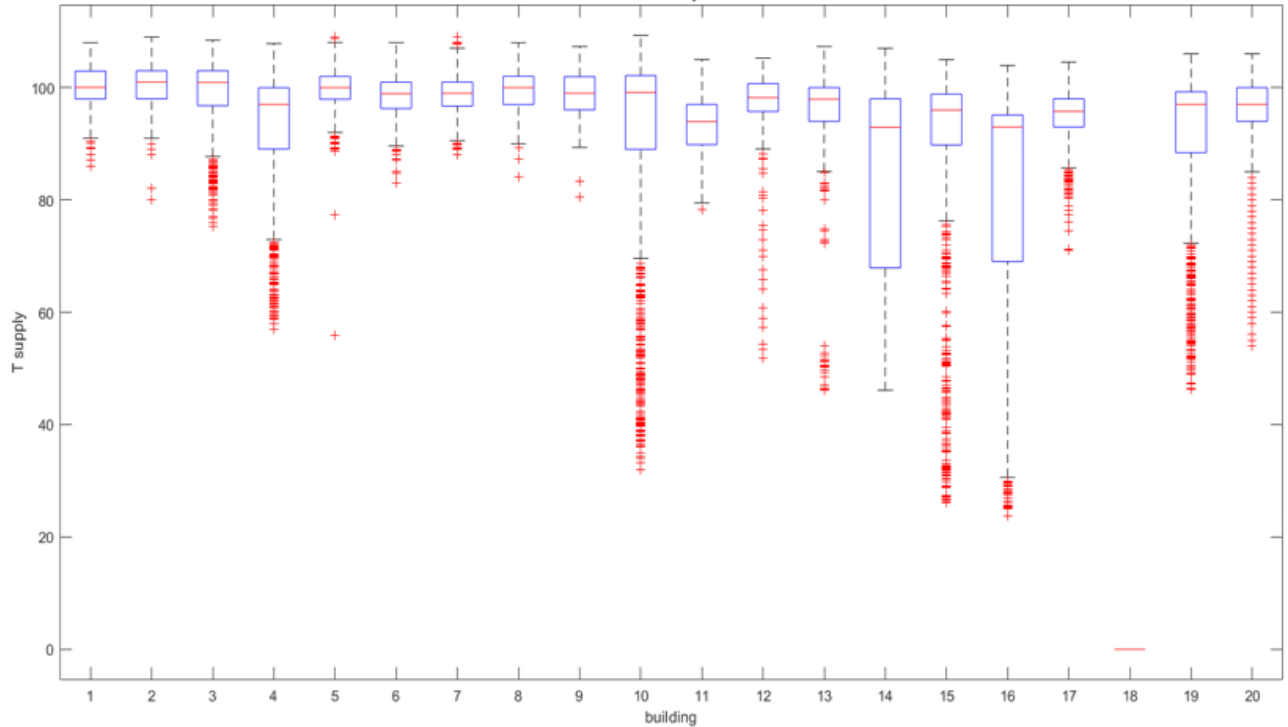


Figure 22 - Box Plot of supply primary temperature for every building in January.

It can be noted that in January the box plots, in addition to showing a higher temperature than the other graphs, have a reduced interquartile range. This is due to the fact that in that month the users will require heat for a longer time, decreasing the possibility of a decrease in temperature as a consequence of the lack of flow request.

As shown in figure 24, in the summer months the variability of the temperature parameter increases. In fact, in this season the buildings are often fed discontinuously according to the demand for domestic hot water. This leads to a significant decrease in the supply temperature measurement to the building during periods of non-power supply. This mechanism is easily identifiable in the box plot relating to building 19 where the out of layers represent the instants of heat request to the domestic hot water storage vessel.

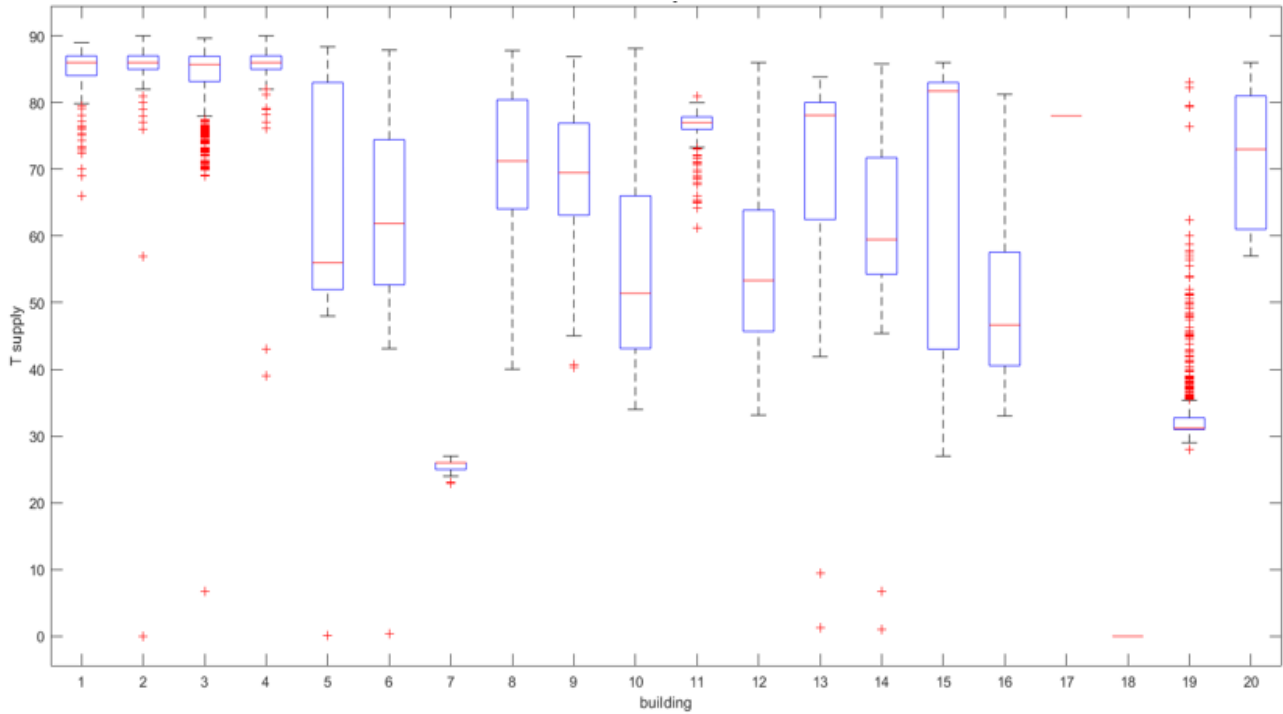


Figure 24 - Box Plot of supply primary temperature for every building in July.

As regards the return temperature, the rate of variability in the values is much higher. This is mainly due to the control logic of the controller that manages the heat exchanger as we will see in chapter 6.4.

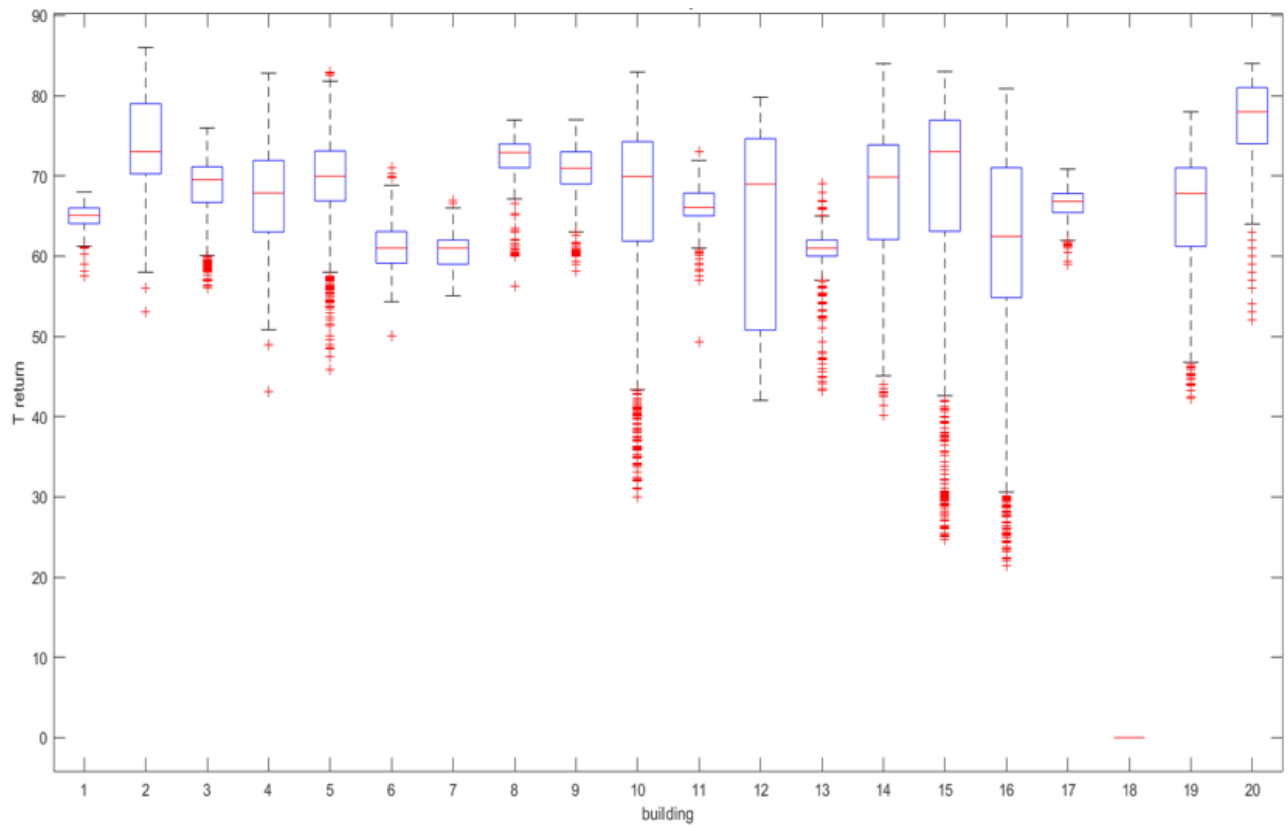


Figure 25 - Box Plot of return primary temperature for every building in January.

## 6. Model

This section presents the models implemented for the simulation of the district heating network starting from the analysis of the pipeline, of the boundary conditions and of the substations in hydraulic terms up to the thermal analysis.

### 6.1 Pipe Model (Hydraulic analysis)

In order to implement subsequent analyzes concerning the thermal analysis as well as for management simplicity, a new pipe model is created. Initially the pipe is modeled to manage only the hydraulic parameters without considering the thermal parameters. The conservation equations of interest are therefore the conservation of mass and the conservation of momentum:

$$\dot{m}_a + \dot{m}_b = 0 \quad (4)$$

$$der(I_s) = I_{b-flows} - F_{s,p} - F_{s,fg} \quad (5)$$

Where:

- $\dot{m}_a$  : is the mass flow-rate at node a;
- $\dot{m}_b$  : is the mass flow-rate at node b;
- $I_s$  : momentum [ $kg * \frac{m}{s}$ ];
- $I_{b-flows}$ : flow of momentum across boundaries [ $kg * \frac{m}{s^2}$ ];
- $F_{s,p}$  : pressure forces [ $kg * \frac{m}{s^2}$ ];
- $F_{s,fg}$  : friction and gravity forces [ $kg * \frac{m}{s^2}$ ].

The mass conservation does not take into account storage effect. If the user want to include the aforementioned effect a simple change of the model should be made.

The momentum equation could be written as:

$$\frac{d(\rho v A)}{dt} = -\frac{d(\rho v^2 A)}{dx} - A * \frac{dp}{dx} - (F_f + A \rho g \frac{dz}{dx}) \quad (6)$$

The  $I_{b-flows}$  term could be set equal to 0 as velocity and area of inlet and outlet node are the same and the gravity effect should be set to 0 as we are considering a closed circuit.

The friction pressure losses are determined through Haaland's formula:

$$\frac{1}{\sqrt{f}} = -1.8 * \log \left[ \left( \frac{\epsilon}{D} \right)^{1.1} + \frac{6.9}{Re} \right] \quad (7)$$

The following figures show a code excerpt:

```
F_fg = A_mean * dp_fg;
Ib_flow = 0;
F_p = A_mean * (Medium.pressure(state_b) - Medium.pressure(state_a));
dp_fg = 1/(-1.8*log10((rug/diameter/3.7)^1.11+6.9/
Modelica.Fluid.Pipes.BaseClasses.CharacteristicNumbers.ReynoldsNumber
(noEvent(abs(port_a.m_flow))/A_mean/d,d,Medium.dynamicViscosity
(state_a),Diameter)))^2 * Length/diameter*0.5*d*(m_flow/A_mean/d)^2;
```

For Momentum balance:

```
If momentumDynamics==Types.Dynamics.SteadyState then
  0 = Ib_flow - F_p - F_fg;
else
  Der(I) = Ib_flow - F_p - F_fg;
end if;
```

The following figure shows the component user interface. As we can see the interface is user-friendly (see chapter 4.1). In fact, the user only has to specify the roughness of the pipe, the length and the diameter.

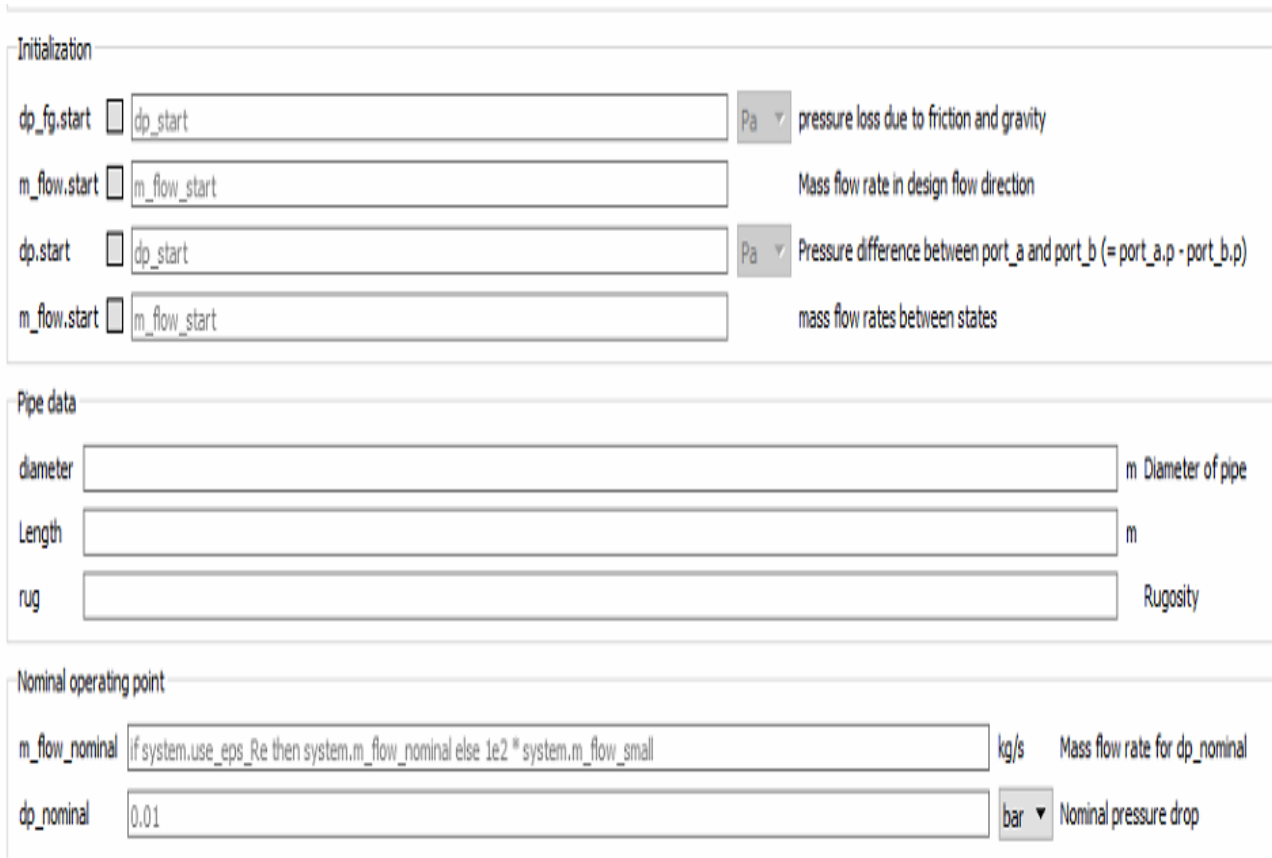


Figure 26 - User interface in OpenModelica of the created pipe.

### 6.1.1 Validation of the model

Before proceeding with the analysis of the case study, it is necessary to verify the effectiveness of the model used in modelling district heating networks.

To demonstrate the effectiveness of the software and components a reference case study has been implemented in *OpenModelica*. The exercise originally solved in *MATLAB* has been taken from Verda-Sciacovelli book [28].

The case study is a district heating network with multiple rings characterized by 14 users. The diameter of the pipes and the flow rate arriving at the users are known.

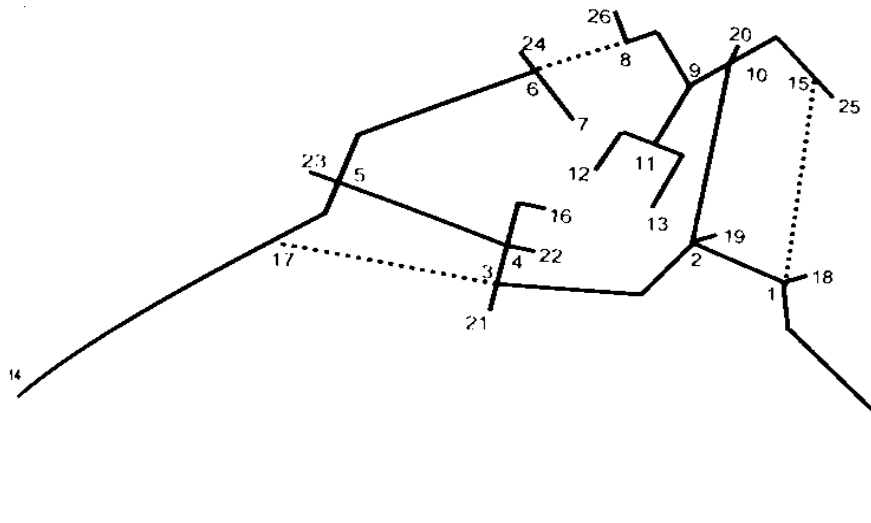


Figure 27 - DH network of the reference case. [28]

Figure 27 shows that the network including dotted lines forms a closed loop and so the components should be able to handle flow-reversal. In the following table the network data are reported:

Table 8 - Variables in the reference case.

BRANCH	L [m]	f [-]	sum( $\beta$ ) [-]	Dcom[mm]	G[kg/s]	Area[m <sup>2</sup> ]	v[m/s]
0-1	660	0.014	2.6	500	513.19	0.20	2.72
1-2	260	0.014	4	500	497.67	0.20	2.64
2-10	360	0.014	4	350	143.6	0.10	1.55
2-3	500	0.014	4.3	450	297.13	0.16	1.95
3-4	100	0.014	4	450	293.25	0.16	1.92
4-5	380	0.014	4	350	156.11	0.10	1.69
5-6	400	0.014	4.3	250	54.33	0.05	1.15
6-7	140	0.014	2	250	23.71	0.05	0.50
6-8	300	0.014	4	250		0.05	
8-9	180	0.014	3.8	250	28.46	0.05	0.60
9-10	60	0.014	4	250	88.4	0.05	1.88
9-11	180	0.014	4	250	59.94	0.05	1.27
11-12	160	0.014	2.9	250	27.6	0.05	0.59
11-13	120	0.014	2.9	250	32.34	0.05	0.69
5-17	180	0.014	4.3	75	31.05	0.00	7.32
4-16	240	0.014	2.9	300	78.92	0.07	1.16
10-15	330	0.014	4.9	50	18.97	0.00	10.06
1-15	380	0.014	4	250		0.05	
3-17	400	0.014	4	250		0.05	
17-14	720	0.014	2	250	31.05	0.05	0.66
1-18	20	0.014	2	125	15.52	0.01	1.32
2-19	20	0.014	2	250	56.92	0.05	1.21
10-20	20	0.014	2	250	36.22	0.05	0.77
3-21	20	0.014	2	75	3.88	0.00	0.91
4-22	20	0.014	2	250	58.21	0.05	1.24
5-23	50	0.014	2	250	70.72	0.05	1.50
6-24	50	0.014	2	250	30.61	0.05	0.65
15-25	50	0.014	2	125	18.97	0.01	1.61
8-26	70	0.014	2	250	28.46	0.05	0.60

Unlike the original exercise was made using a constant friction factor of 0.014, the model implemented in *OpenModelica* considers constant roughness. The determination of the roughness is made using the Colebrook formula for the first branch because there the mass flow rate is the highest and using  $f=0.014$ :

$$\varepsilon = \left( 10^{-\frac{1}{2\sqrt{f}}} - \frac{2.51}{Re * \sqrt{f}} \right) * 3.7 * D \quad (8)$$

The calculations shows an equivalent roughness of 0.1086 mm. It should be noted that since the exercise to be performed with  $f = \text{constant} = 0.014$ , the roughness of each pipe should be varied to achieve the desired coefficient of friction. The selected approach considers the roughness of the pipes as constant.

In order to test the effectiveness of both the calculation of pressure losses and the management of flow-reversal the created component has been tested through the reference exercise [28] :

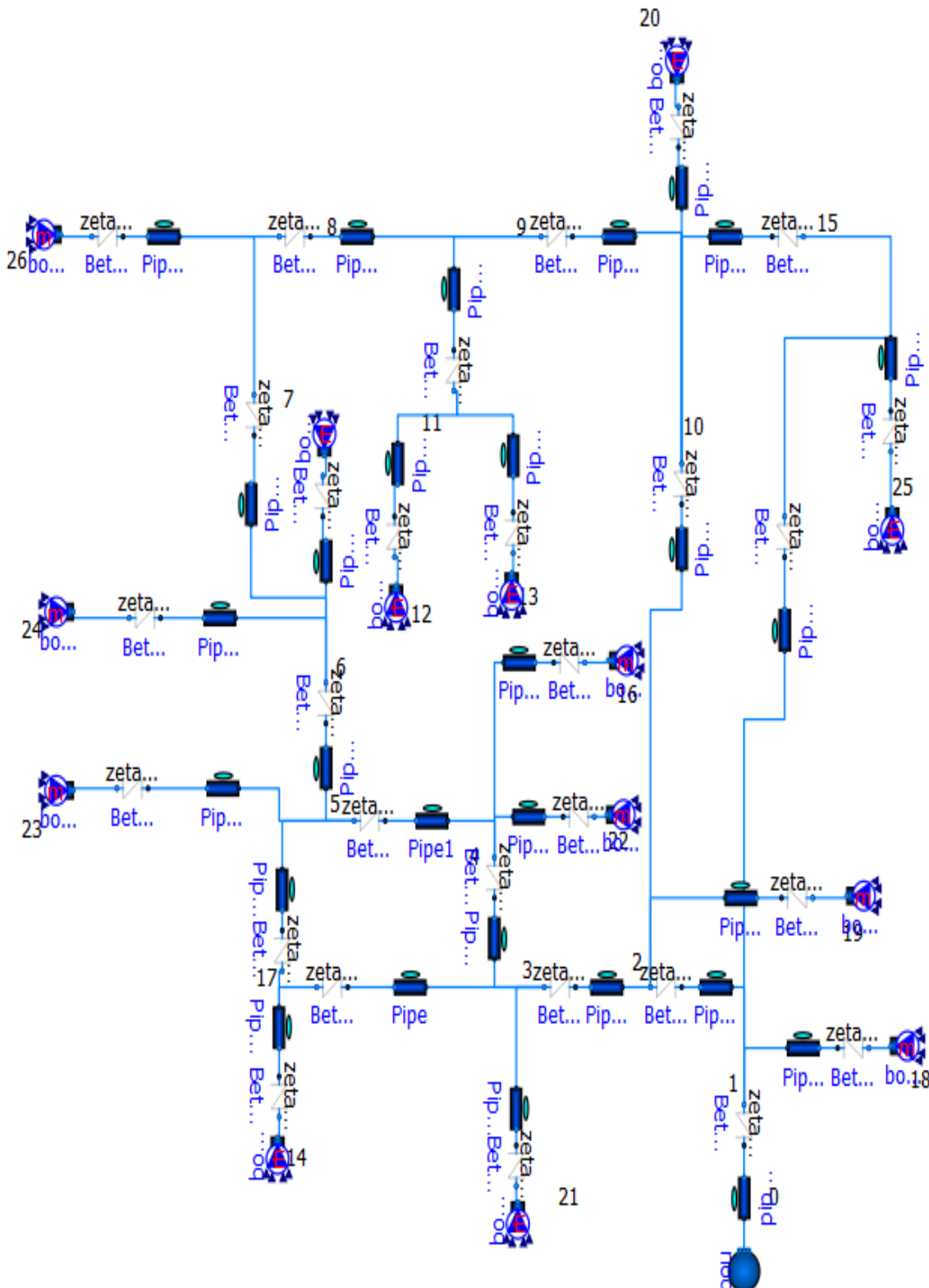


Figure 28 - Diagram view in OpenModelica of the reference exercise using the created pipe.

The figure below shows the pressure at the various nodes of the network. Except for small deviations due to the assumption on the roughness the results obtained are practically identical to those reported in the original exercise performed in *MATLAB* environment.

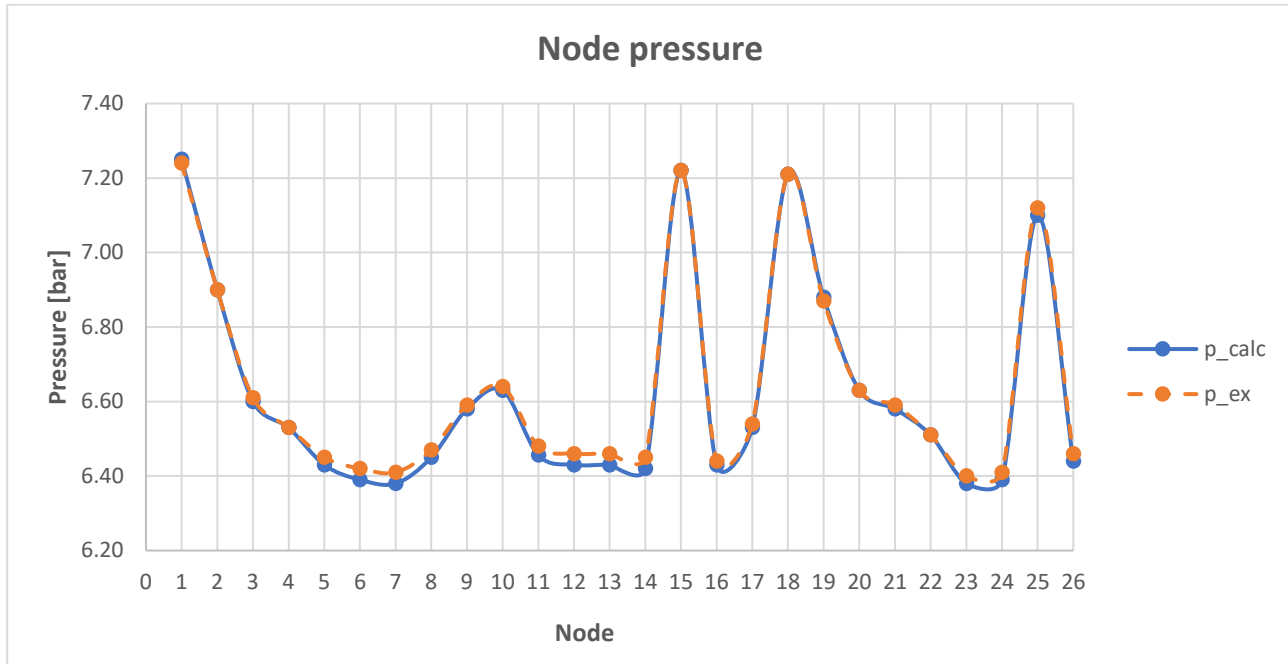


Figure 29 - Pressure vs node for the reference exercise calculated with the new pipe and from the reference.

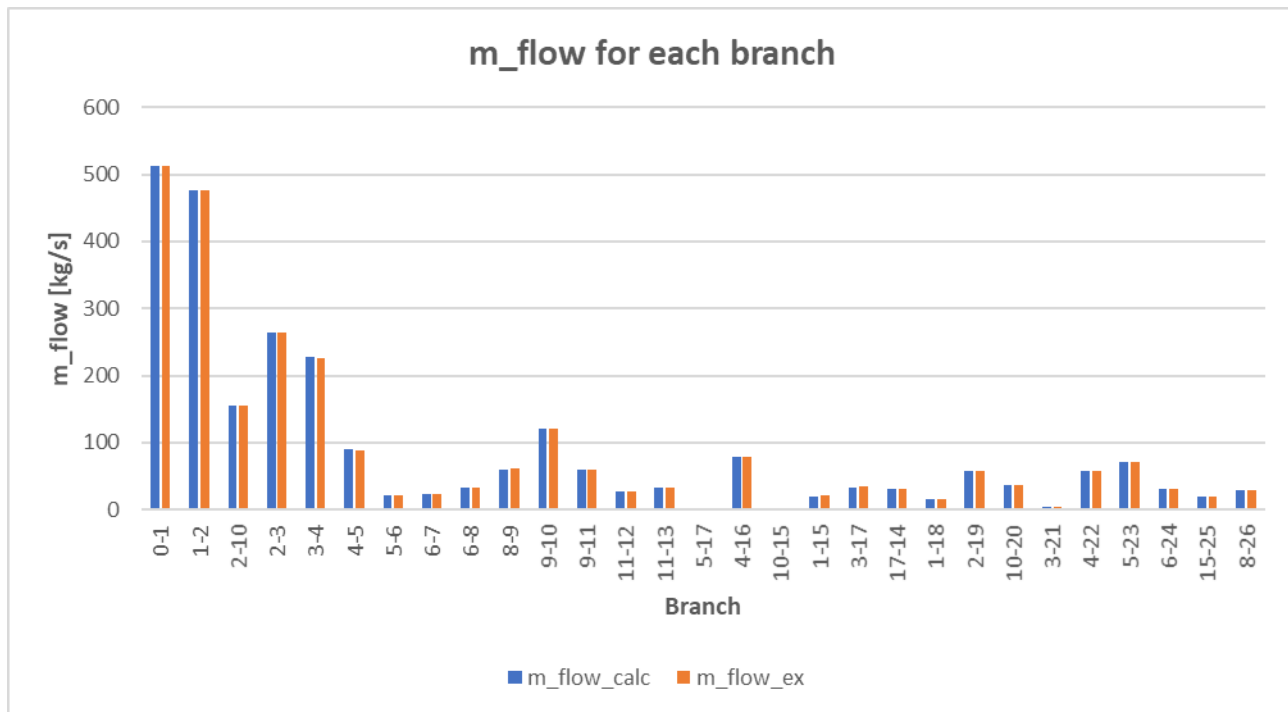


Figure 30 - Mass flow-rate for each branch in the reference exercise and calculated with the new pipe.

Furthermore a comparison with the results obtained in the same network using static pipe has been made:

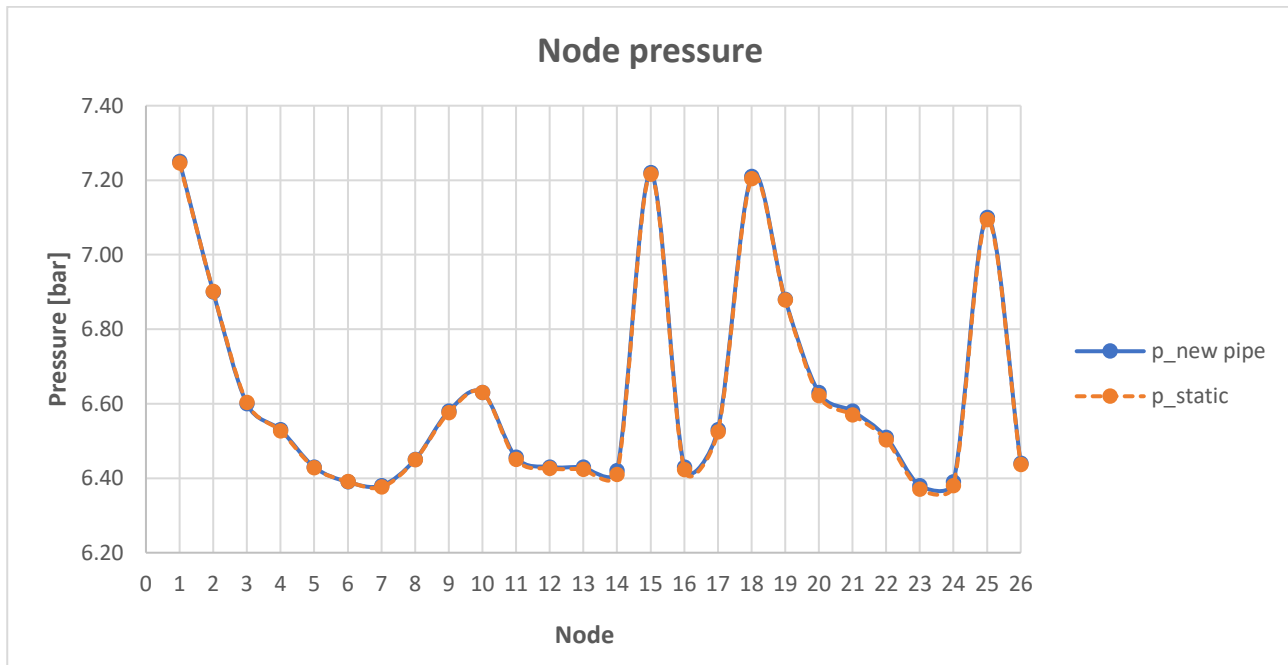


Figure 31 - Pressure vs node for the reference case using created pipe and using static pipe.

The results show an almost perfect match confirming that the gap from the original exercise data is solely due to the roughness hypothesis. The component created is able to handle flow-reversal and the result obtained are coherent, as a consequence we can assume the component appropriate to simulate district heating network.

It is possible to consider the component validated for hydraulic calculations.

## 6.2 Boundary conditions of the model

The *Modelica* model requires specific boundary conditions as input. In fact, like all hydraulic circuits, the pressure differential determines the flow rate circulating in the network. The pressure boundary conditions will not be fixed but will vary according to the oscillations in the operation of the network due to the variability of the loads. Furthermore, a constraint is necessary for the temperature entering the batch under analysis.

Since only one pressure measurement point is available for the batch analyzed, which is not positioned at the beginning of the batch, the known value must be used to return to initial conditions at the entry point using the back-modeling technique.

The figure shows the batch dwg including the pressure measurement point highlighted with a red circle.



Figure 32 - AutoCAD plan of the portion of the district heating under analysis.

Knowing the diameter of the pipes and their lengths as well as the curves and T-joints the model is able to determine both linear and concentrated pressure losses.

Two *Modelica* models were implemented, one for the supply and one for the return, in order to evaluate the value of supply and return pressure at the inlet/outlet point. Furthermore, for these models it is necessary to know the flows passing through the network which enter the model through boundary conditions entering or leaving the buildings.

From the model it is possible to see how the measuring point is a pressure boundary condition and the other boundary conditions are the mass flows to the various buildings:



Mass flow-rate boundary used for each building.



Pressure boundary at measuring point.

a) Supply Model

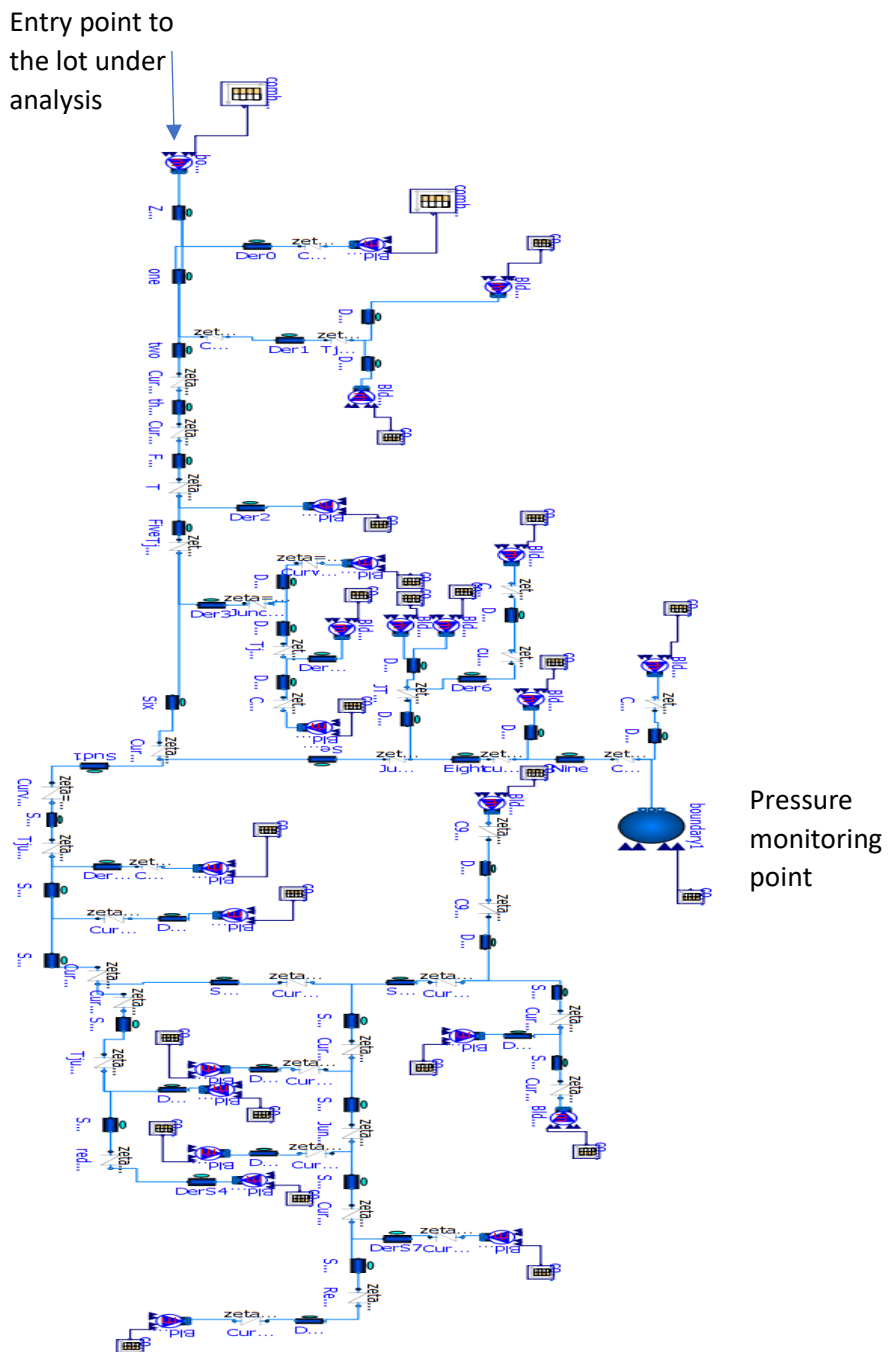


*Figure 33 - Diagram view in OpenModelica of the supply network under analysis.*

Pressure boundary is an existing component (*Modelica Standard Library*) that is used to set the pressure at different points of the network. In this model, the pressure constraint is positioned in the only point of the network where the pressure measurement is available while the boundary condition at the users' level is set as given mass flow, which is provided by the monitoring data.

Mass flow sources prescribe a certain mass flow at various points in the network. From the mass flows the model calculates the pressure required to obtain the given mass flow. Hence, the pressure required will depend not only on the constraint flow but also on the constraint in pressure. The drawback of a mass flow constraint is that instead of having a system where the valve controls the flow by managing the pressure drop the mass flow is provided by the boundary. Moreover the use of mass constraints often requires higher calculation times since it is necessary to add the mass flow of each user in relation to the different load profiles (an example from this network is given by the mass flow source near linked to the first pipe of the network that is the sum of all the mass-flows in the network). The decision to use a model of this type to return to an expression under pressure is therefore a winning choice.

As the model calculates the pressure required to obtain given mass flow, the calculated pressure values at the entry point to the lot of buildings could be determined. After having determined these values it was possible to formulate a correlation that links the inlet flow with the supply pressure to the lot itself:

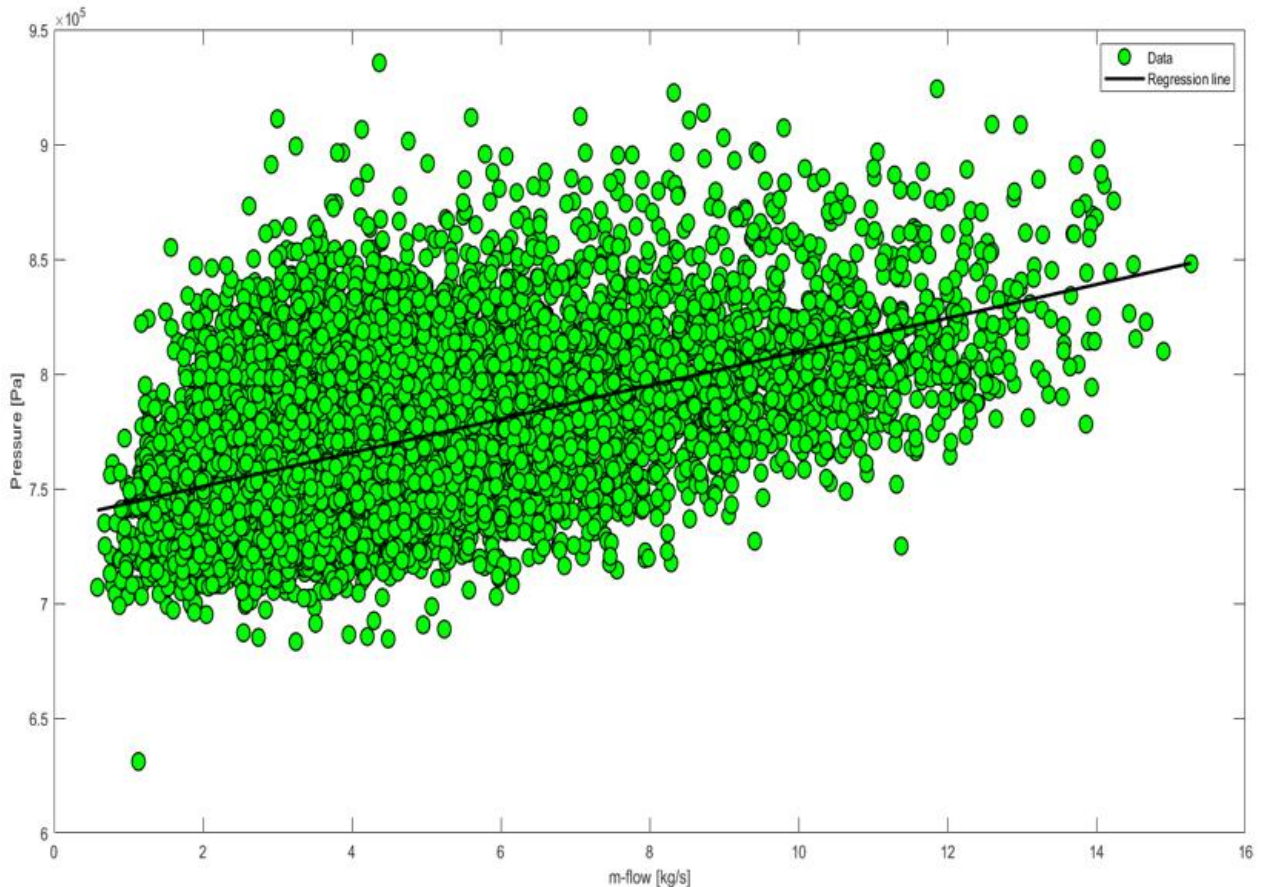


Figure 34 - Pressure at the inlet of the network vs mass-flow entering in it.

$$p = 7333 m_{flow} + 7.36 e^5 \quad (9)$$

The same approach was used for the return network:

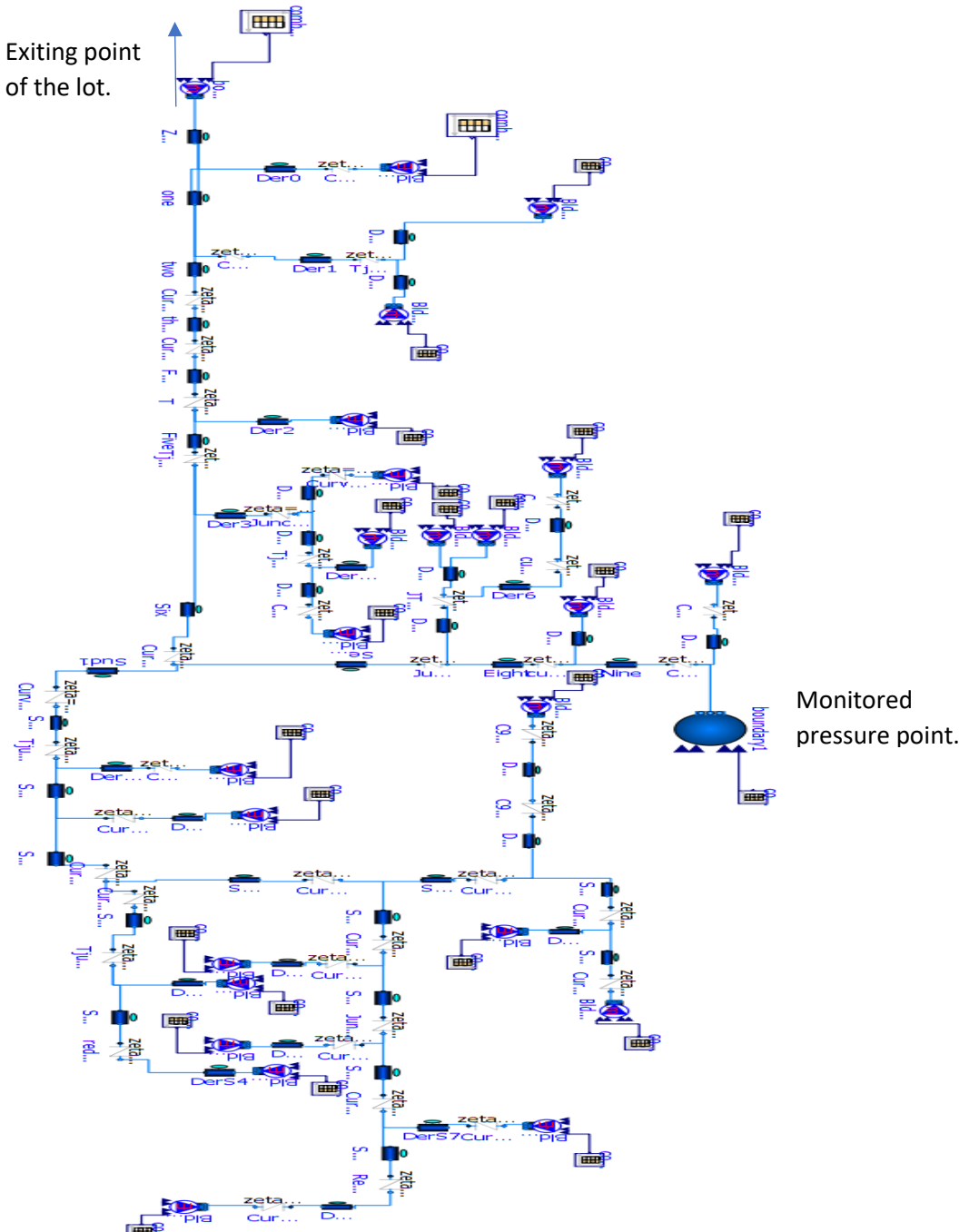


Figure 35 - Diagram view in OpenModelica of the return network under analysis.

The only difference from the previous model (the one for the supply) is that the mass flows are exiting the buildings rather than entering and the constraint in pressure is that of the return.

Using the pressure values at the entry point to the lot, it was possible to formulate a correlation that links the outlet flow with the return

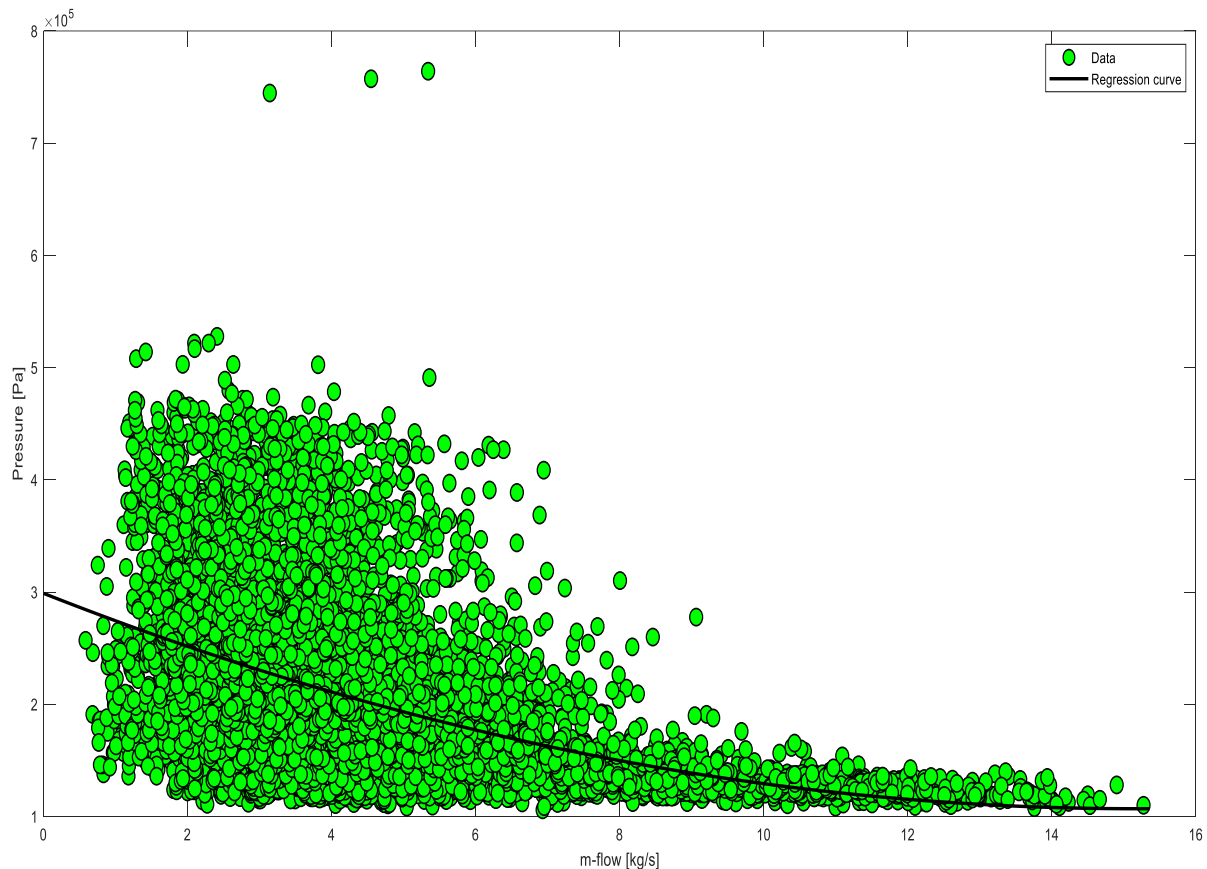


Figure 36 - Pressure exiting the lot vs mass flow.

$$p = 833.2 m_{flow}^2 - 2.529 e^4 m_{flow} + 2.9883 e^5 \quad (10)$$

### 6.3 Boundary condition testing

Following the correlations obtained through regression, the one obtained through the latter was used as the pressure boundary condition of the model. The other boundary conditions based on mass-flow affect the primary flow rates for each building at each time step.

Compared to the model described previously, we note how the flow constraint of the previous model has become a pressure constraint. Furthermore, the constraint on the measuring point which has become our "benchmark" is no longer present. The aim is to check whether the results at the measuring point are comparable to the real ones.

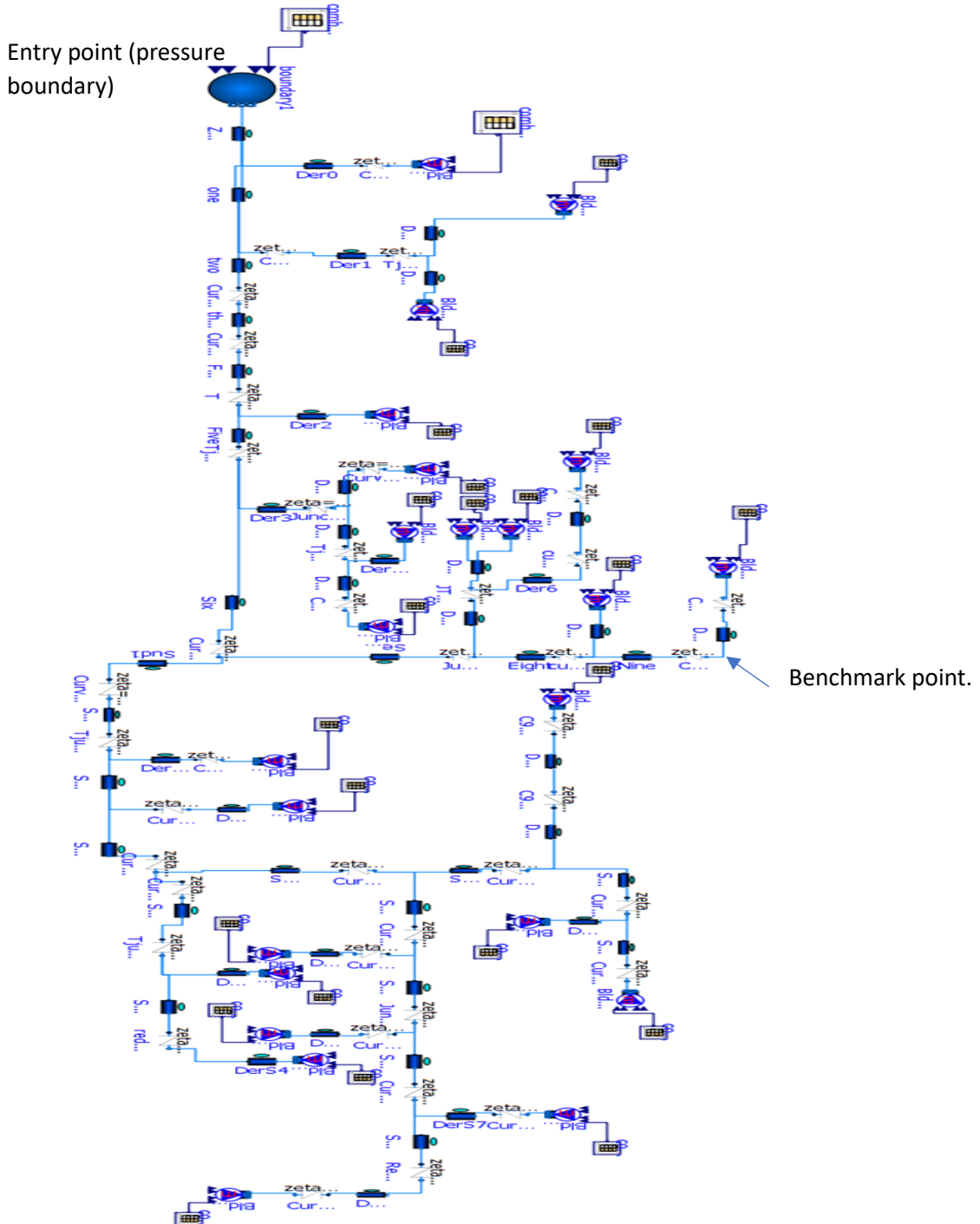


Figure 37 - Diagram view in OpenModelica of the boundary conditions testing model.

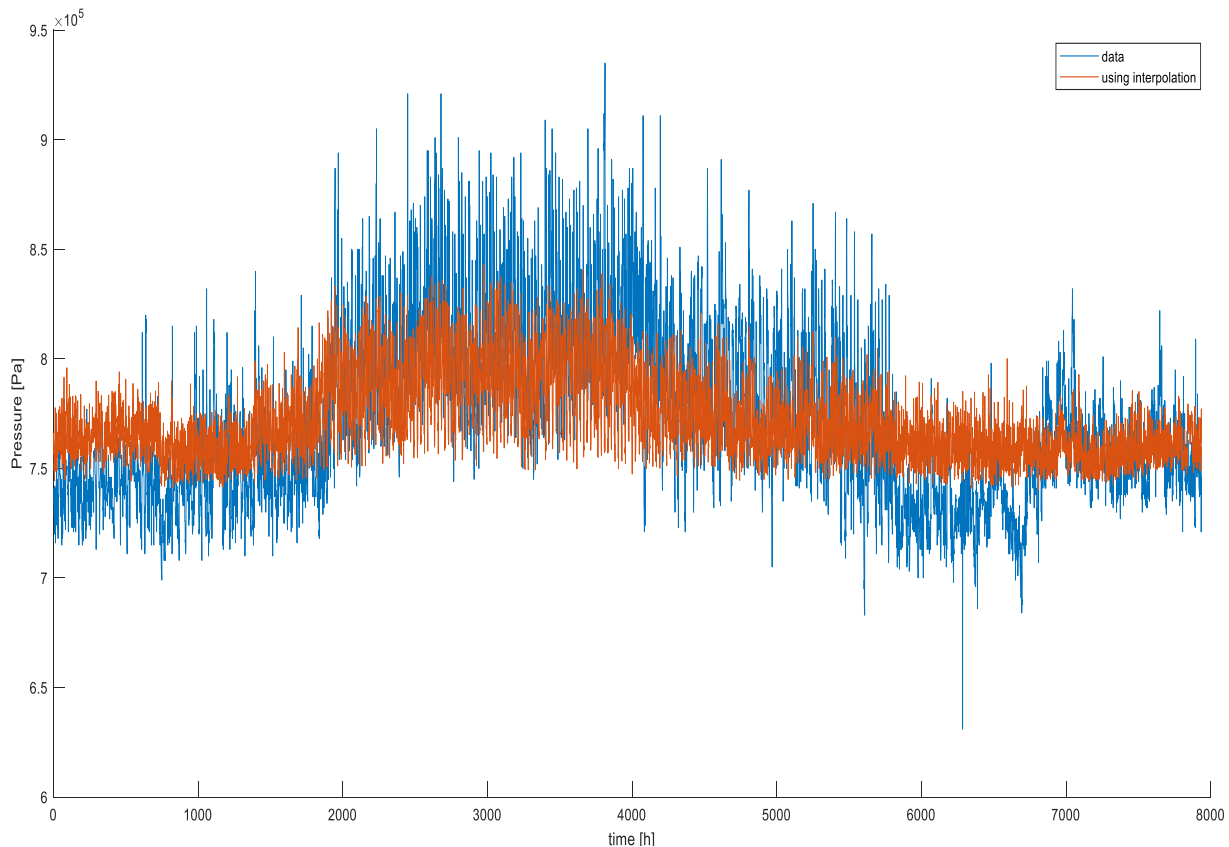


Figure 38 - Measured and modelled pressure at measuring point vs time.

The two curves, although presenting a similar trend, are strongly staggered. In particular, the resulting interpolated curve is particularly flattened with respect to the data.

This is due to the **large dispersion of pressure data** as the inlet flow varies. The dispersion is due to the fact that for the same flow rate the losses are different in relation to the users that require power and to the variation of the input data.

To show the data dispersion at measuring point a graph reporting measured pressure value versus mass flow-rate is shown in figure 39.

From this figure we can see how the dispersion of the data is mainly due to the variation of the measurement point. This is due to the fact that by evaluating a portion of the network, the average pressure in the network can vary with the heating demands upstream and downstream (not analyzed).

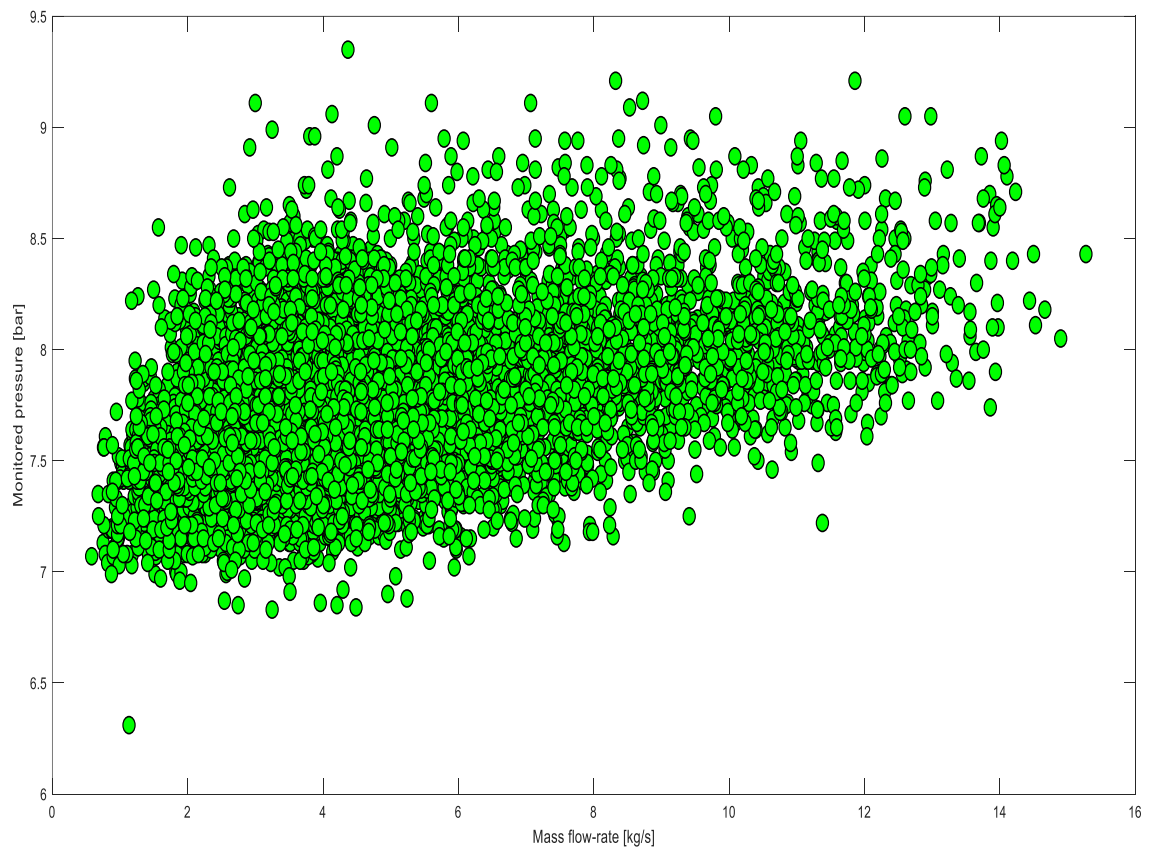


*Figure 39 - Measured pressure vs mass flow-rate in the measure point from monitored data.*

It is evident that the dispersion is mainly linked to the monitoring data as the pressure losses in the portion of the network analyzed are of minor entity.

It is evident that by simulating only a portion of the network this approximation is necessary.

## 6.4 Analysis of the heat exchange substation

The substation in district heating networks consist of three major parts: a valve, a heat exchanger and a controller. The controller regulates the mass flow into the consumer to ensure that the heat demand is met by acting on the valve. The mass flow into the consumer depends on the differential pressure between the supply and return pipes associated to the substation. The heating flow rate corresponding to a certain mass flow is also dependent on the temperature difference of the thermal fluid upstream and downstream the heat exchanger. The heat flow rate is given by equation 11 :

$$PP = m_{flow} * c_p * (T_s - T_r) \quad (11)$$

Different approaches have been tested to define the flow through the substation:

- a) Correlation between heat load and mass-flow-rate;
- b) Correlation between outside temperature and mass-flow-rate;
- c) Correlation between outside temperature, power and mass-flow-rate;
- d) Correlation between supply temperature to the secondary, power and mass flow.

- a) The first valve control equation tested is based on the power parameter only. This type of control is effective only in the case in which the delivery and return temperatures assume approximately constant values as we can see in equation 11.  
If we look at the following figures we note, in fact, that the curve follows the trend of the real values but has a large dispersion:

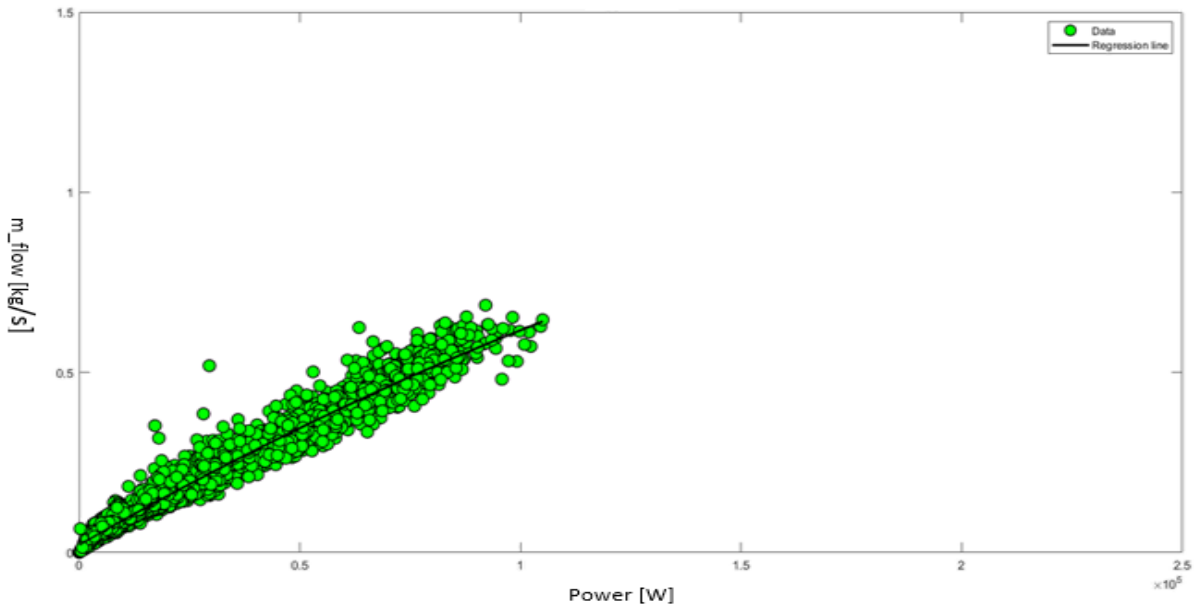


Figure 40 - Regression curve, mass flow-rate vs power for a building.

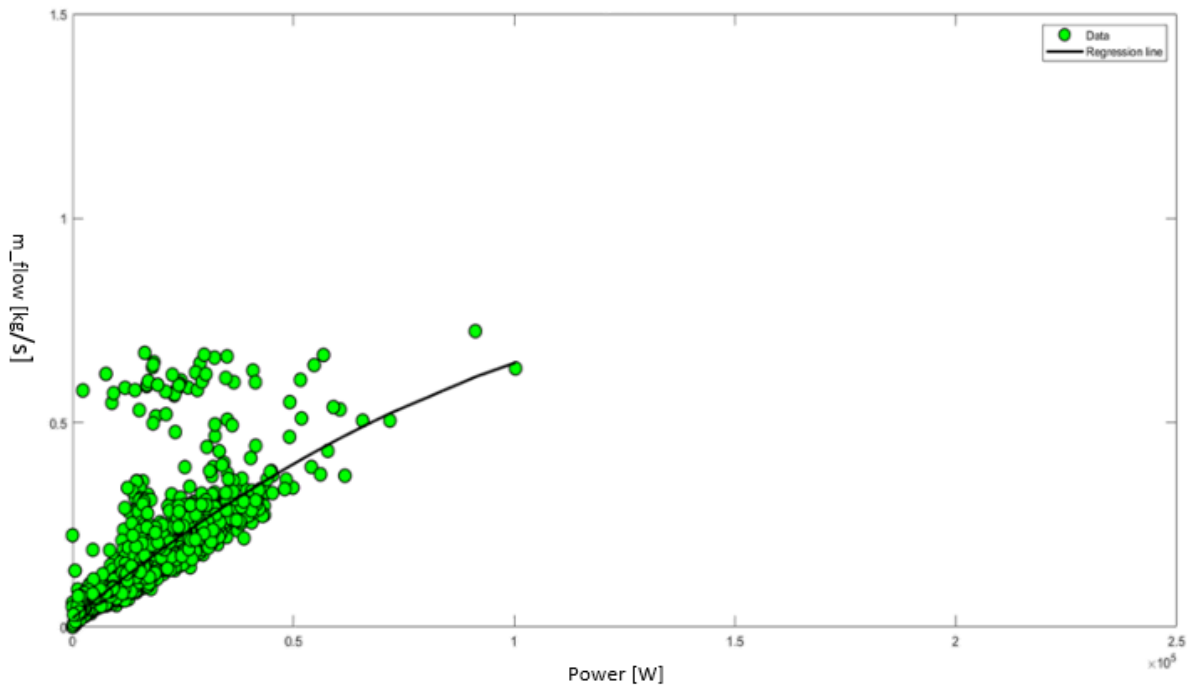


Figure 41 - Regression curve, mass flow-rate vs power for a building.

It is therefore evident that this approach is not adequate for our interests.

- b) The second type of valve control tested is based on the outside temperature.

Also in this case, the dispersion of the data is very large as the parameter does not consider the stochastic changes in load related to the domestic hot water service and also does not consider the temperature difference to primary.

Looking figure 42 we see that this approach is not satisfactory:

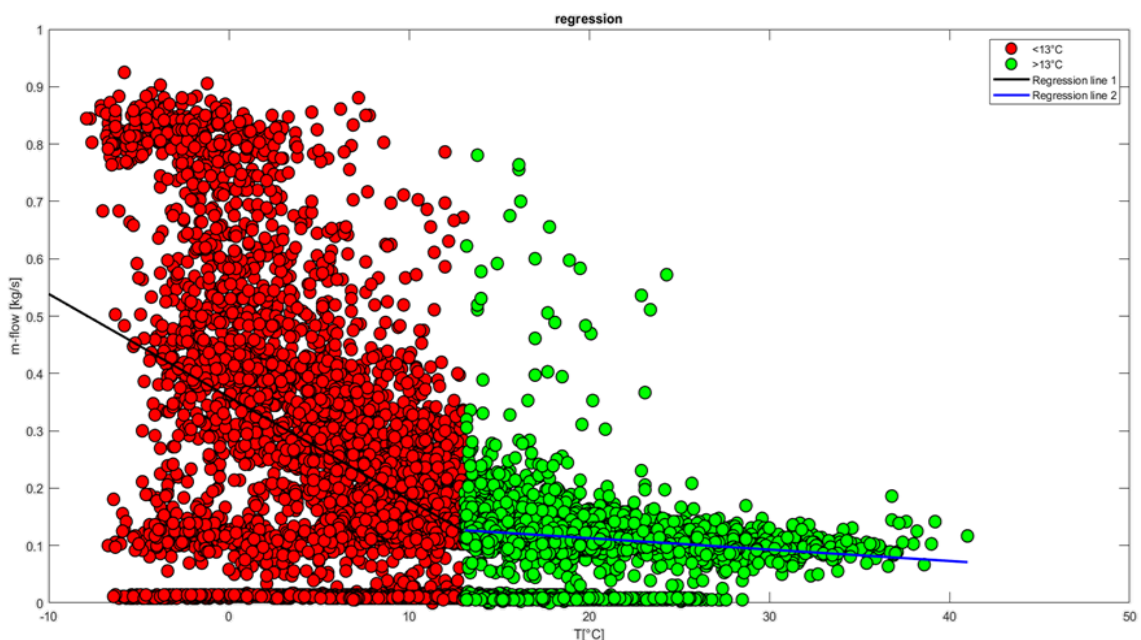


Figure 42 - Regression mass flow-rate vs outside temperature for a building.

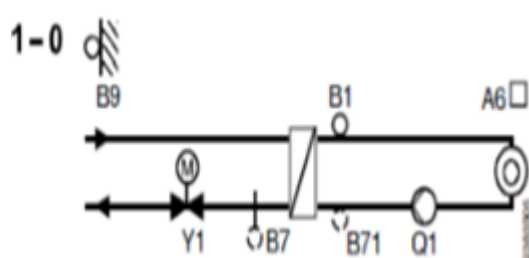
- c) The third type of valve control tested considers both the influence of external temperature and power. In this way, both the variable that manages the delivery temperature to the secondary is controlled through the climatic curve and the stochasticity of the domestic hot water needs through the power parameter.

The controllers used by the network are RVD230 and RVD250 Siemens [29].

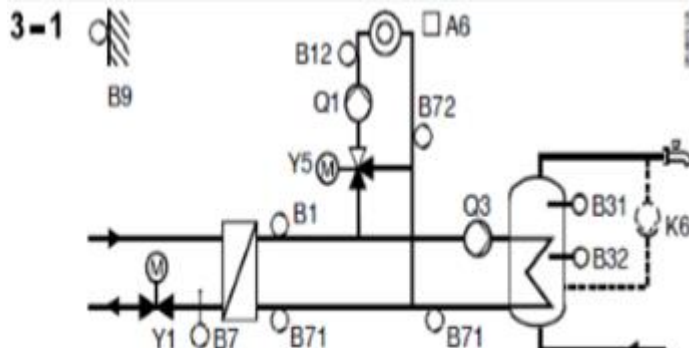
The RVD is a multifunction control unit that supervises the flow temperature of a heating circuit and a DHW system.

- The functionality of the controller covers only the types of systems with direct connection to the district heating circuit. It has been specifically designed for small to medium-sized residential systems and for non-residential systems.
- The RVD230 has 7 heating plants and 11 pre-loaded DHW plants. By combining the different plants together, it is possible to configure 28 different types of plants.

The types of plants present in the analyzed network are:



A6	Room unit
B1	Heating circuit supply temperature sensor
B7	Primary return temperature sensor
B71	Secondary return temperature sensor
B9	Outside temperature sensor
Q1	Circulator of heating circuit
Y1	Motorized 2-way valve



A6	Room unit
B1	Common temperature sensor
B12	Heating circuit supply temperature sensor
B31	Storage temperature sensor 1
B32	Storage temperature sensor 2
B7	Primary return temperature sensor
B71	Secondary return temperature sensor or D.H.W return
B72	Heating circuit return temperature sensor
B9	Outside temperature sensor
K6	Circulating pump (optional)
Q1	Circulator of heating circuit
Q3	Intermediate circulator for D.H.W circuit
Y1	Motorized 2-way valve
Y5	Heating circuit mixing valve

Figure 43 - Different types of substation adopted in the network under analysis.

The controller sets the delivery temperature to the secondary through the use of a climatic curve dependent on the external temperature.

On the basis of the known configurations, the different climatic curves for each building were generated. An example is shown below:

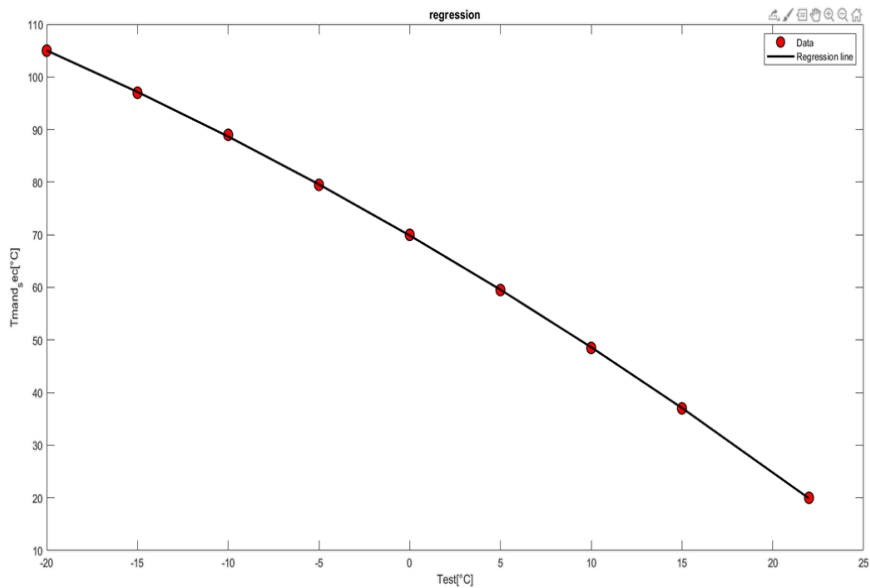


Figure 44 - Climatic curve for one substation controller.

Furthermore, the controller imposes a limitation of the maximum return temperature to the primary. This control is carried out aiming at reducing heat dissipation. The lower the return temperature the lower the heat dissipation through return circuit.

The type of control is shown in the diagram:

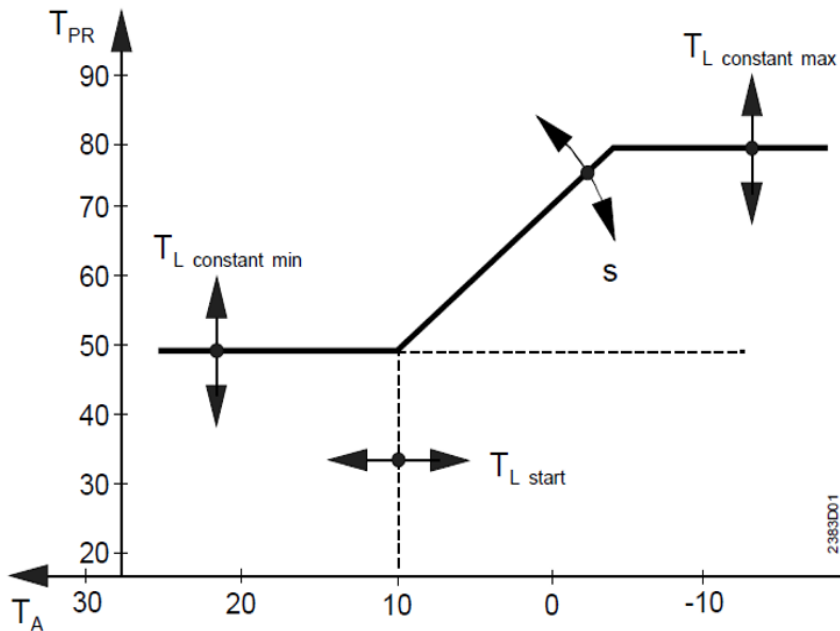


Figure 45 - Graph explaining the return temperature control at primary side.

Where:

- $T_A$  : Outside temperature [ $^{\circ}\text{C}$ ];
- $T_{PR}$  : Return temperature at primary side [ $^{\circ}\text{C}$ ];

The current limit value is determined as follows:

- If the outdoor temperature is higher than or equal to the compensation start value ( $T_{L\ start}$ ), the current limit value is the constant  $T_{L\ constant\ min}$ .
- If the outdoor temperature is lower than the compensation start value ( $T_{L\ start}$ ), the current limit value is calculated entering the curve in figure 45.

In any case, the current value of the  $T_L$  limit cannot be greater than the upper limit value.

Considering a correlation that links the mass flow with the external temperature and the power, the physical properties of the problem are summarized in the interpolating parameters.

In particular:

- ❖ The outdoor temperature parameter is a reflection of the supply temperature to the secondary as well as the maximum return to primary temperature limit;
- ❖ The power parameter contains information related to the flow rate and temperature delta in the secondary, as well as the user's DHW request.

Interpolating surfaces were then developed taking into account the three above-mentioned parameters. The interpolating equations are shown in the following tables:

Table 9 - Interpolation equation of substations control for all the different buildings.

$$m_{flow} = K[1] + K[2] * T_{out} + K[3] * PP + K[4] * PP * T_{out}$$

Building	K1	K2	K3	K4
<b>10243</b>	2.29E-02	2.60E-05	5.08E-06	1.80E-07
<b>10165</b>	2.16E-01	-6.59E-04	4.08E-06	1.92E-07
<b>10162</b>	1.95E-02	4.75E-04	6.53E-06	1.12E-07
<b>10158</b>	-5.86E-02	2.30E-03	8.71E-06	2.26E-07
<b>10157</b>	-1.87E-02	6.30E-04	5.78E-06	2.12E-07
<b>10110</b>	-1.60E-03	1.05E-04	6.19E-06	5.63E-08
<b>10264</b>	7.23E-02	-1.40E-03	4.91E-06	4.26E-07
<b>10241</b>	5.15E-02	-4.72E-04	4.76E-06	4.30E-07
<b>10245</b>	1.61E-02	-1.20E-04	4.83E-06	4.00E-07
<b>10552</b>	-3.88E-02	1.70E-03	7.78E-06	3.52E-07
<b>10551</b>	2.55E-02	-2.36E-04	5.66E-06	6.30E-08
<b>10164</b>	-3.60E-03	6.63E-04	8.73E-06	2.85E-07
<b>10549</b>	8.60E-03	-2.94E-04	8.84E-06	2.84E-07
<b>10163</b>	-2.50E-02	1.20E-03	7.48E-06	5.96E-07
<b>10545</b>	2.57E-02	-5.43E-04	1.48E-06	8.65E-07
<b>10521</b>	-1.12E-02	3.76E-04	7.94E-06	1.34E-07
<b>10224</b>	6.60E-02	-2.00E-03	8.06E-06	5.33E-07
<b>10263</b>	-6.90E-03	1.70E-03	6.47E-06	3.10E-07

By way of example, the graph of the interpolating surface with respect to the real points for a building is shown below:

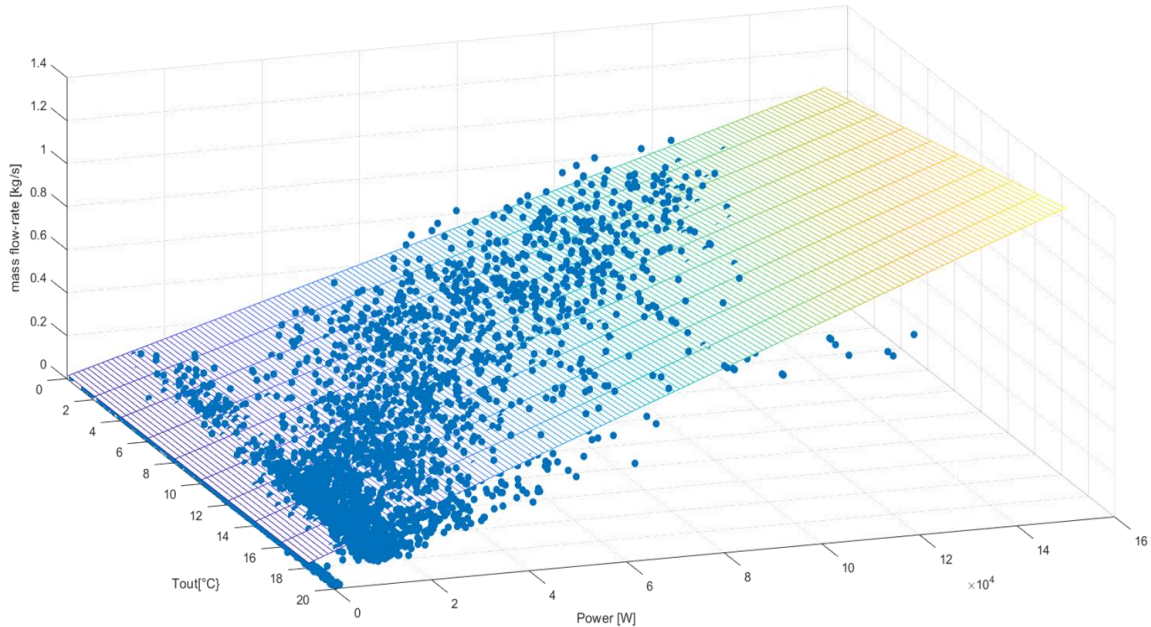


Figure 46 - Interpolating surface for a building

We can see how the surface interpolates the real data in a good way. At this point it is necessary to create components in *OpenModelica* capable of managing the valve control as well as the heat exchange to the exchanger:

- **Valve model:**

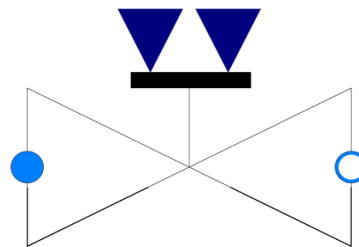


Figure 47 - Icon view of valve model implemented in OpenModelica..

The valve component acquires as input the external temperature and the power exchanged at the substation and uses them to define the flow-through and therefore the necessary pressure drop. *Modelica* requires flow through components and connectors. The component was then implemented in such a way as to be able to handle near-zero flow conditions.

Mass flow is defined according to the equation:

$$m_{flow} = K[1] + K[2] * T_{out} + K[3] * PP + K[4] * PP * T_{out} \quad (12)$$

Where:

- $K[1], K[2], K[3], K[4]$  are the coefficients of the interpolation equation;
- $T_{out}$  is the outside temperature;
- $PP$  is the exchanged power at the substation.

The user view of the component looks like this:

## Parameters

General	Assumptions	Advanced	Modifiers
<b>Component</b> Name: valveLinear_me4			
<b>Class</b> Path: ValveLinear_me4 Comment: Valve for water/steam flows with linear pressure drop			
<b>Initialization</b> m_flow.start <input type="text"/> m_flow_start <span style="float: right;">Mass flow rate in design flow direction</span> dp.start <input type="text"/> dp_start <span style="float: right;">Pa <input type="button" value="▼"/> Pressure difference between port_a and port_b (= port_a.p - port_b.p)</span>			
<b>Coefficients</b> coefficient <input type="text"/> coefficient <span style="float: right;">b1 b2 b3 b4</span>			

Figure 48 - User view of valve model created in OpenModelica.

- **Heat exchanger:**

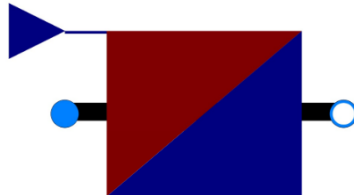


Figure 49 - Icon view of heat exchanger model implemented in OpenModelica.

The heat exchanger component, starting from the input power information and the mass flow rate managed by the valve, causes a loss of heat and therefore of fluid temperature. It is also possible to set a nominal pressure drop of the component starting from which the latter proportionally processes the pressure drop for each different flow through.

A code excerpt is reported below:

```

hSet = Q_flow / m_flow + instream(port_a.h_outflow);
Xi_instream=instream(port_a.Xi_outflow);
port_a.h_outflow = instream(port_b.h_outflow);
port_b.h_outflow = hSet;
F_fg = A_mean * dp_fg;

```

- **Substation Model**

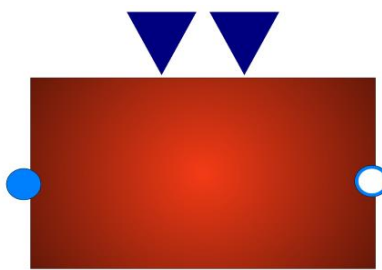


Figure 50 - Icon view of substation model created in OpenModelica.

The substation component incorporates the previous two models for a better graphical display as well as a more usable user interface. In fact, only the parameters of the coefficients and of the nominal pressure and mass flow and initial temperature are required from the user as we can see in the following figure:

## Parameters

General    Modifiers

Component  
Name: exc2

Class  
Path: exc2  
Comment:

Coefficients  
coefficient  b1 b2 b3 b4

Exchanger  
m\_flow\_nominal  kg/s  
dp\_nominal  Pa  
T\_start  K

Figure 51 - User interface for substation model created in OpenModelica.

- d) Since it is possible to determine the delivery temperature to the secondary on the basis of the external temperature through the climatic curve (see figure 44), an interpolation surface has been created which, instead of considering the external temperature as a parameter, considers the delivery temperature to the secondary. It should be noted that this temperature has minimum limits below which the climatic curve is not considered and, in this case, the temperature value in delivery to the secondary is set equal to the limit. The imposition of this limit means that for almost all the buildings under analysis the temperature is equal to the constraint as already shown in the graphs analyzed in chapter 5.1. The following graph shows the interpolation surface for a building:

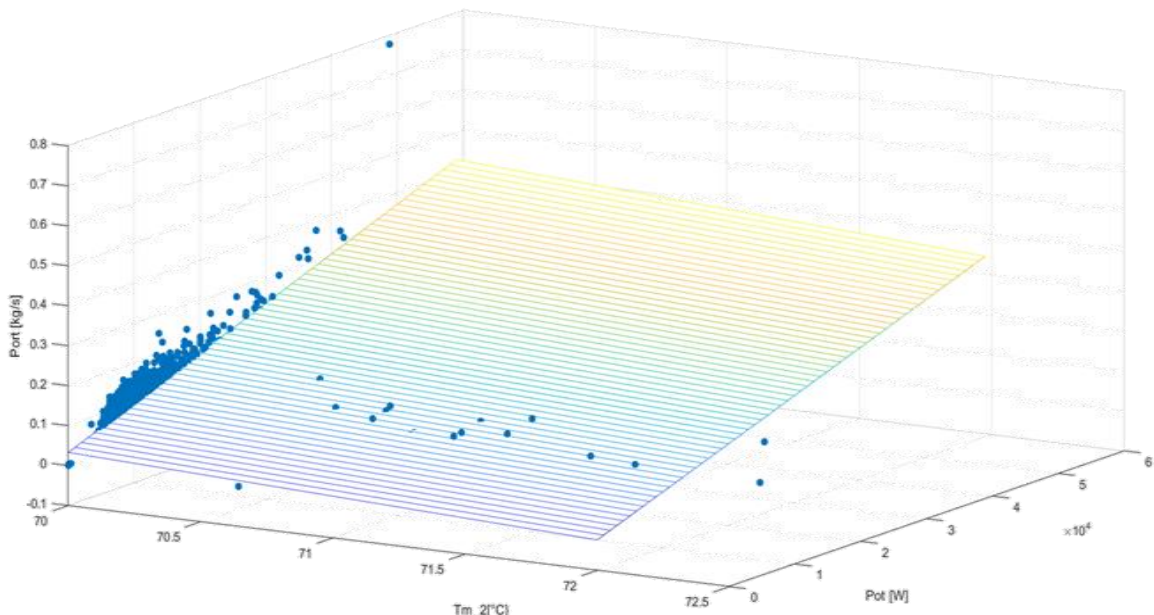


Figure 52 - Interpolating surface mass flow-rate vs power and secondary supply temperature.

Figure 52 shows how for most cases the temperature is equal to the limit, leading to results similar to those obtained with the a) approach already described, which proved to be not effective.

It is therefore possible to say that with the data provided, approach c) is the one that best simulates the actual behavior of the network.

## 6.5 Network Model

Based on the assumptions described and using the specially created components, the complete model of the portion of the network under analysis was developed. As regards the distribution part, the pipes have been modeled according to the indications described in chapter 4.1 and using the Haaland pipe model described in chapter 6.1 while for the substation the model just described has been used.

The boundary conditions are those obtained through the hydraulic analysis described in chapter 6.2 both for supply and return. We can see that unlike the previous models there are only two boundary conditions, supply pressure and return pressure specifically. Supply and return pressure are the variables that determine the dynamics of the mass flow (see chapter 4.1).

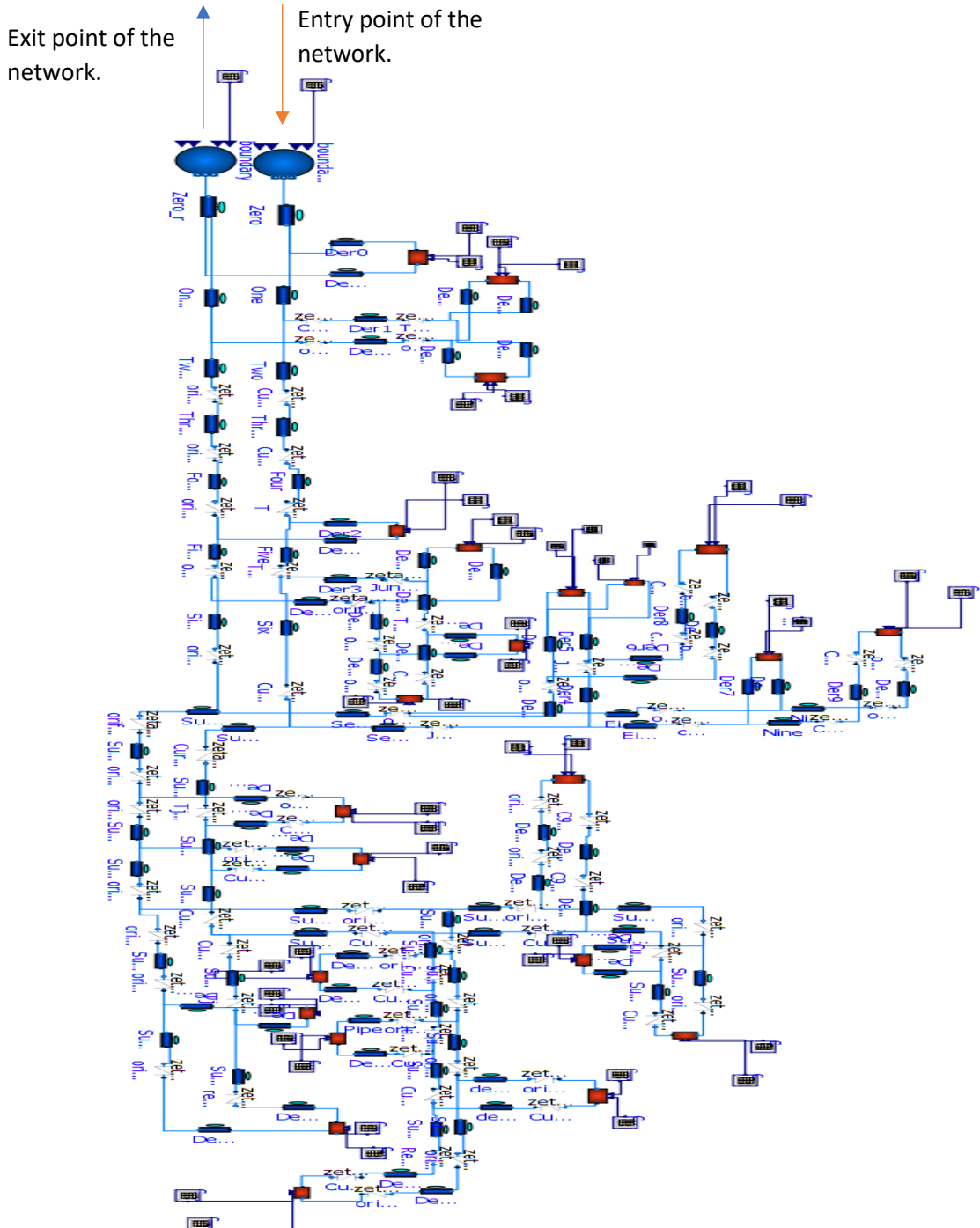


*Figure 53 - Diagram view in OpenModelica of the entire simulated network.*

Through the simulation of the entire hydraulic model the deviation between the simulated flow value compared to the real value is then evaluated.

The results are plotted by means of a box plot:

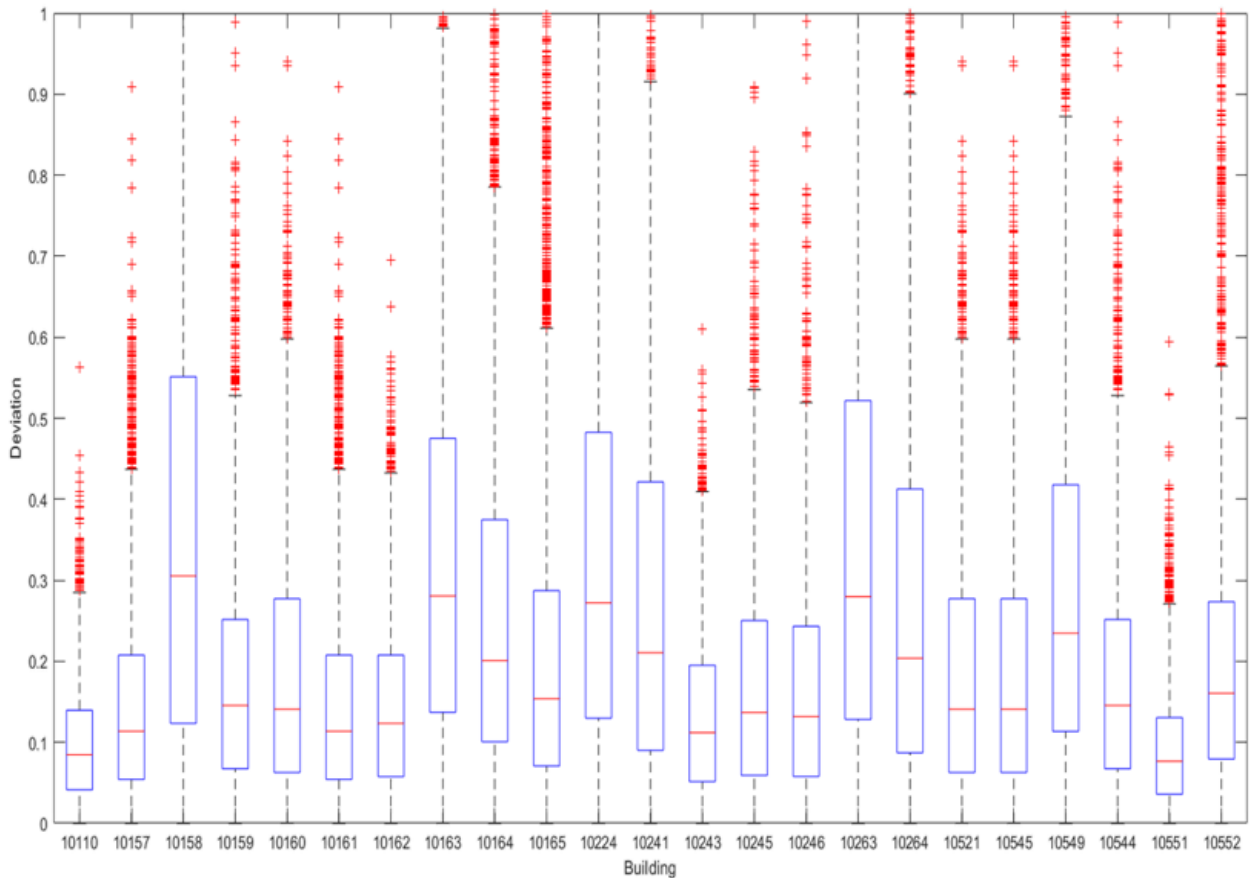


Figure 54 - Mass flow-rate deviation between simulated and real values for each building.

The results, although acceptable, show these drawbacks:

- The controller modulates the valve in the primary circuit of the substation according to various controlled parameters:
  - ❖ External temperature: is used as an input in the climatic curves to determine the values of the supply temperature to the secondary and the maximum return temperature to the primary in order to limit heat dissipation . While being able to determine the delivery temperature through the climatic curve as shown in Chapter 6.4, the missing information in the available monitoring data on the return temperature in the secondary circuit and the corresponding flow-rate represents a limitation in the evaluation.
- The parameters recorded have different sampling times and therefore the measurements from one building to another are temporally staggered and, moreover, the number of recorded parameters is different from building to building as shown by the charts shown in chapter 5.1.

Since the model had to follow a temporal logic linked to timestep, it was necessary to interpolate some values for different buildings in order to simulate the entire time span that goes from September 2018 to July 2019. The interpolation, albeit carried out according to logic of linearity or proximity based on the evaluated data, it always carries with it a certain degree of intrinsic approximation.

- The data on external temperature is available for a limited number of buildings and when available it is not recorded at the same time in which the other parameters are recorded (for example flow rate and flow temperature to primary). This has led to the assumption of an identical external temperature for all buildings that do not present information regarding this parameter. Although the assumption is consistent as the lot is located on an area of 0.18 km<sup>2</sup>, and the more distant buildings have a distance of 0.6 km, for two adjacent buildings it resulted from the data analysis that the measured values are appreciable different, as reported in Figure 55. This affects the interpolation surface in actual conditions.

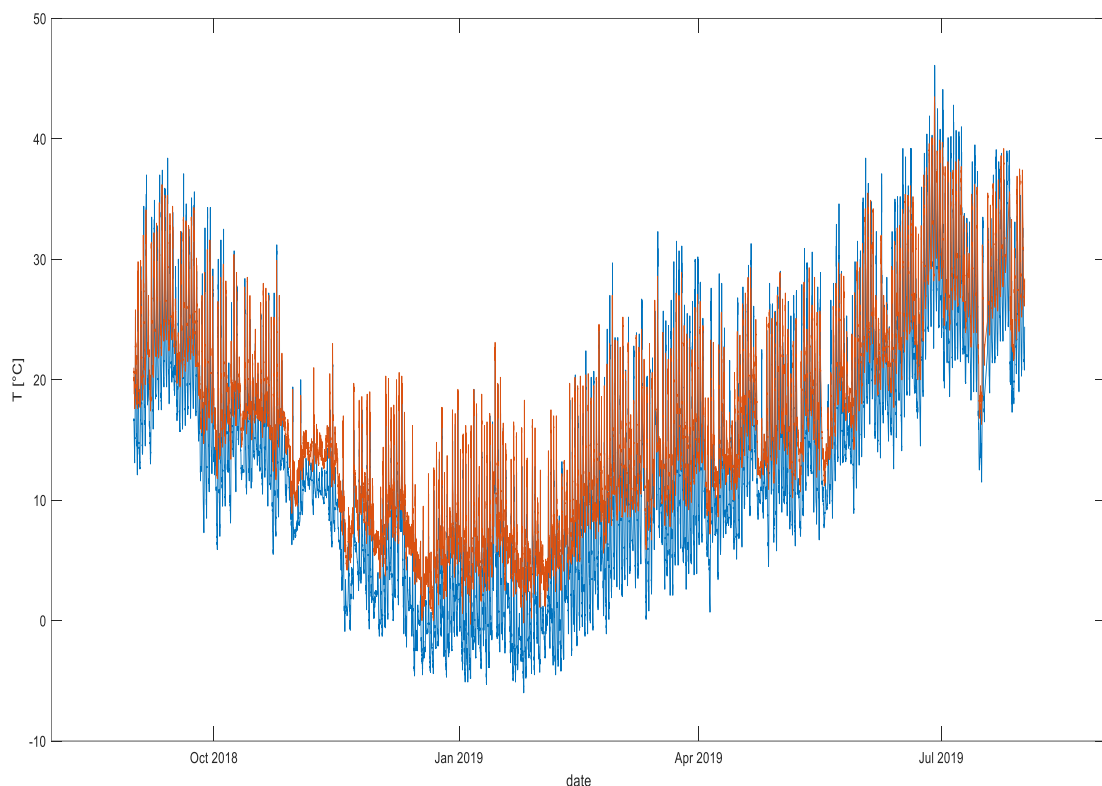
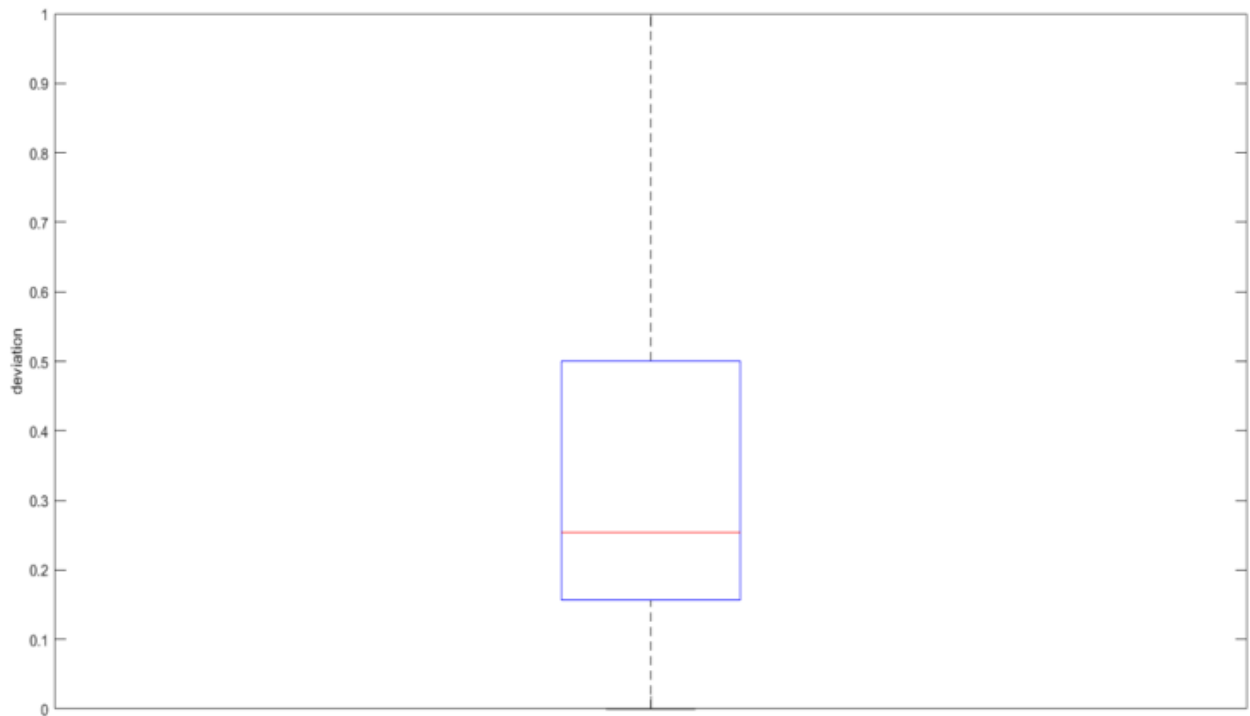


Figure 55 - Outside temperature from real data for two adjacent buildings.



*Figure 56 - Deviation of outside temperature for two adjacent buildings.*

Despite these issues, the results are considered satisfactory. This is due to the fact that the physical properties are summarized in the interpolating parameters, in particular:

- The outdoor temperature is proportional to the supply temperature in the secondary circuit of the substation, as well as to the maximum temperature limit in the return pipe of the primary circuit;
- The power parameter contains the information related to the flow rate and temperature delta to the secondary circuit of the substation, as well as the user's DHW request.



## 6.6 Thermal analysis

The analyzes carried out so far mainly included the hydraulic parameters of the network. The aim of the work is to model district heating networks both in hydraulic and thermal terms using *OpenModelica* software. An analysis of the thermal parameters relating to the network is therefore necessary.

In a district heating network the thermal dissipations in the distribution network must be evaluated for the sizing of the network. The distance between the heat production plant and the users is such as to be able to generate appreciable variations in the supply temperature. District heating pipes are therefore characterized by an important thickness of insulation.

For the analysis of the network "premant" or equivalent pipes are considered. The insulation values of the "premant" pipes are shown in figure 58. «Premant» is the patented name of a pre-insulated system with plastic sheath for long-range district heating. The system has been designed for direct installation in the ground. The solution provides for an insulating layer in closed cell polyurethane foam ( $\lambda < 0.026 \text{ W/mK}$ ). [30]

The "premant" pipes are supplied for single sections of 6 - 12 meters length. Furthermore, the pipes are available in three different categories of insulating thickness as shown in the figure:

**PREMANT**

Nominal diameter	Steel tube d x s	Insulation thickness 1 D	Insulation thickness 2 D	Insulation thickness 3 D	Length m	Buried pipe volume l/m
DN	mm	mm	kg/m	mm	kg/m	mm
20	26.9 x 2.6	90	2.76	110	3.19	125
25	33.7 x 2.6	90	3.17	110	3.60	125
32	42.4 x 2.6	110	4.56	125	5.01	140
40	48.3 x 2.6	110	5.08	125	5.44	140
50	60.3 x 2.9	125	6.30	140	6.69	160
65	76.1 x 2.9	140	7.79	160	8.36	180
80	88.9 x 3.2	160	9.22	180	9.84	200
100	114.3 x 3.6	200	13.34	225	14.44	250
125	139.7 x 3.6	225	16.21	250	17.56	280
150	168.3 x 4.0	250	21.10	280	22.85	315
200	219.1 x 4.5	315	31.36	355	34.34	400
250	273.0 x 5.0	400	45.49	450	50.02	500
300	323.9 x 5.6	450	58.90	500	64.08	560
350	355.6 x 5.6	500	67.02	560	74.01	630
400	406.4 x 6.3	560	85.25	630	94.15	670
450	457.2 x 6.3	630	99.11	670	104.90	710
500	508.0 x 6.3	710 (670)	115.50	800	130.20	900
600	610.0 x 7.1	800	150.20	900	165.90	1000
700	711.0 x 8.0	900	190.10	1000	207.40	1100
800	813.0 x 8.8	1000	232.80	1100	251.90	1200
900	914.0 x 10.0	1100	288.70	1200	310.30	-
1000	1016.0 x 11.0	1200	346.90	-	-	6
						776.00

Figure 57 - Technical data sheet of Premant pipes (1) [30].

Furthermore, the technical data sheet provides for each type of pipe the conductance and thermal dissipation per linear meter:

#### Thermal losses q (W / m) for the pipe

PREMANT	Valore U W/mK	Temperatura media di esercizio T <sub>e</sub> [°C]							
		50 °C	60 °C	70 °C	80 °C	90 °C	100 °C	110 °C	120 °C
26.9 - 90	0.1292	5.2	6.5	7.8	9.0	10.3	11.6	12.9	14.2
33.7 - 90	0.1572	6.3	7.9	9.4	11.0	12.6	14.2	15.7	17.3
42.4 - 110	0.1607	6.4	8.0	9.6	11.2	12.9	14.5	16.1	17.7
48.3 - 110	0.1843	7.4	9.2	11.1	12.9	14.7	16.6	18.4	20.3
60.3 - 125	0.2054	8.2	10.3	12.3	14.4	16.4	18.5	20.5	22.6
76.1 - 140	0.2410	9.6	12.0	14.5	16.9	19.3	21.7	24.1	26.5
88.9 - 160	0.2484	9.9	12.4	14.9	17.4	19.9	22.4	24.8	27.3
114.3 - 200	0.2599	10.4	13.0	15.6	18.2	20.8	23.4	26.0	28.6
139.7 - 225	0.3002	12.0	15.0	18.0	21.0	24.0	27.0	30.0	33.0
168.3 - 250	0.3557	14.2	17.8	21.3	24.9	28.5	32.0	35.6	39.1
219.1 - 315	0.3887	15.5	19.4	23.3	27.2	31.1	35.0	38.9	42.8
273.0 - 400	0.3779	15.1	18.9	22.7	26.5	30.2	34.0	37.8	41.6
323.9 - 450	0.4342	17.4	21.7	26.0	30.4	34.7	39.1	43.4	47.8
355.6 - 500	0.4239	17.0	21.2	25.4	29.7	33.9	38.2	42.4	46.6
406.4 - 560	0.4514	18.1	22.6	27.1	31.6	36.1	40.6	45.1	49.6
457.2 - 630	0.4548	18.2	22.7	27.3	31.8	36.4	40.9	45.5	50.0
508.0 - 710	0.4413	17.7	22.1	26.5	30.9	35.3	39.7	44.1	48.5
610.0 - 800	0.5380	21.5	26.9	32.3	37.7	43.0	48.4	53.8	59.2
711.0 - 900	0.6097	24.4	30.5	36.6	42.7	48.8	54.9	61.0	67.1
813.0 - 1000	0.6840	27.4	34.2	41.0	47.9	54.7	61.6	68.4	75.2
914.0 - 1100	0.7550	30.2	37.7	45.3	52.8	60.4	67.9	75.5	83.0
1016.0 - 1200	0.8315	33.3	41.6	49.9	58.2	66.5	74.8	83.1	91.5
									99.8

Figure 58 - Technical data sheet of premant pipe (2). [30]

The linear dissipation assumes steady state operation, and does not consider the thermal inertia of the pipe and its delay time.

To evaluate the heat losses of the network, different pipe models were created that implement different solutions. Furthermore, the software was initially validated for simulations in the thermal field.

### 6.6.1 Validation of the model

In order to validate the subsequent components created, it is necessary to evaluate a component already present in OpenModelica that will be used as benchmark. A compact model was first built using different components of the Modelica standard Library [26] [31]. The goal for the benchmark model is the creation of a single model in which both the parameters relating to the pipeline and those relating to the ground are manageable.

It is necessary to use and merge at least three components from *Modelica* [26] and *DisHeatLib* [32] libraries:

- 1) dynamic pipe;
- 2) Thermal conductance;
- 3) Soil.

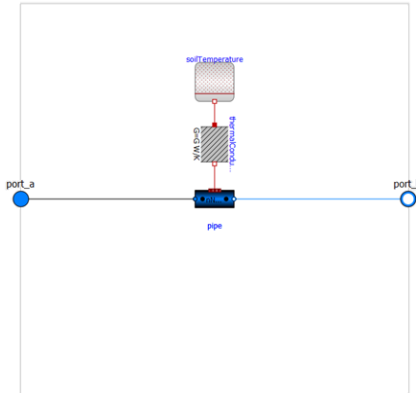


Figure 59 - Diagram view of the composed component.

The control on the pipe component is carried out through the user-selectable parameters:

- Length;
- Number of nodes;
- Roughness;
- Diameter;
- Initial pressure;
- Initial temperature;
- Use of heat exchange.

As regards the thermal conductance, the control takes place on the quantity itself.

Ground side it is possible to:

- Set either a constant temperature or undisturbed soil;
- In case of undisturbed soil, the average annual temperature value as well as the time when the coldest day occurs can be set;
- Set the annual variation in soil temperature;
- Set the depth of the associated buried pipe.

For this analysis the soil temperature is considered constant equal to 12.3 ° C (average soil temperature in Grugliasco) [31].

Dynamic pipe uses finite volume analysis to determine the temperature of the carrier fluid at the exit of the pipe.

So, to evaluate the dissipation on each volume, both the conductance and the component that simulates the ground must be vectorized, as shown in the code excerpt below. The associated connector will then consider all the nodes and the thermal dissipation will evolve throughout all the interested nodes.

```
Modelica.Thermal.HeatTransfer.Components.ThermalConductor[pipe.nNodes]
  thermalConductor (G=G*pipe.dxs);

DisHeatLib.Boundary.SoilTemperature[pipe.nNodes] soilTemperature(
  each T_amp=T_amp,
  each T_const=T_const,
  each T_mean=T_mean,
  each alpha=alpha,
  each inputType=DisHeatLib.BaseClasses.InputTypeSoilTemp.Constant,
  each t_min=t_min,
  each z=z);
```

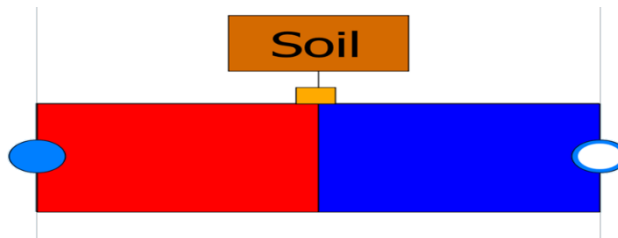


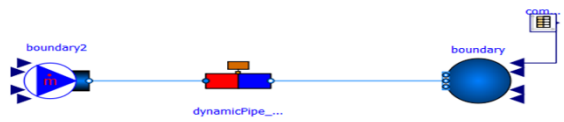
Figure 60 - Icon view of the composed component.

### 6.6.2 Validation of the components and methodology used

In order to assess the effectiveness of the component that are used as benchmark, the steady state behavior is assessed for a typical section of pipe, verifying the consistency of the outlet temperature with that which would be obtained using the linear dissipation value reported on figure 61.

A simple model is then implemented characterized by:

- One boundary condition in mass-flow and temperature (boundary 2 component);
- One boundary condition in pressure (boundary component);
- “Dynamicpipe\_soil” component that manages the heat exchange with the ground.



It is then possible to proceed to the validation by setting a supply temperature of 80 ° C and a constant flow rate of 3.2 kg / s. As regards the geometry of the pipes, diameter was set equal to 0.2 m and total length was set to 66 meters. Furthermore, the conductance values are set according to figure 61 (technical data sheet):

PREMANT	Valore U W/mK	Temperatura media di esercizio T <sub>a</sub> [°C]								
		50 °C	60 °C	70 °C	80 °C	90 °C	100 °C	110 °C	120 °C	130 °C
26.9 - 90	0.1292	5.2	6.5	7.8	9.0	10.3	11.6	12.9	14.2	15.5
33.7 - 90	0.1572	6.3	7.9	9.4	11.0	12.6	14.2	15.7	17.3	18.9
42.4 - 110	0.1607	6.4	8.0	9.6	11.2	12.9	14.5	16.1	17.7	19.3
48.3 - 110	0.1843	7.4	9.2	11.1	12.9	14.7	16.6	18.4	20.3	22.1
60.3 - 125	0.2054	8.2	10.3	12.3	14.4	16.4	18.5	20.5	22.6	24.6
76.1 - 140	0.2410	9.6	12.0	14.5	16.9	19.3	21.7	24.1	26.5	28.9
88.9 - 160	0.2484	9.9	12.4	14.9	17.4	19.9	22.4	24.8	27.3	29.8
114.3 - 200	0.2599	10.4	13.0	15.6	18.2	20.8	23.4	26.0	28.6	31.2
139.7 - 225	0.3002	12.0	15.0	18.0	21.0	24.0	27.0	30.0	33.0	36.0
168.3 - 250	0.3557	14.2	17.8	21.3	24.9	28.5	32.0	35.6	39.1	42.7
219.1 - 315	0.3887	15.5	19.4	23.3	27.2	31.1	35.0	38.9	42.8	46.6
273.0 - 400	0.3779	15.1	18.9	22.7	26.5	30.2	34.0	37.8	41.6	45.3
323.9 - 450	0.4342	17.4	21.7	26.0	30.4	34.7	39.1	43.4	47.8	52.1
355.6 - 500	0.4239	17.0	21.2	25.4	29.7	33.9	38.2	42.4	46.6	50.9
406.4 - 560	0.4514	18.1	22.6	27.1	31.6	36.1	40.6	45.1	49.6	54.2
457.2 - 630	0.4548	18.2	22.7	27.3	31.8	36.4	40.9	45.5	50.0	54.6
508.0 - 710	0.4413	17.7	22.1	26.5	30.9	35.3	39.7	44.1	48.5	53.0
610.0 - 800	0.5380	21.5	26.9	32.3	37.7	43.0	48.4	53.8	59.2	64.6
711.0 - 900	0.6097	24.4	30.5	36.6	42.7	48.8	54.9	61.0	67.1	73.2
813.0 - 1000	0.6840	27.4	34.2	41.0	47.9	54.7	61.6	68.4	75.2	82.1
914.0 - 1100	0.7550	30.2	37.7	45.3	52.8	60.4	67.9	75.5	83.0	90.6
1016.0 - 1200	0.8315	33.3	41.6	49.9	58.2	66.5	74.8	83.1	91.5	99.8

Figure 61 - Highlighting of the linear dissipation for the analyzed case.

Pipe data

nNodes	<input type="text" value="2"/>
length	<input type="text" value="66"/> m
diameter	<input type="text" value="0.2"/> m
roughness	<input type="text" value="0.025"/> mm ▾

Conductance

G	<input type="text" value="0.3887 * dynamicPipe_soil.length"/> W/K
---	---

Soil

inputType	<input type="text" value="DisHeatLib.Boundary.BaseClasses.InputTypeSoilTemp.Constant"/> ▾	Model for ground temperature
T_const	<input type="text" value="12.3"/> degC ▾	Constant temperature

Figure 62 - User interface in OpenModelica for the example analyzed.

Considering the parameters described above, the temperature at state\_b in steady state should be:

$$T_b = -\frac{W}{m} * l * \frac{1}{c_p * m_{flow}} + T_{state_a} = 79.866 \text{ } ^\circ\text{C}$$

Where:

- $T_b$  : Temperature at state b [ $^\circ\text{C}$ ];
- $\frac{W}{m}$  : linear heat dissipation [ $\frac{W}{m}$ ];
- $l$  : length of the pipe [m];
- $c_p$  : specific heat of the medium [ $\frac{J}{kg \text{ } K}$ ];
- $m_{flow}$ : mass flow rate [ $\frac{kg}{s}$ ];
- $T_{state\_a}$  : Temperature at state a [ $^\circ\text{C}$ ];

The simulation result at steady state is  $T_b = 79.87 \text{ } ^\circ\text{C}$  (see figure 63). It can, therefore, be said that the simulation provides reliable results with respect to the technical data sheet and that, therefore, the approach is correct.

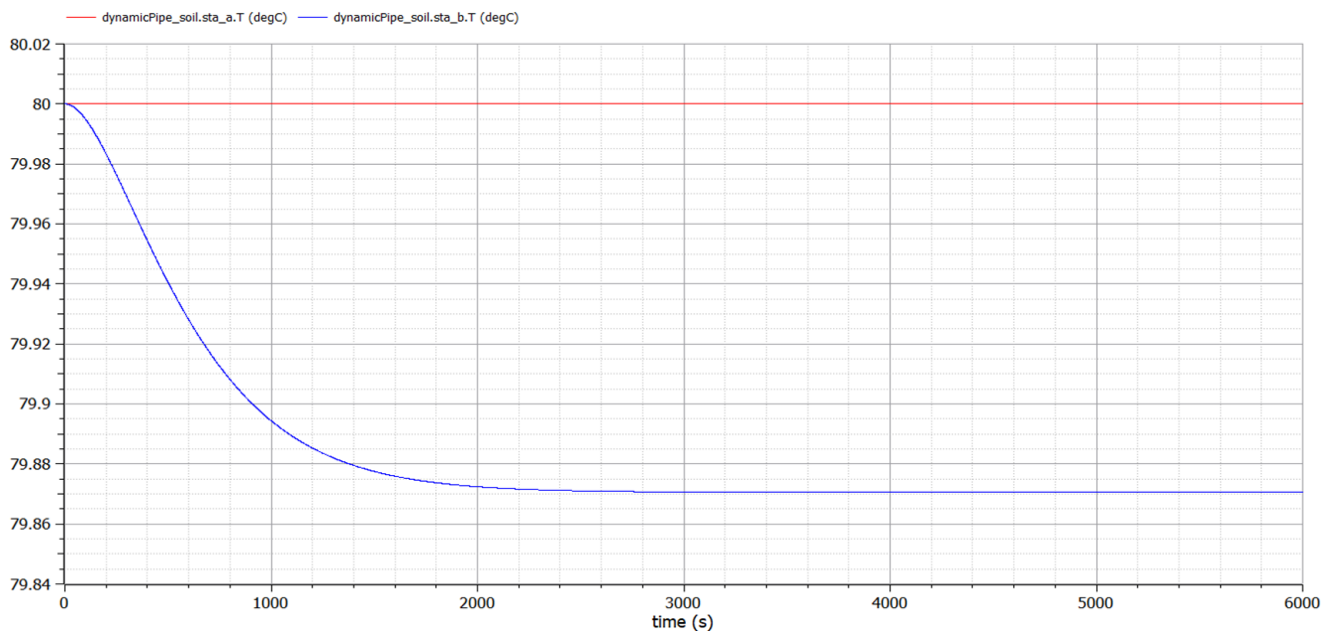


Figure 63 - Evolution of pipe state temperature for the example analyzed.

### 6.6.3 Validation of pipe model (1)

The first pipe model determines the outlet temperature through an equation determined by a previous analysis of the finite volumes. The output variable is the outlet temperature and the input parameters are the flow-rate and the inlet temperature.

From the following table we can see an example related to the first pipe of the network of how the plane interpolates the input data:

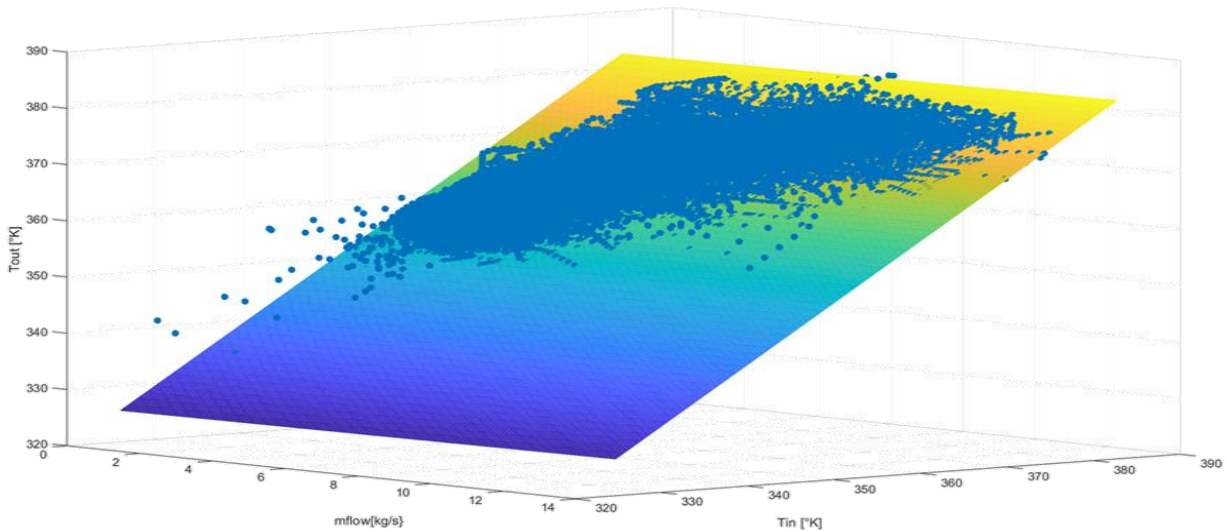


Figure 64 - Interpolation plane for the determination of outlet pipe temperature for one pipe.

The following graphs show the evolution of the inlet and outlet temperature of the pipeline in the case of finite volume analysis and in the case of using the interpolating plane (figure 65) and the deviation between the two values (figure 66).

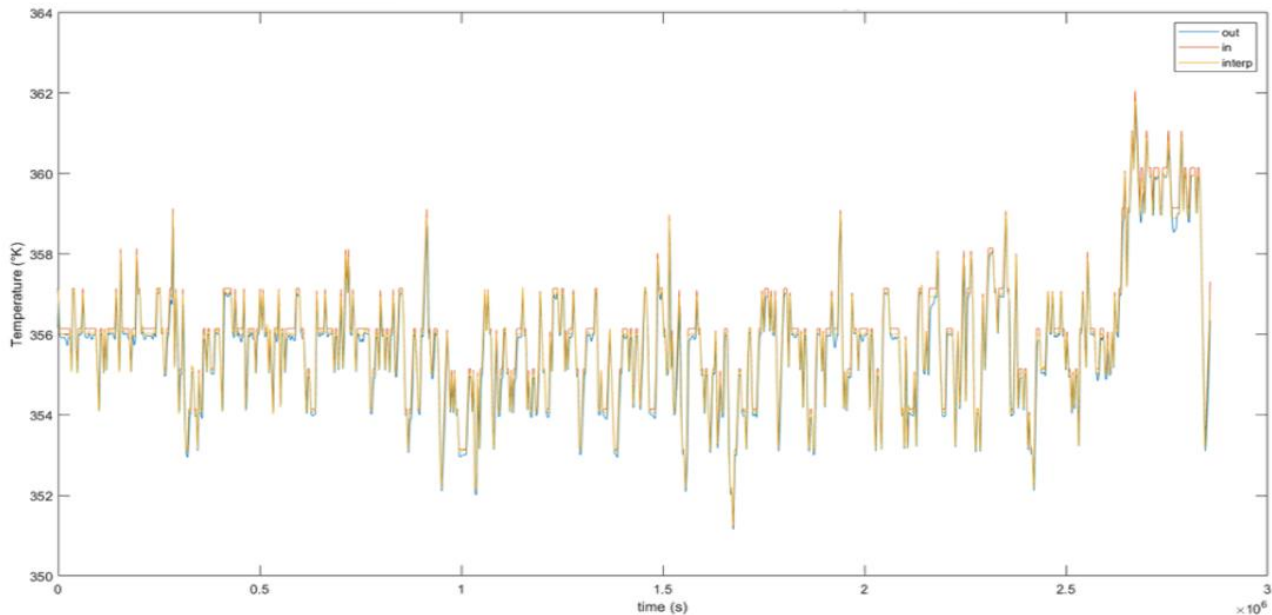


Figure 65 - Comparison of obtained results through finite volume and through the use of the interpolation plane.

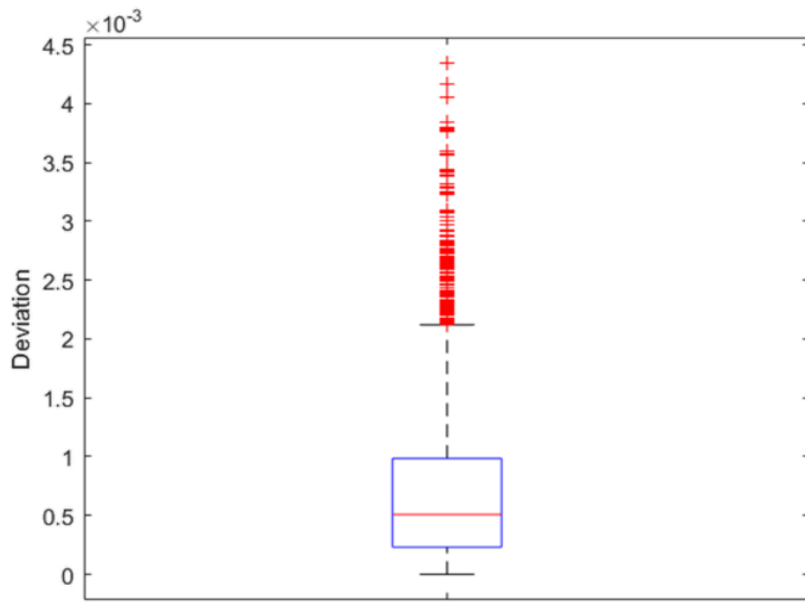


Figure 66 - Deviation between finite volume method and used method.

As we can see from the two graphs, this pipe leads to good results but, on the other side, the finite volume analysis is computationally very expensive, and for this reason, this model has been discarded.

#### 6.6.4 Validation of new pipe model (2)

In order to improve the model, a new pipe model has been created which, using the `delay()` function in *Modelica*, uses the temperature information at the previous instant in the equation. This generates good results, similar to those obtained using finite volumes as this solution allows to partially take into account the effects of inertia and hydraulic transmissivity.

With the root mean squares method an equation is generated and takes into account the flow temperature at the previous instant, the flow temperature at the evaluated instant and the flow-rate.

```

hSet=Medium.specificEnthalpy(Medium.setState_pTX(p=port_b.p,
T=coefficient[1]+coefficient[2]*port_a.T+coefficient[3]*delay(port_a.T,1)+coefficient[4]*port_a.m_flow, X=Xi_instream)) ;
Q_flow=m_flow*(hSet-inStream(port_a.h_outflow));
Xi_instream=inStream(port_a.Xi_outflow);
port_a.h_outflow=inStream(port_b.h_outflow);
port_b.h_outflow=hSet;
F_fg=A_mean*dp_fg;

```

The graphs below show a better behavior compared to the previous pipe model:

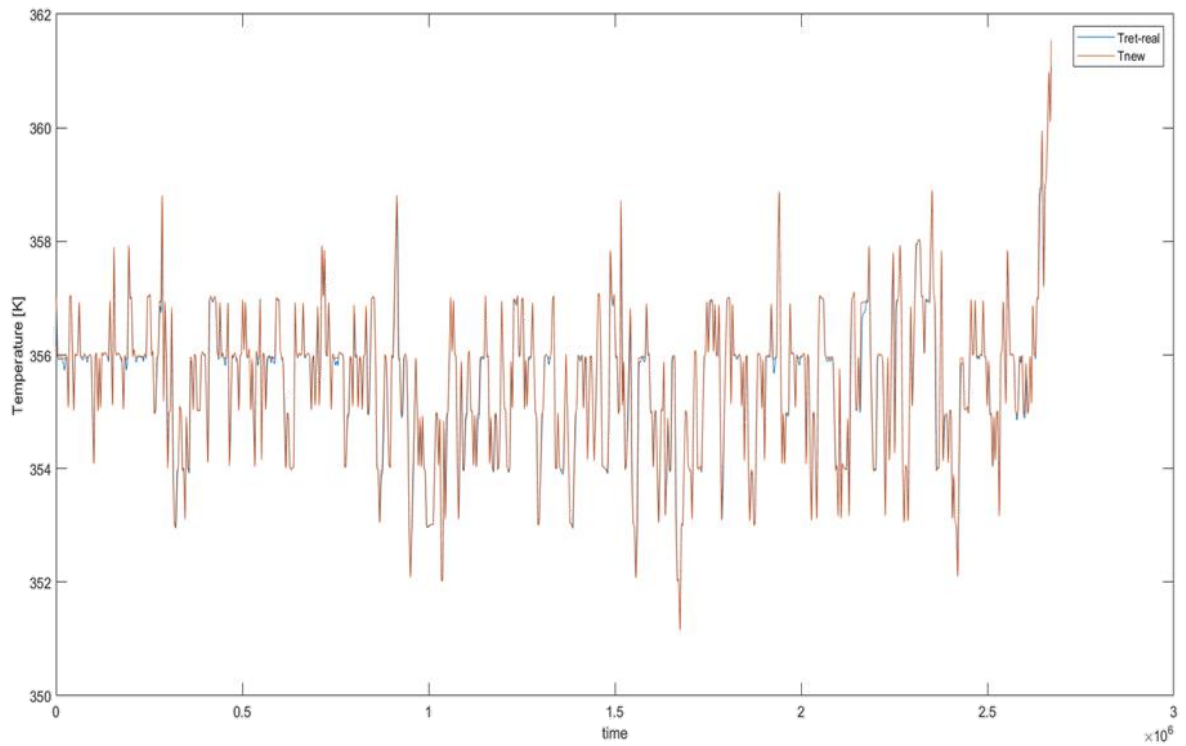


Figure 67 - Comparison of outlet temperature obtained through finite volume and through new pipe model.

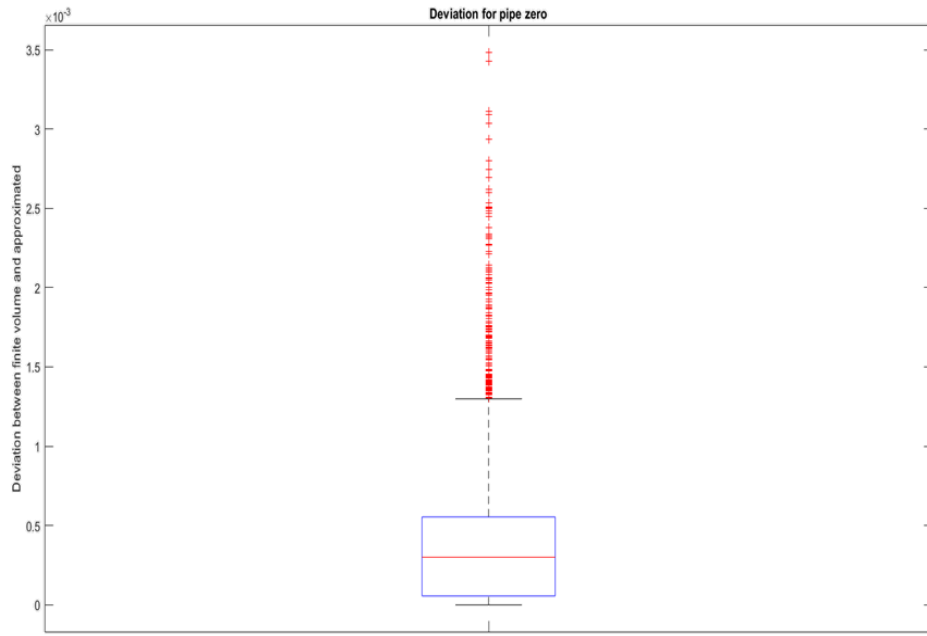


Figure 68 - Deviation between new implemented method and finite volume method.

While leading to better results, this model also has the limit of requiring a prior simulation using finite volumes, therefore it is computationally expensive as well.

### 6.6.5 Validation of new pipe model (3)

The one-dimensional energy balance in the pipe is represented by the following partial differential equation:

$$\frac{dT}{dt} + \frac{m_{flow}}{\pi r^2 \rho} \frac{dT}{dx} + \frac{1}{\pi r^2 \rho c_p} q(T(x)) = 0 \quad (13)$$

where  $q(T(x))$  describes the heat loss to the surrounding environment along the length of the pipe and depends on the boundary conditions. The heat loss may often be described as a linear function of the temperature difference between boundaries :

$$q(T(x)) = k S (T(x) - T_{boundary}) \quad (14)$$

where  $k$  is the thermal conductivity of the surroundings (water, soil) and  $S$  is the shape factor.

If the mass-flow is constant, an explicit solution to equation 13 can be derived through Laplace-transformation and integration over the pipe length. In the case of time-varying flows the equation can be solved by applying the method of characteristics. Temperature at the outlet of a pipe with length  $L$  is then given by [22]:

$$T(L, t) = T_{boundary} + (T_{in}(t - \tau) - T_{boundary}) e^{-\frac{\tau}{\tau_p}} \quad (15)$$

Equation 15 replaces and does not require any more a finite volume simulation. This equation is the basis of the *spatialDistribution* function implemented in commercial softwares like *Dymola* but not yet implemented in *OpenModelica*.

The first implementation of a model using the above equation has led to excellent results. The calculation was in fact repeated on the zero pipe analyzed through different methods previously defined showing the following results:

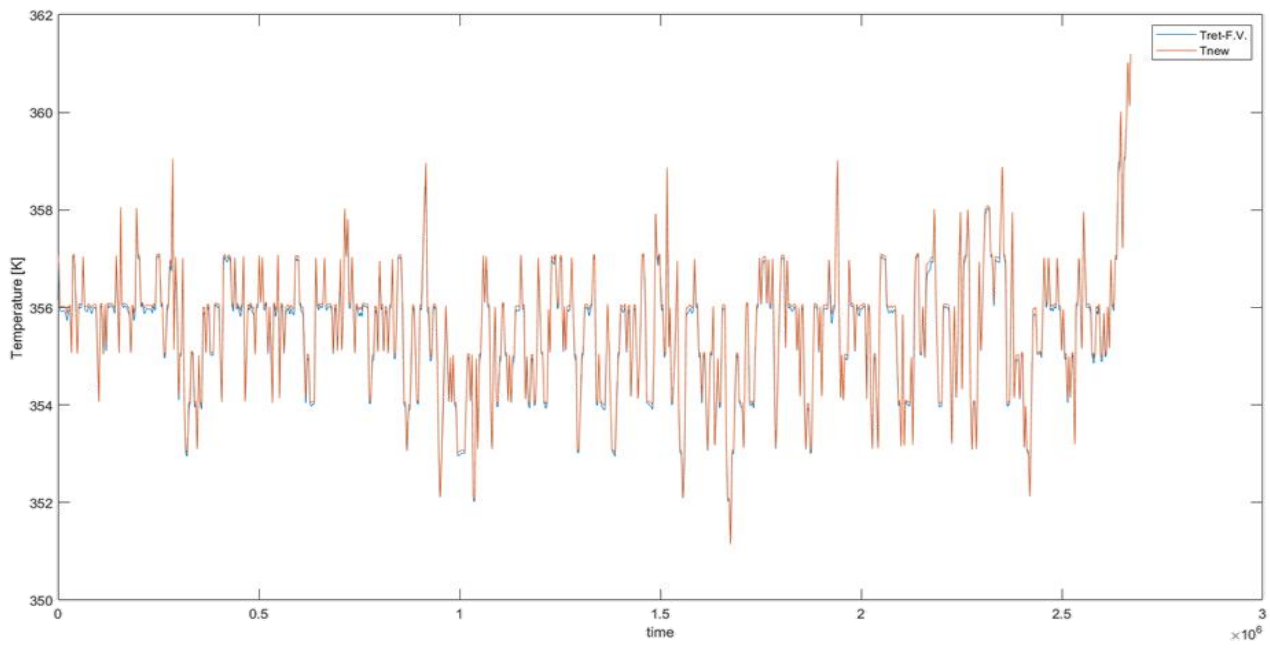


Figure 69 - Outlet temperature for pipe zero using finite volume and using the new implemented pipe.

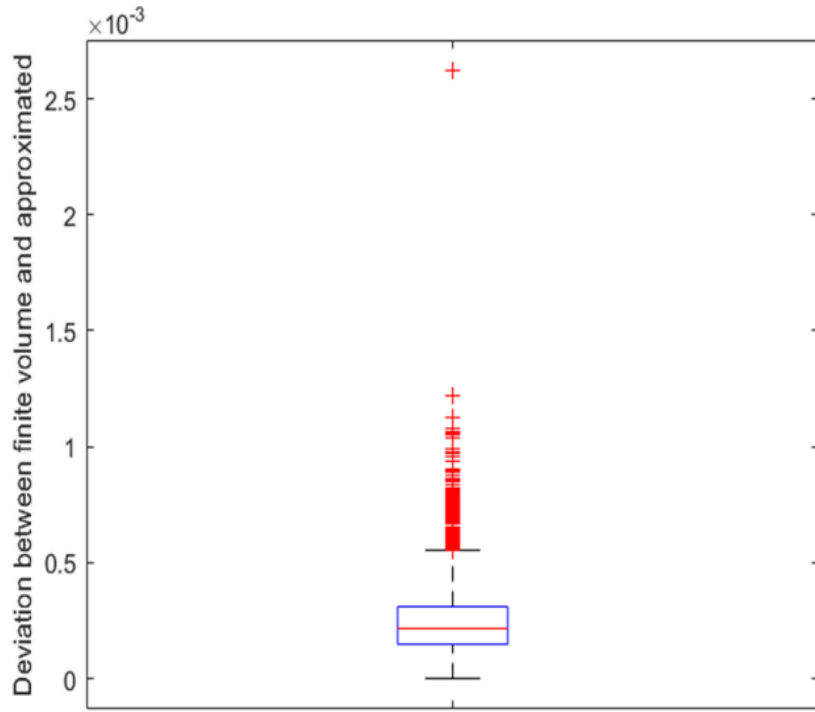


Figure 70 - Outlet temperature deviation between finite volume and new implemented method.

The graphs show a marked improvement over the results obtained through the other models. Furthermore, in addition to a better accuracy, the model does not have to go through the finite volume analysis, hence drastically reducing the calculation times.

Figure 71 shows the user interface of the newly created component. The editable parameters are:

- Pipe diameter;
- Length of the pipe;
- Conductivity of insulation;
- Roughness;
- Thickness of insulation;
- Temperature of the ground.

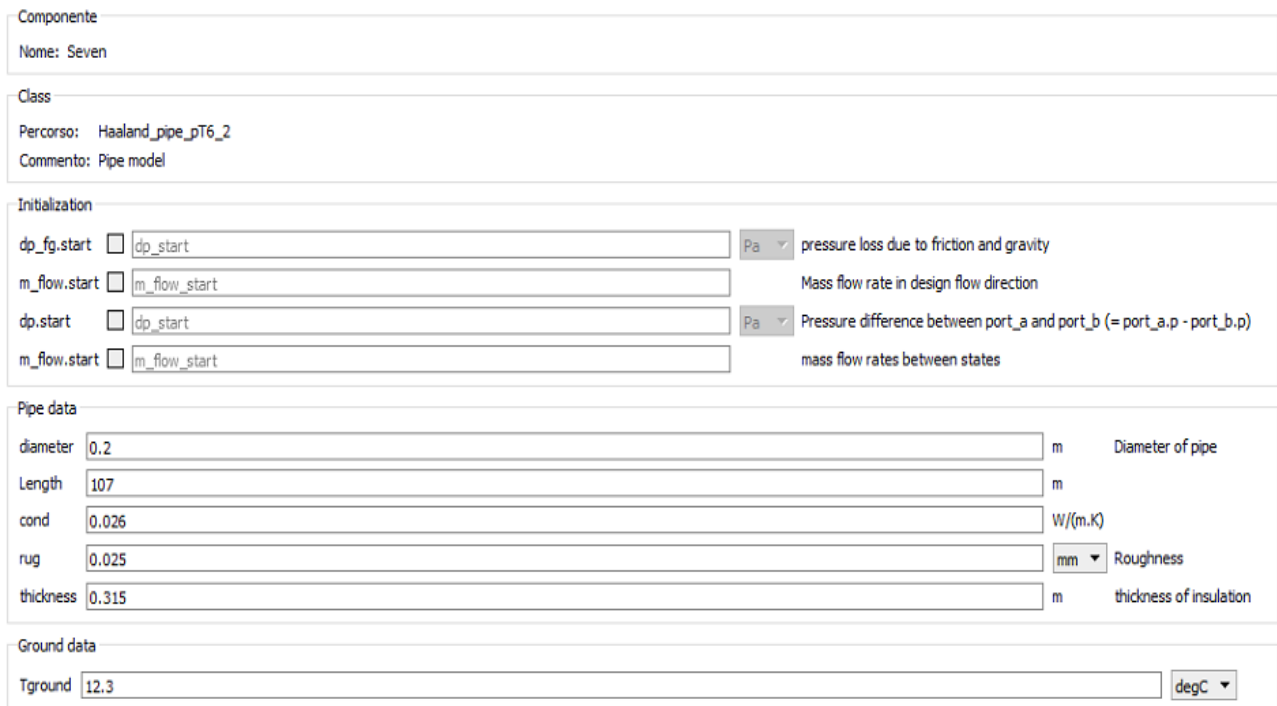


Figure 71 - User interface in OpenModelica of the new pipe.

The interface adopted is user-friendly. As already widely emphasized this was a key aspect in the creation of each component presented over the entire work.

In order to make the component effective from a computational point of view, it is necessary to avoid the generation of events.

Events are generated in one of two ways. First, they can be generated by conditional expressions. If conditional expressions only involve the variable time, then we call them “time events”. The time variable is a built-in, global variable that is treated as an “input” to all models. If events are generated because of conditional expressions that involve solution variables, then we call them “state events”. Events express the fact that there is an abrupt change in the behavior of the system. But it’s important to point out that events are not just describing a change but also specifying when it changes.

A typical example of event generation is presented in Modelica by example book [33] : Consider an example, where the system began in an equilibrium state. At the start of the simulation, there are no significant dynamics.

Since nothing is really changing in the system, the integrator is unlikely to accumulate significant integration error. So, in order to minimize the amount of time required to complete the simulation, variable time step integrators will, in such circumstances, increase their step size.

“There is, however, a risk in doing this. The risk is that the integrator may get “blind-sided” by a sudden disturbance in the system. If such a disturbance were to occur, the integrator’s assumptions that a large step will not lead to significant integration error would not be true.

The question then becomes, how can the integrator *know* when it can take a large time step and when it cannot. Typically, these integration schemes use a kind of trial and error approach. They try to take large step and then estimate the amount of error introduced by that step. If it is less than some threshold, then they accept the state (or perhaps try a larger step). If, on the other hand, the step introduces too much error, then they try a smaller step. But they cannot know how small a step will be required to get under the error threshold, which means they will continue to blindly try smaller and smaller steps.” [33]

A state event is an event that depends on the solution trajectory. State events are much more complicated to handle. Unlike time events, where the time of the event is known *a priori*, a state event depends on the solution trajectory. So we cannot entirely avoid the searching for the point at which the event occurs.

If a state is started extremely close to an event, due to the numerical imprecision it is not possible to know whether the step is starting right after an event has just occurred or whether a step is starting where an event is just about to occur.

The *noEvent* operator suppresses this special event handling. Instead, it does what most users expected would happen in the first place, which is to evaluate the conditional expression for every value of the state.

The following figure shows a code excerpt that uses the operator to avoid the phenomenon just described.

```

tau=noEvent(floor(Length/((port_a.m_flow+0.00001)*4/(d*pi*diameter^2))) ;
hSet=Medium.specificEnthalpy(Medium.setState_pTX(p=port_b.p,T=Tground+
(max(delay(port_a_T,tau,2671200),Tground)-Tground)*e^(-
Length/(m_flow/(d*pi*diameter^2/4))/taup)));
Q_flow=m_flow*(hSet-inStream(port_a.h_outflow));
Xi_instream=inStream(port_a.Xi_outflow);
port_a.h_outflow=inStream(port_a.h_outflow);
port_b.h_outflow=hSet;
F_fg=A_mean*dp_fg;
Ib_flow=0;
F_p=A_mean*(Medium.pressure(state_b)-Medium.pressure(state_a));
dp_fg=1/(-
1.8*log10((rug/diameter/3.7)^1.11+6.9/Modelica.Fluid.Pipes.BaseClasses.Cha-
racteristicNumbers.ReynoldsNumber(noEvent(port_a.m_flow))/A_mean/d,s,Mediu-
m.dynamicViscosity(state_a),diameter))^2*Length/diameter*0.5*d*(m_flow/A_-
mean/d)^2;
```

Furthermore as in the model different combitimetables are used as input data in the model (e.g. outside temperature and heat demand at substation) time events are suppressed by imposing noEvent operator at the different combitimetables used. Using this operator each abrupt change of a variable in time inside the table does not cause an increase of computational time.

## 6.7 Thermal model

Once the components and method used have been validated, the model is implemented with the aim of evaluating the heat dissipation of the delivery circuit.

*Table 10 - Linear conductance for the different pipes present in the network under analysis.*

Diameter	Linear conductance [W/m/K]
DN200	0.3887
DN150	0.3557
DN65	0.241
DN50	0.2054
DN40	0.1843
DN32	0.1607

The conductance value is prescribed for each different pipe in accordance with the table 10 and with the effective length of the section analyzed.

Initially the model of the supply circuit of the network is evaluated for ten minutes timesteps and considering one node every 12 meters in length. In this model no substations are present but only boundary in mass flow-rate at building level.

The following figure shows the delivery model:

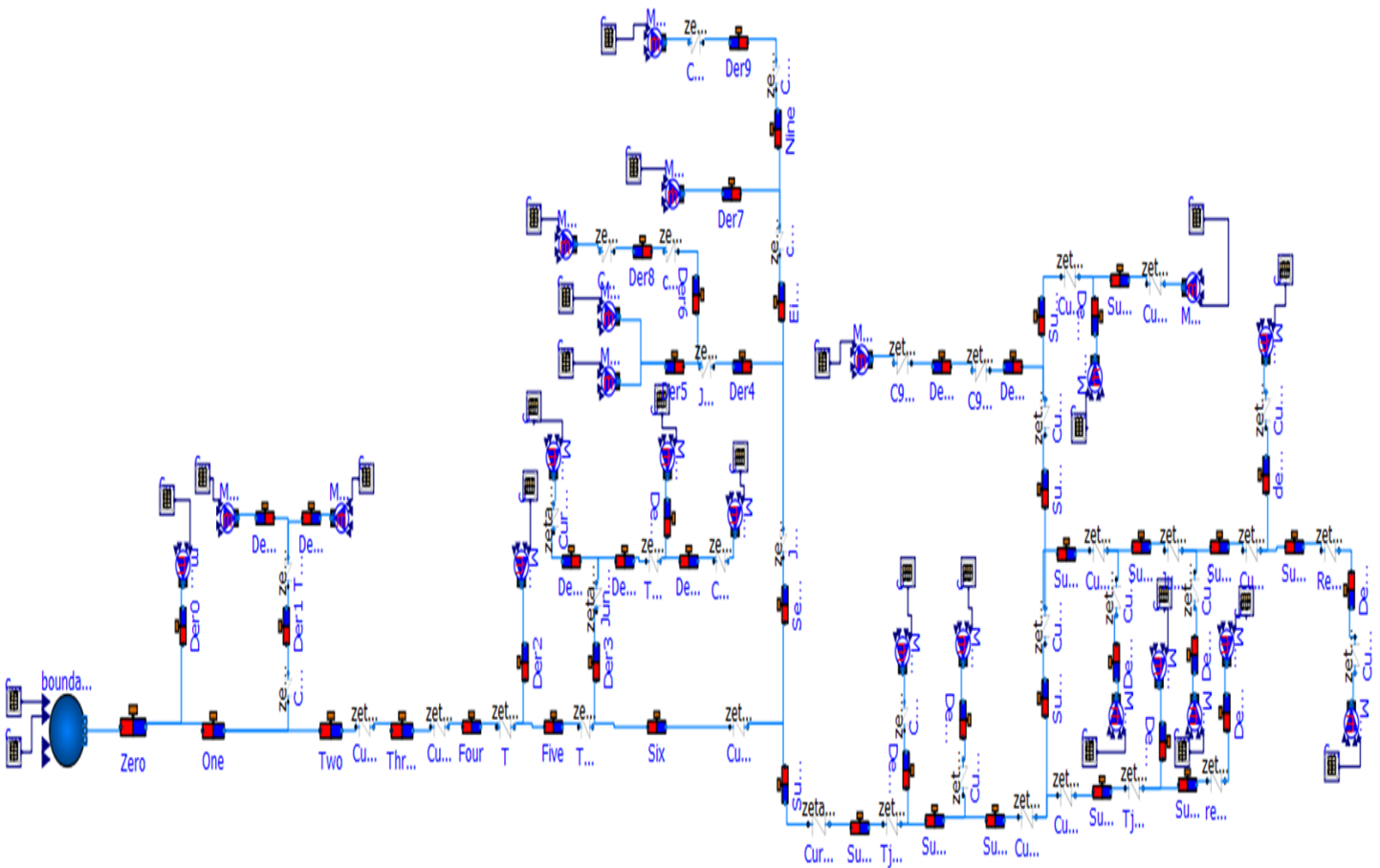


Figure 72 - Thermal model for the supply in OpenModelica using finite volumes.

The model was simulated for the month of January. In the month analyzed the finite volume analysis brought to an extremely high calculation time as shown in the following figure:

```
timer
  1.31042s      reading init.xml
  0.154661s     reading info.xml
  0.0308515s [ 0.0%] pre-initialization
  119.972s [ 13.3%] initialization
  0.0803568s [ 0.0%] steps
  22.2583s [ 2.5%] solver (excl. callbacks)
  1.18814s [ 0.1%] creating output-file
  0.125097s [ 0.0%] event-handling
  0.889997s [ 0.1%] overhead
  757.791s [ 84.0%] simulation
  902.336s [100.0%] total
```

*Figure 73 - Simulation time using dynamic pipe.*

Using the new component specifically created and avoiding as much as possible the generation of conditional and temporal events, the simulation time is strongly decreased:

```
timer
  0.234293s      reading init.xml
  0.0350693s     reading info.xml
  0.0162303s [ 0.0%] pre-initialization
  96.4309s [ 80.1%] initialization
  0.0030027s [ 0.0%] steps
  6.15247s [ 5.1%] solver (excl. callbacks)
  0.343928s [ 0.3%] creating output-file
  0.179864s [ 0.1%] event-handling
  0.479014s [ 0.4%] overhead
  16.7454s [ 13.9%] simulation
  120.351s [100.0%] total
```

*Figure 74 - Simulation time using new pipe.*

Chapter 7 shows a comparison between the results obtained using the new implemented pipe with respect to the dynamic pipe and to monitored value.

Using the new implemented pipe it was possible to perform a simulation of the entire network (considering also substations) for the month of January in about 15 minutes.

Given the reduced calculation times, it was decided to simulate the entire network under analysis including the supply and return circuits and heat exchange substations.

The necessary assumption is always that the flow rate circulating in the network is equal to the sum of the flow rates determined by the component of the different substations.

To decide which timestep to use, different simulations were performed using different timesteps. Initially an independence in time for the month of January was carried out using 10 minutes and 1 minutes timestep for the entire network showing the following results:

$$\text{Deviation} = \text{abs}\left(\frac{T_{1\text{min}} - T_{10\text{min}}}{T_{1\text{min}}}\right) * 100$$

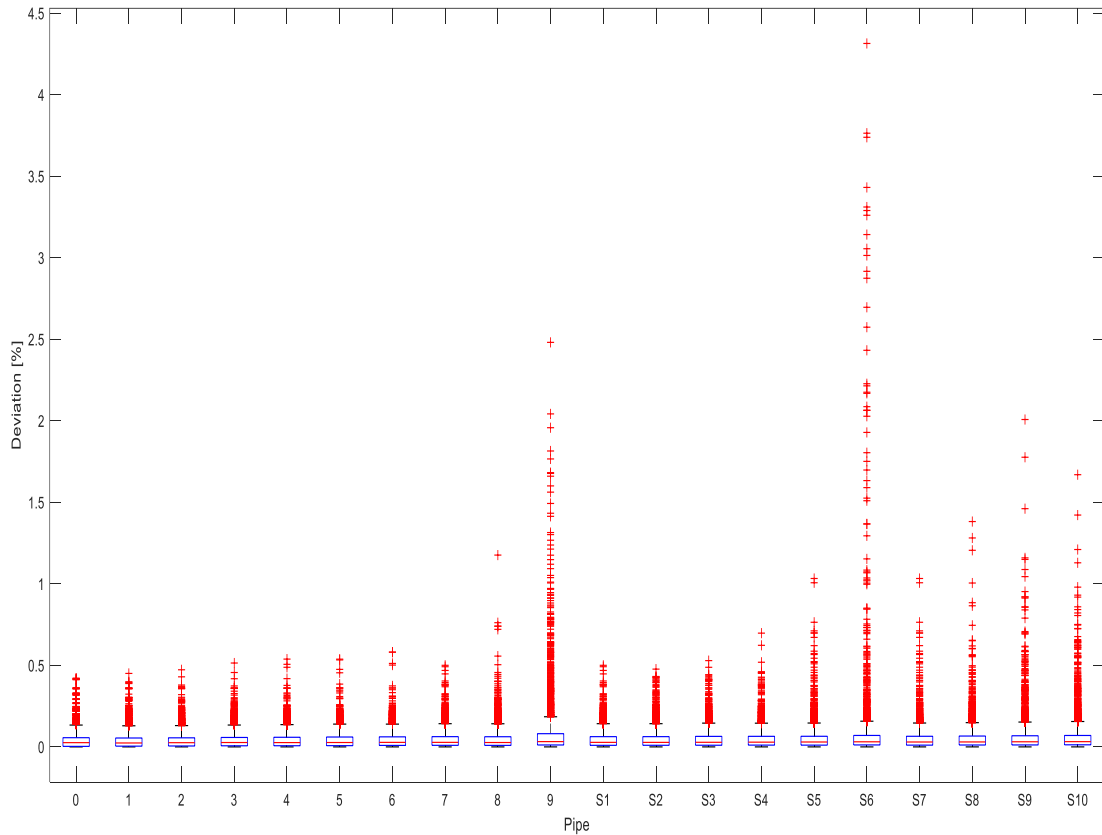


Figure 75 - Deviation on inlet temperature using 1 minute time-step or 10 minutes time-step.

The results obtained show that the simulations show an average percentage deviation much lower than 0.5%.

As the simulation with a one-minute timestep required a calculation time of approximately 25% greater than that with a 10-minute timestep it was decided not to evaluate the simulation with 1-minute timestep.

Furthermore a simulation with 30-minute timestep has been evaluated. The independence in time is shown in the following figure:

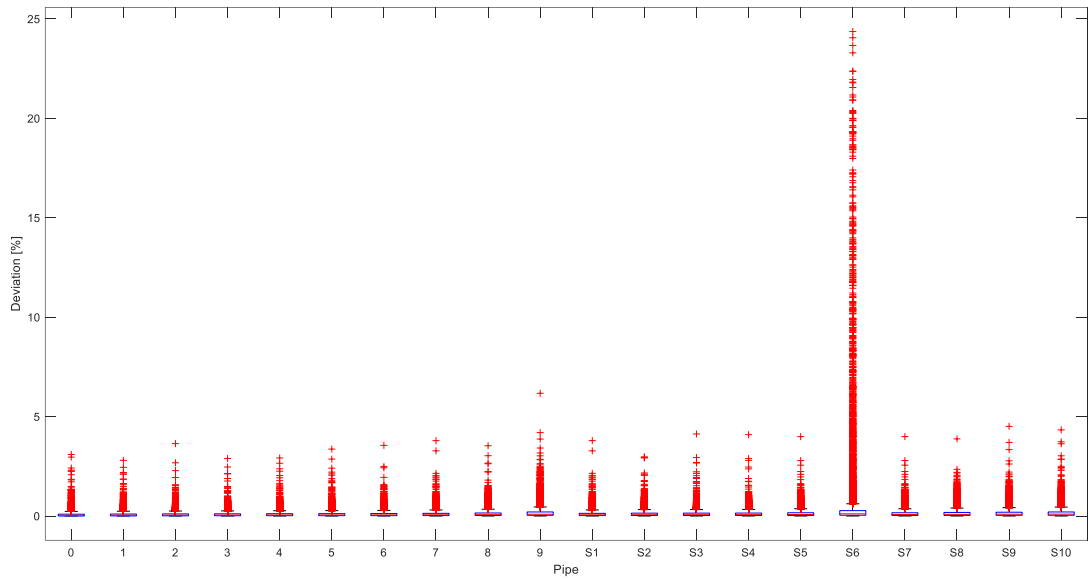


Figure 76 - Deviation of inlet temperature using 10 minutes time-step and 30 minutes time-step.

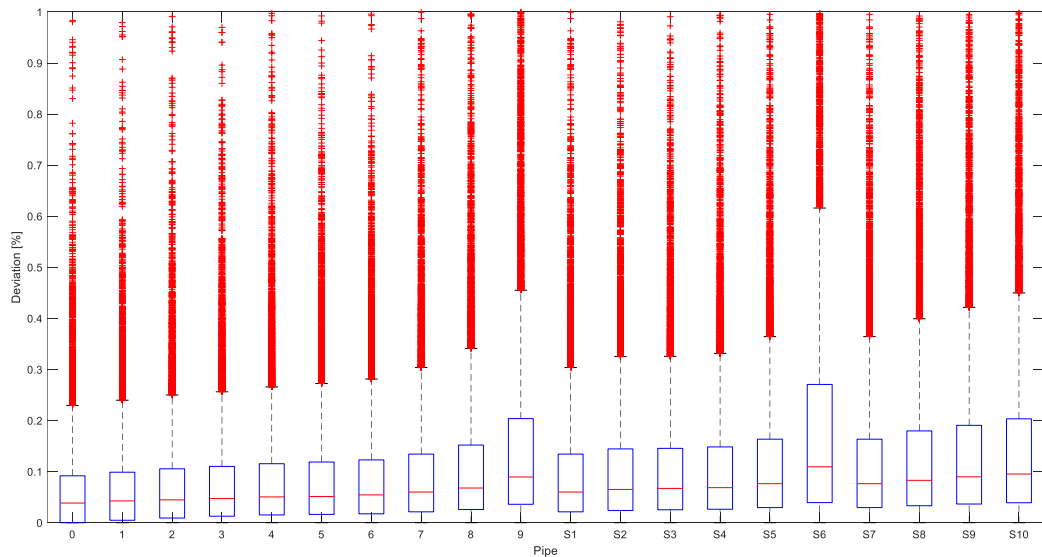


Figure 77 - Particular of the deviation.

Using a 30-minute time-step, the simulation is still reliable.

The calculation times in the case of timestep 10 minutes are shown in figure 79 while with timestep 30 min in figure 78:

```

0.507554s      reading init.xml
0.0741218s     reading info.xml
0.0080731s [ 0.0%] pre-initialization
  1054.18s [ 4.9%] initialization
  0.114914s [ 0.0%] steps
0.0046925s [ 0.0%] solver (excl. callbacks)
  8.37777s [ 0.0%] creating output-file
  2914.22s [ 13.5%] event-handling
  16.7392s [ 0.1%] overhead
  17627.7s [ 81.5%] simulation
 21621.3s [100.0%] total

```

Figure 79 - Simulation time using 10 minutes time-step.

timer	
0.503123s	reading init.xml
0.0728625s	reading info.xml
0.0077883s [ 0.0%]	pre-initialization
1064.14s [ 11.8%]	initialization
0.332719s [ 0.0%]	steps
0.0036554s [ 0.0%]	solver (excl. callbacks)
2.39764s [ 0.0%]	creating output-file
1291.85s [ 14.4%]	event-handling
3.87587s [ 0.0%]	overhead
6634.69s [ 73.7%]	simulation
8997.3s [100.0%]	total

Figure 78 - Simulation time using 30 minutes time-step.

We can see that the total simulation time is approximately 6 hours using 10 minute timestep while it is approximately 2.5 hours using 30 minute timestep.

The simulation was carried out through a computer with the following specifications:

- RAM 64 Giga;
- 8 core;
- VRAM 8 Giga;
- 500 Giga HDD;
- Operating system Windows 10 64 bit.

The reduced calculation times allow to simulate the network in acceptable times and with reliable results given that each component has been validated.

As already specified, the major limitation of the model lies in the fact that the simulation involves a portion of the network and therefore it is necessary to assume that the through-flow is equal to the sum of the batch flow.

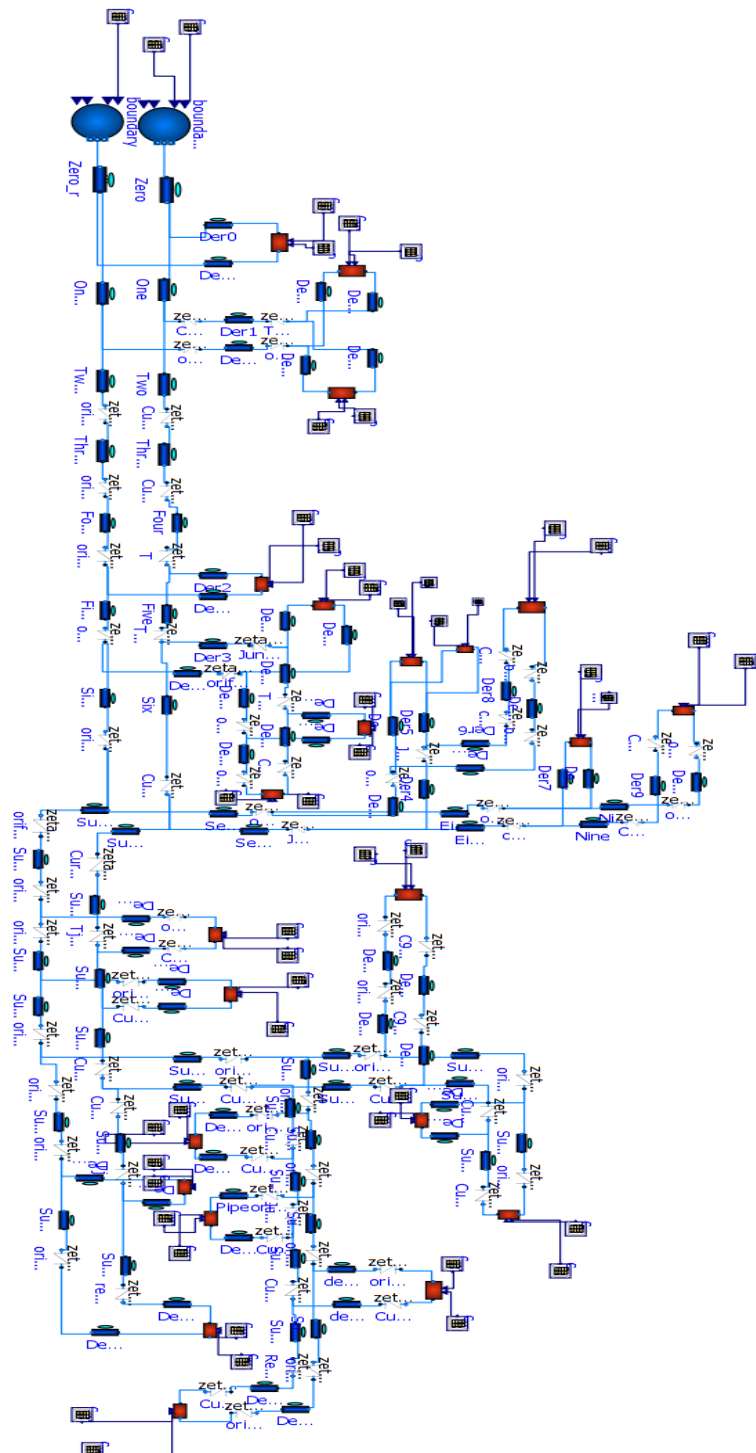


*Figure 80 - Complete model in OpenModelica.*



## 7. Results

A series of graphs regarding the simulation carried out are shown below:

- Comparison between dynamic pipe, implemented pipe and monitored data for the supply circuit in January;
- Delivery and return temperature for some pipes;
- Quantities of interest to substations.

The following figure shows how the new model implemented is able to simulate the temperature entering the substation with comparable accuracy and in a shorter time.

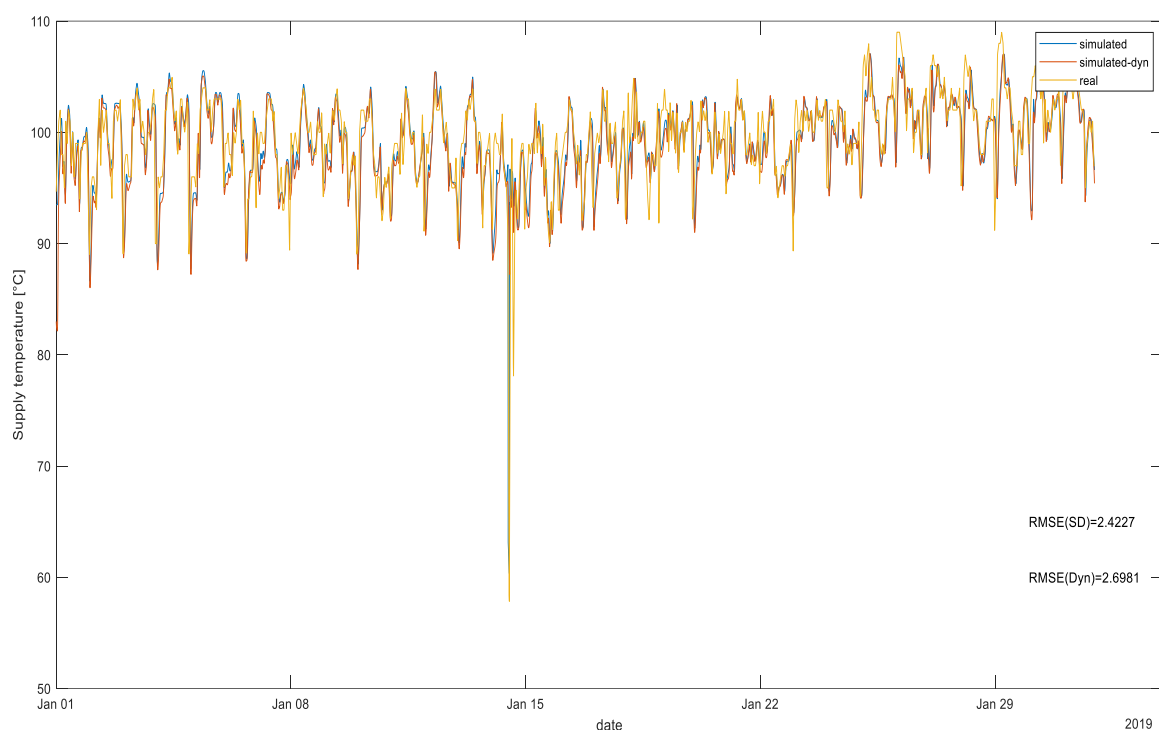


*Figure 81 - Inlet temperature at one substation using new pipe, dynamic pipe and monitored data.*

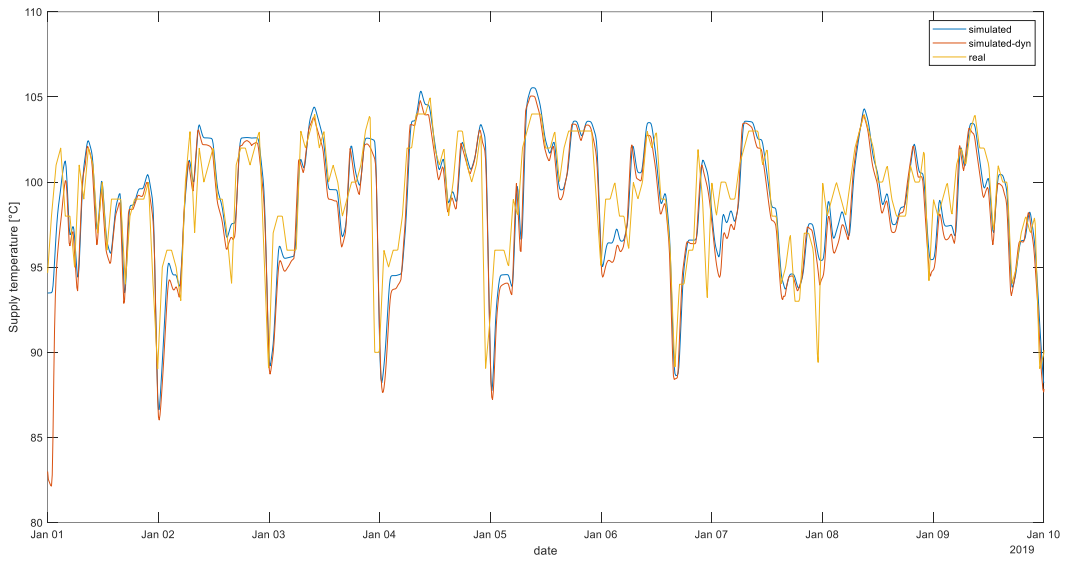


Figure 82 - Particular of figure 81.

As regards the delivery temperature, it is clearly necessary to start from the evaluation of the first pipe in the network. In fact, it has at the entrance the constraint imposed (real temperature in the first building increased taking into account the losses):

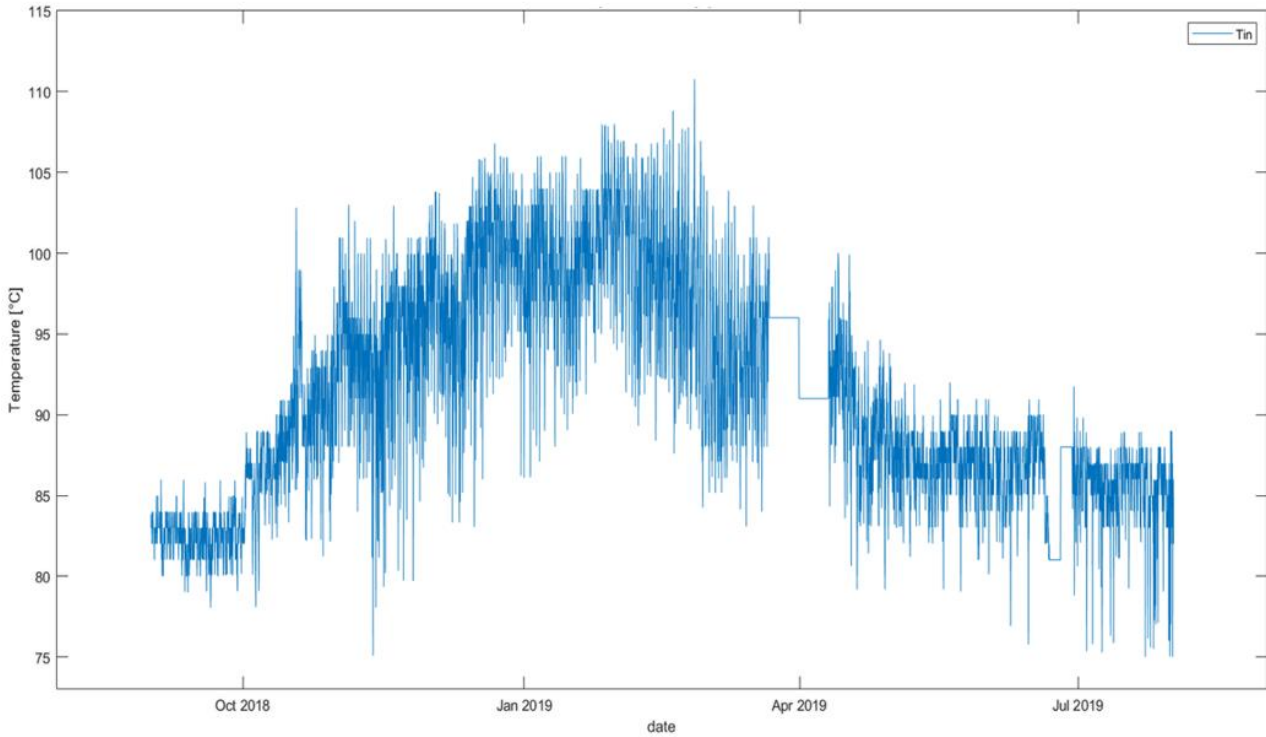


Figure 83 - Inlet temperature vs datetime for the first pipe in the network.

Subsequently, the inlet temperature to pipe 9 is shown (the last of the first main backbone). The graph shows a trend similar to that of the initial pipeline but offset both upwards and downwards. In fact, the heat dissipations will lead to a decrease in the inlet temperature to the final pipe, while in the event of a sudden change from a higher temperature to a lower one in the initial pipe, they will cause a higher supply temperature for pipe 9 due to the hydraulic transmissivity .

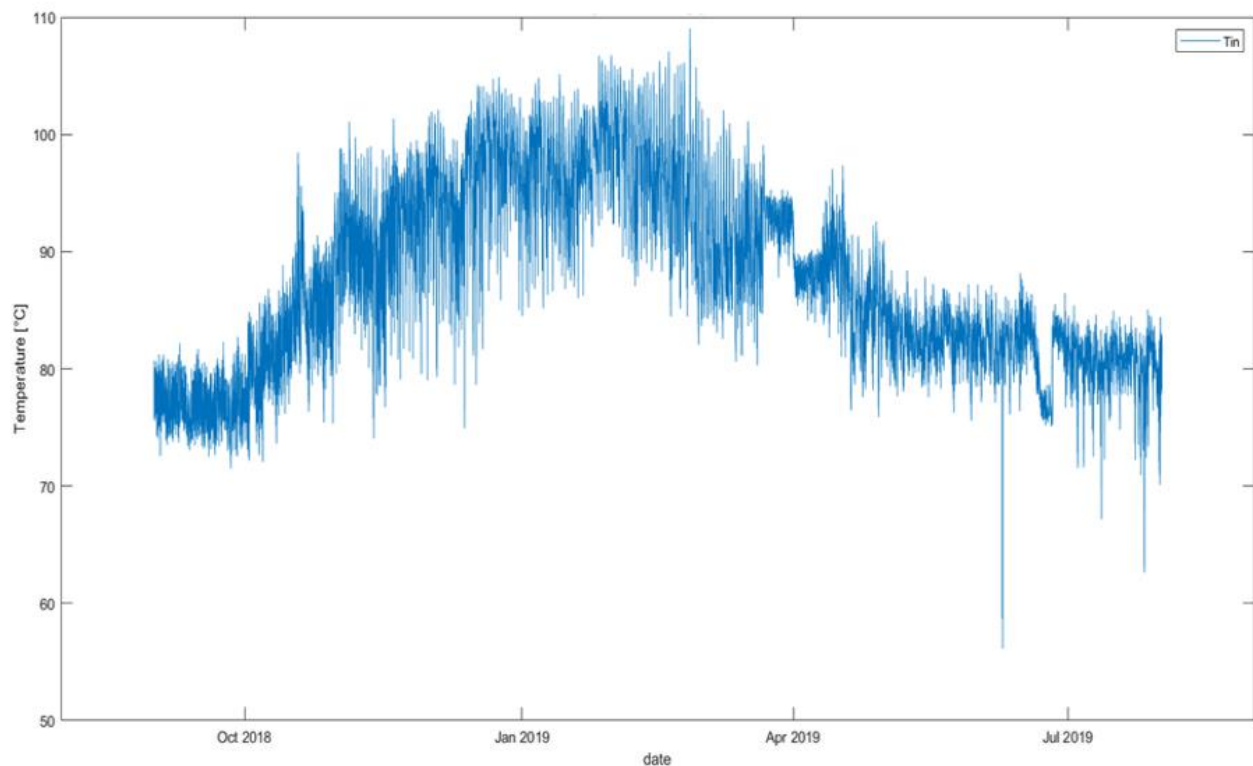


Figure 84 - Simulated inlet temperature of pipe 9.

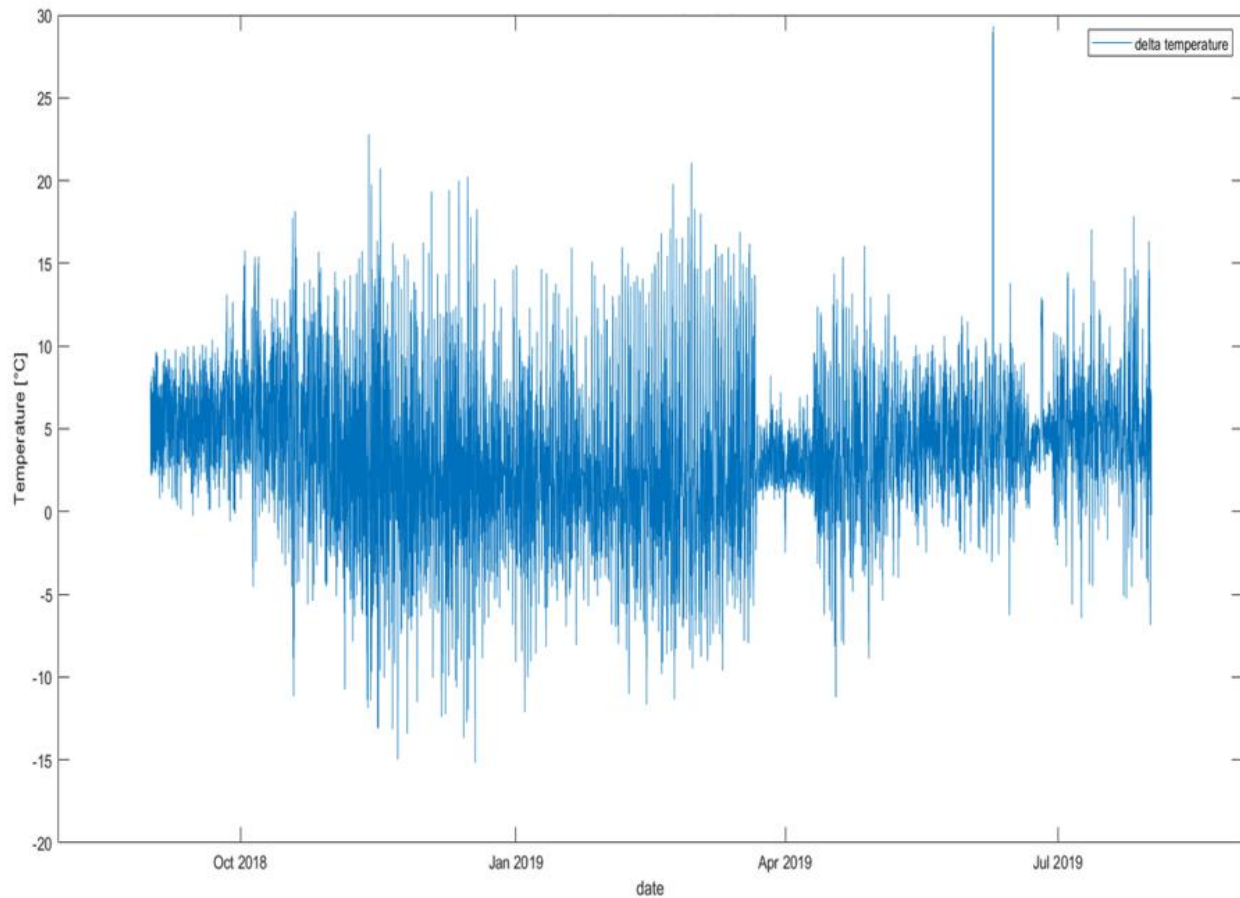


Figure 85 - Delta inlet temperature between first pipe and pipe 9.

Another situation that may arise is presented in the following graph. In the event that the flow rate is very close to zero for a sufficiently long interval of time, the temperature leaving the pipeline will go to the asymptote (the soil temperature assumed as constant equal to the average soil temperature in Grugliasco):

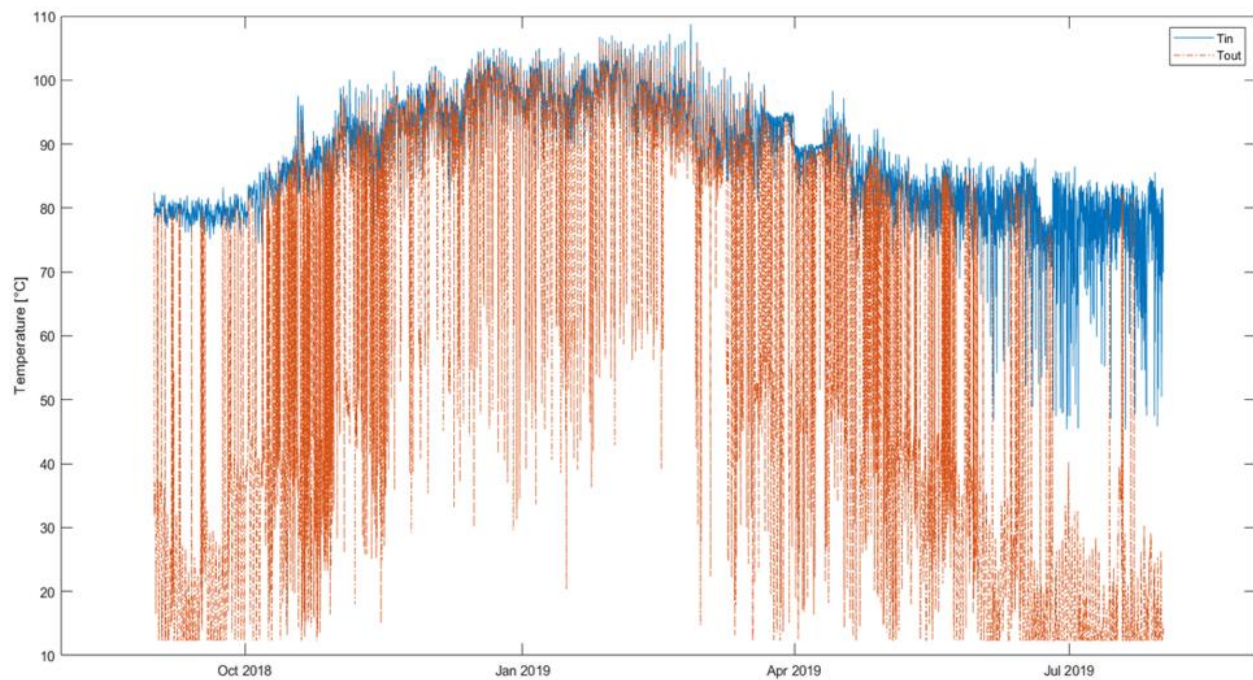


Figure 86 - Example of asymptote temperature reaching.

This graph shows the flow rate parameter related to the pipe considered in the previous graph:

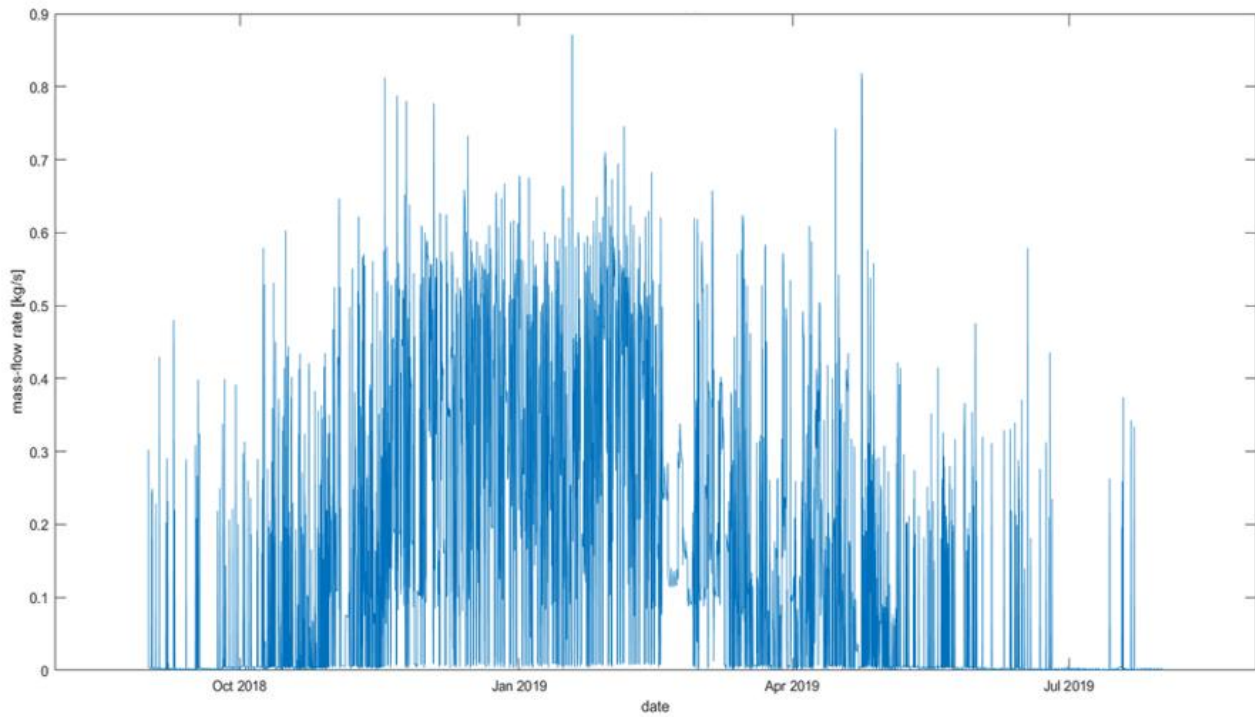
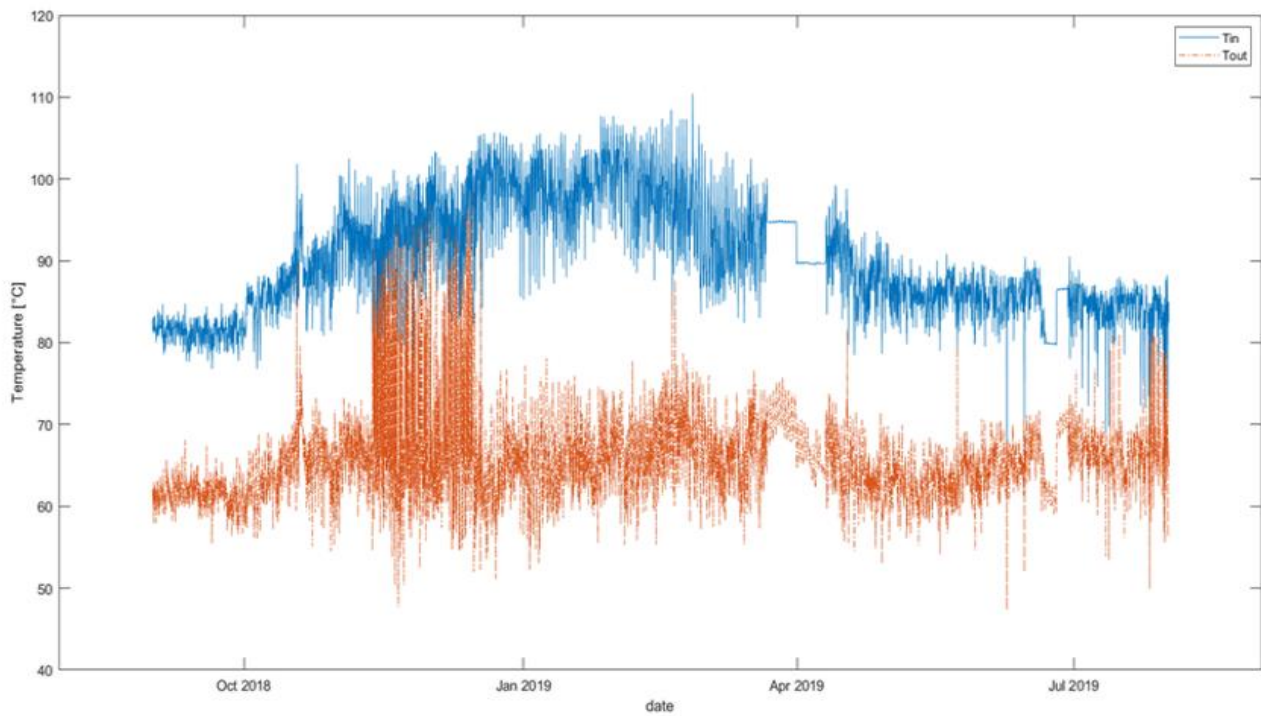


Figure 87 - Mass flow-rate vs date for the pipe analyzed.

The following figure shows the evolution of the temperature parameter at a substation :



*Figure 88 - Evolution of inlet and outlet temperature at a substation.*

It can be seen how the outlet temperature is greatly reduced following the exchange. Furthermore, high outlet temperatures occur when the flow-rate through the heat exchanger is reduced but the power required tends to zero, see subsequent figures.

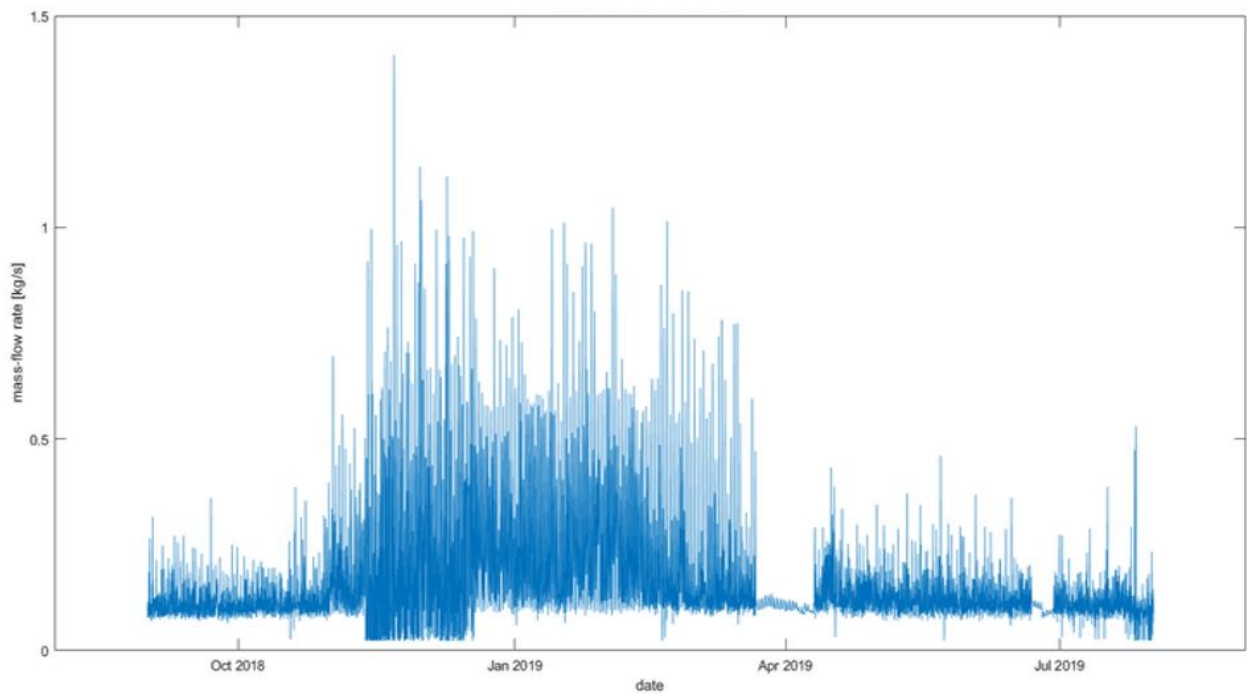


*Figure 89 - Mass flow-rate at substation.*

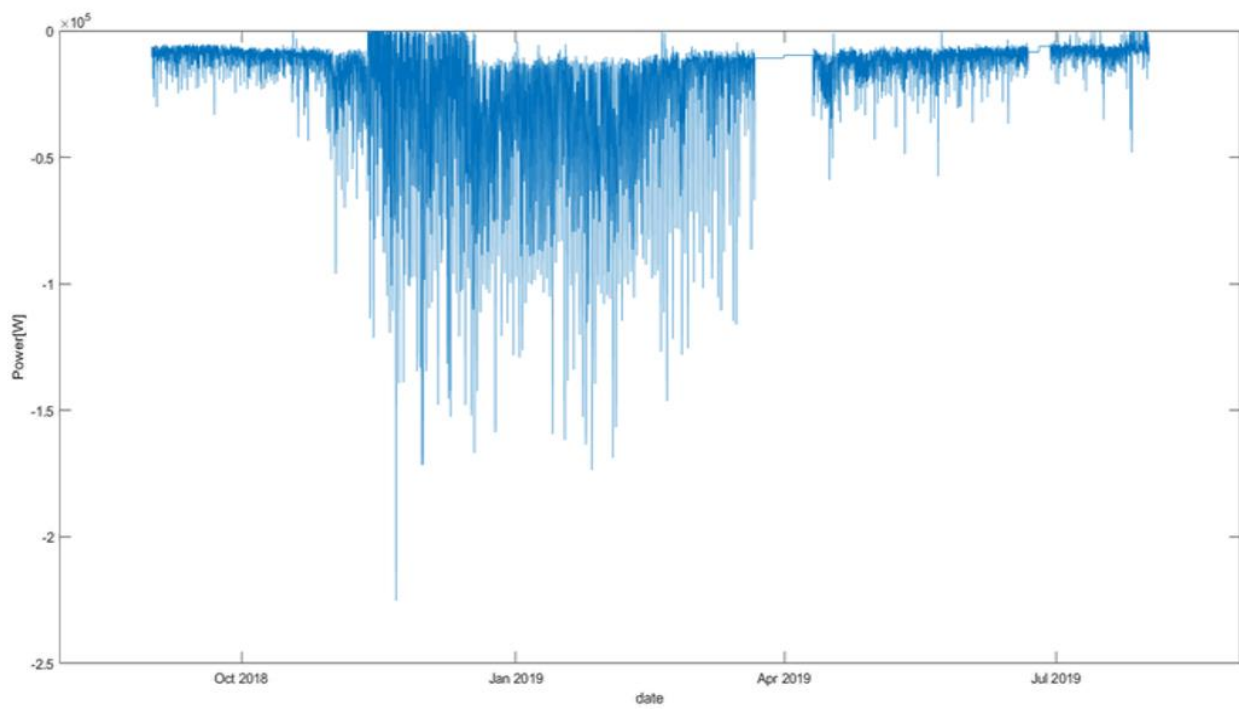


Figure 90 - Power exchanged at substation analyzed.

As regards the month of January, the surface maps of the inlet temperature to the pipes of the main backbone are reported on a daily and monthly basis:

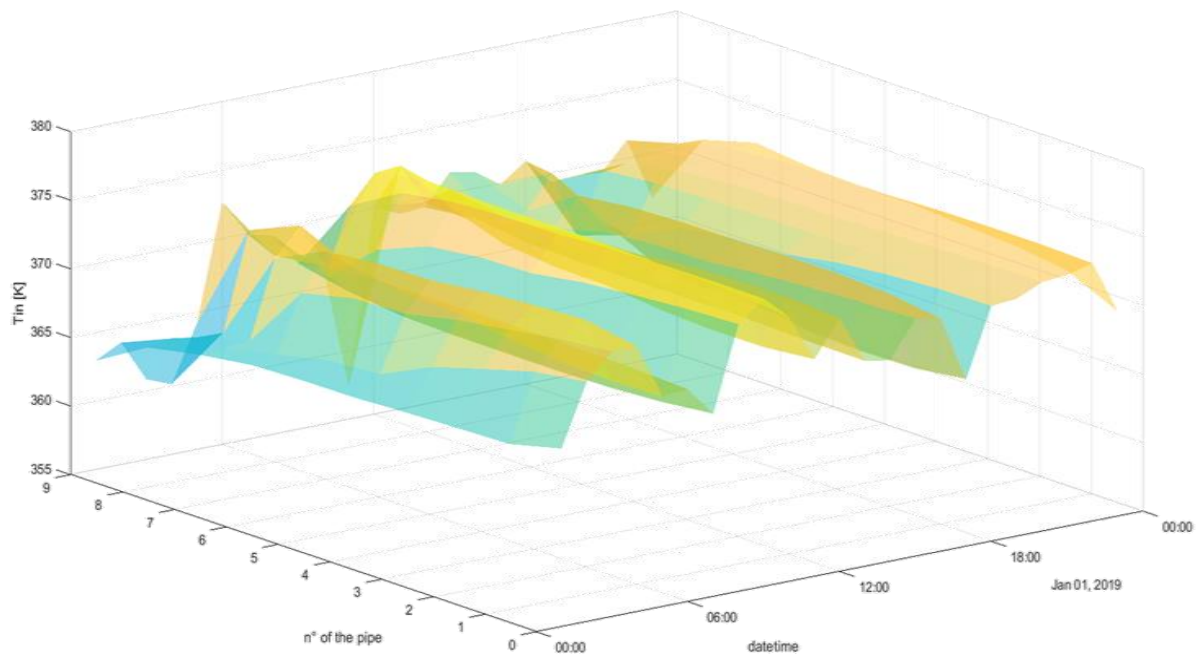


Figure 91 - Daily surface plot of inlet temperature for different pipes.

The daily surface shows the fact that the temperature at the last pipe can be greatly reduced if the flow through is small. It also shows a typical trend of the temperature evolution during the day with two peaks in the early morning (from 5:30 to 7 and from 10 to 11) and an evening peak before dinner time.

The chart on a monthly basis shows the repetition of what has been analyzed for the single day:

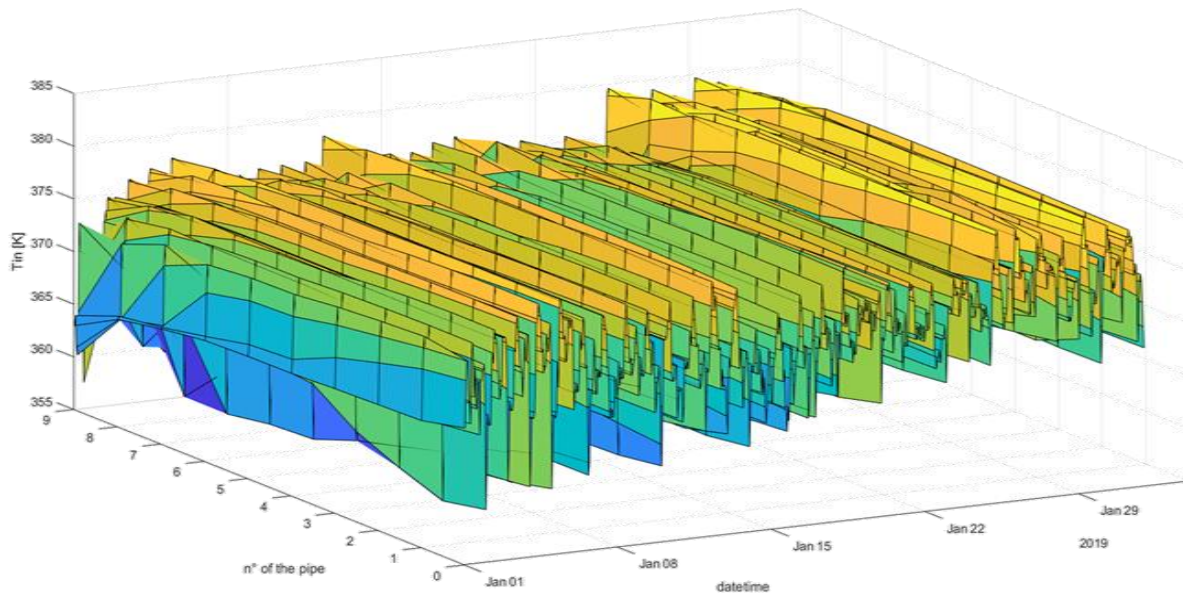


Figure 92 - Monthly surface plot of inlet temperature for different pipes.

## 7.1 Comparison with monitoring data

To fully define the work carried out, the simulated results were compared with the monitoring data.

Since it is known that it is necessary to consider the flow-rate circulating in the network equal to the sum of the flow-rates required by the substations under analysis, it was decided to compare the simulations with the monitoring data for the month of January. In fact, in this month, the users tend to require more heat and therefore the flow rate circulating in the network is greater. This tends to limit the greater heat losses that would be obtained from the model caused by a longer travel time of the carrier fluid inside the pipes. In fact, considering the sum of the flow rates of the users under analysis, the speed of the fluid inside the pipes will be reduced compared to the real case.

The comparison shows a high accuracy of the model despite the limitations related to simulating a portion of the network.

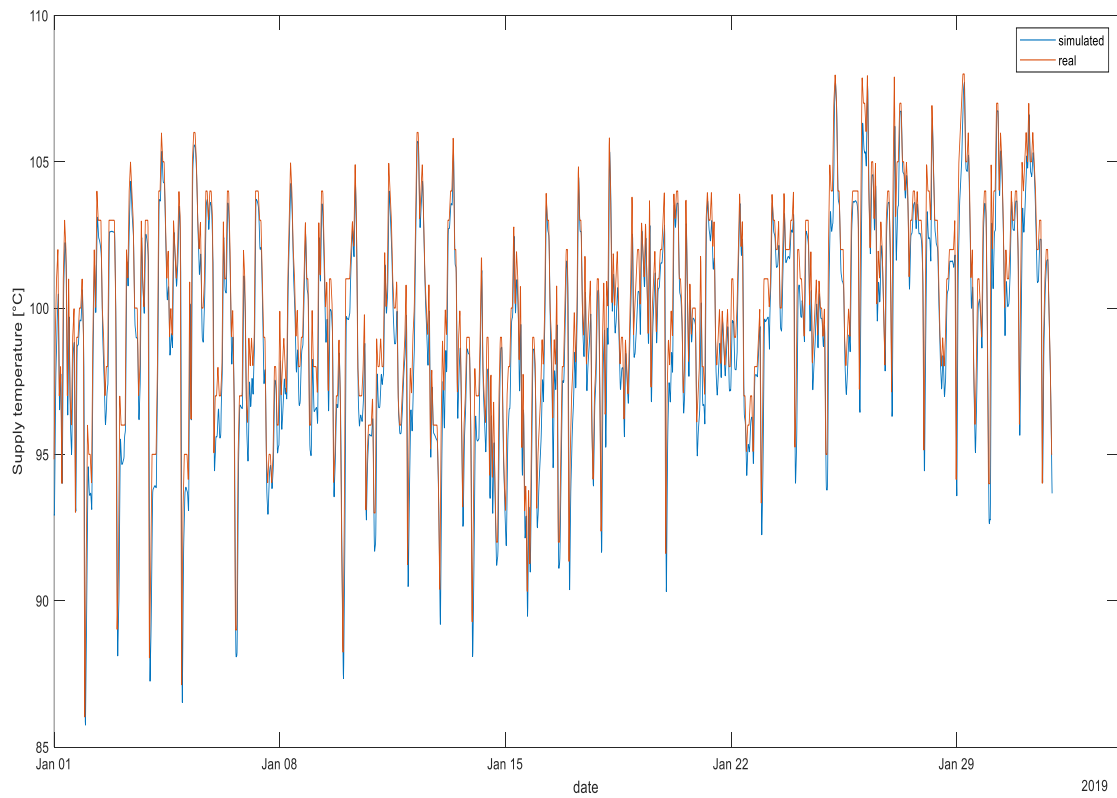


Figure 93 - Inlet temperature at substation 10243 simulated and real.

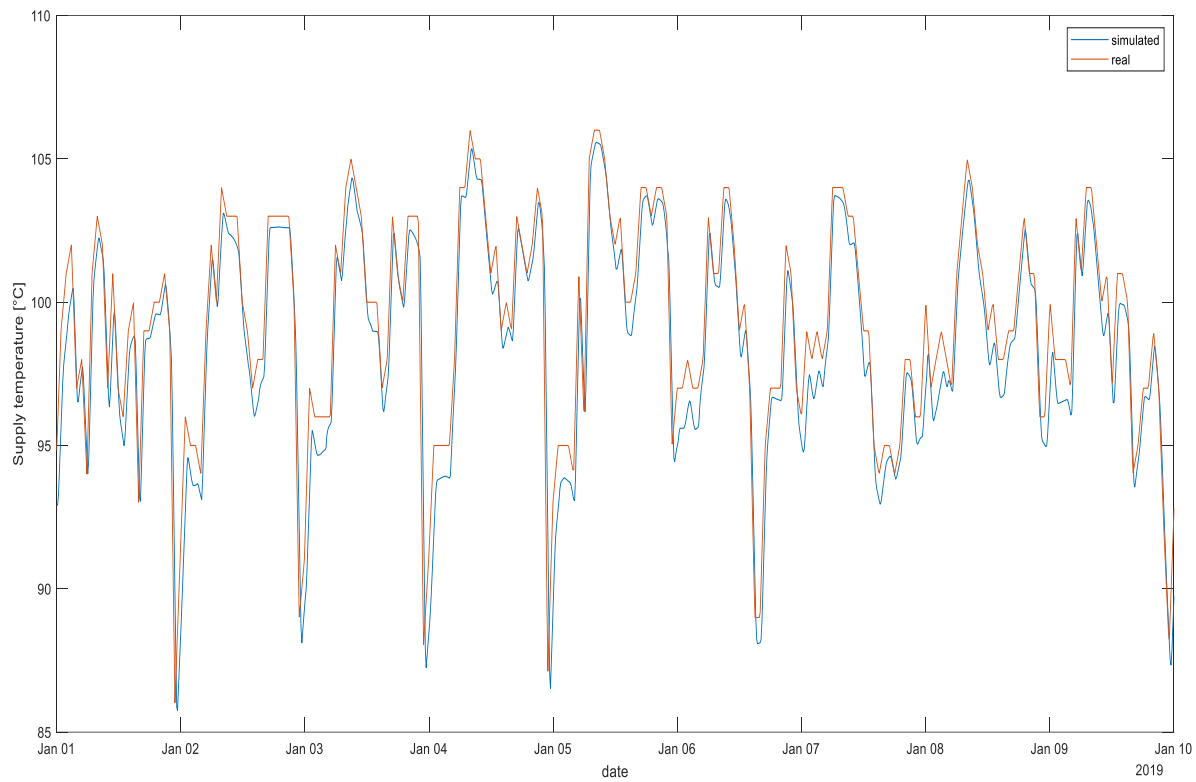


Figure 94 - Particular of figure 93.

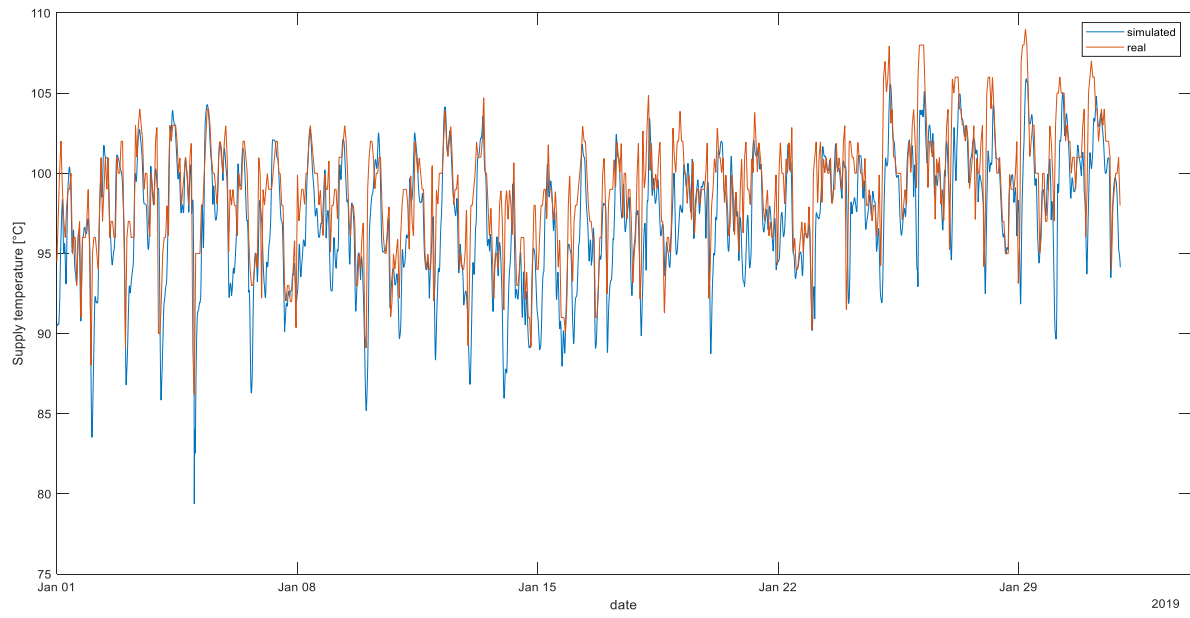


Figure 95 - Inlet temperature at substation 10110 simulated and real.

By way of example, results are reported for two other buildings:

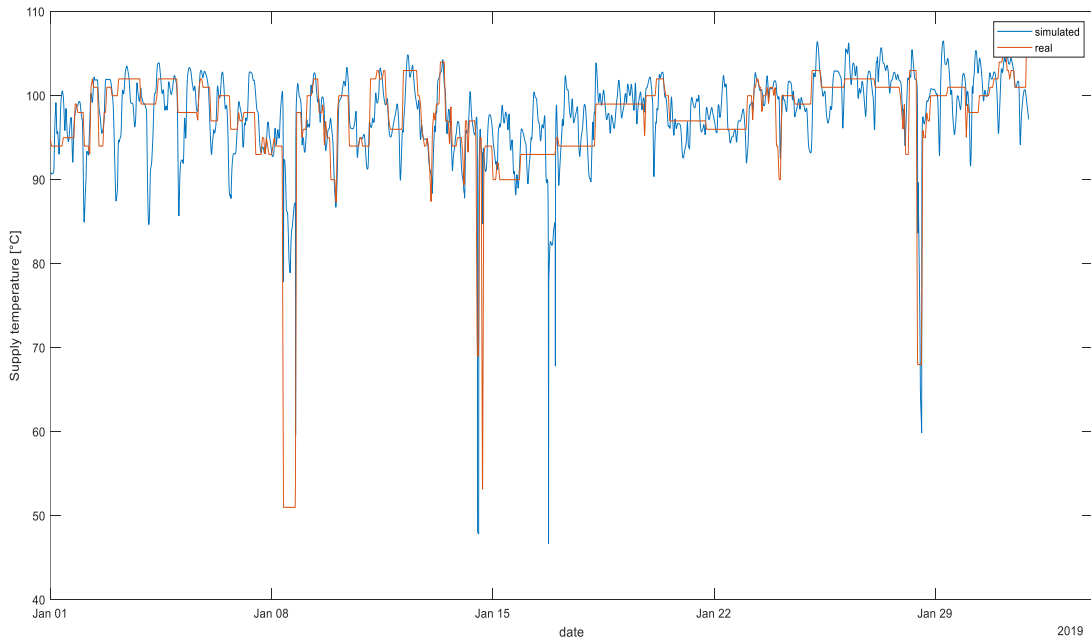


Figure 96 - Inlet temperature at substation 10552 simulated vs real.

Figure 96 shows that the real temperature presents a discordant trend to that obtained from the simulation. This is due to the fact that for that building in January the monitoring data are scarce and the interpolation of the data led to unreliable results (constant behavior through time) with respect to the actual operation. Figure 97 shows the diagram with the availability of hourly data for the various months. The diagram shows the availability of at least one data for each hour of the day. It can be seen that the building generally has less than 10 hourly data per day for the month of January. The simulation performed can therefore be a useful analysis tool for periods of missing data.

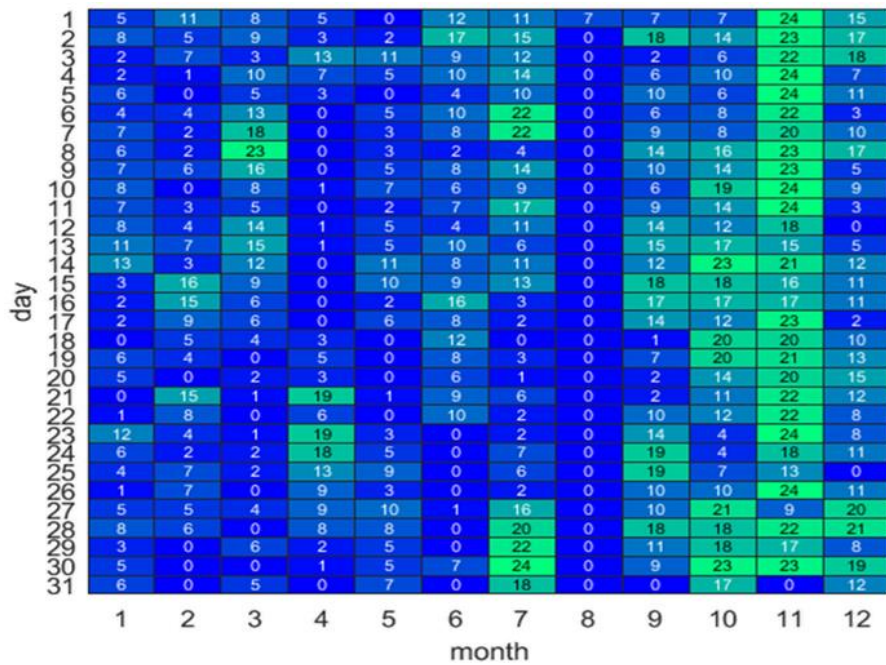
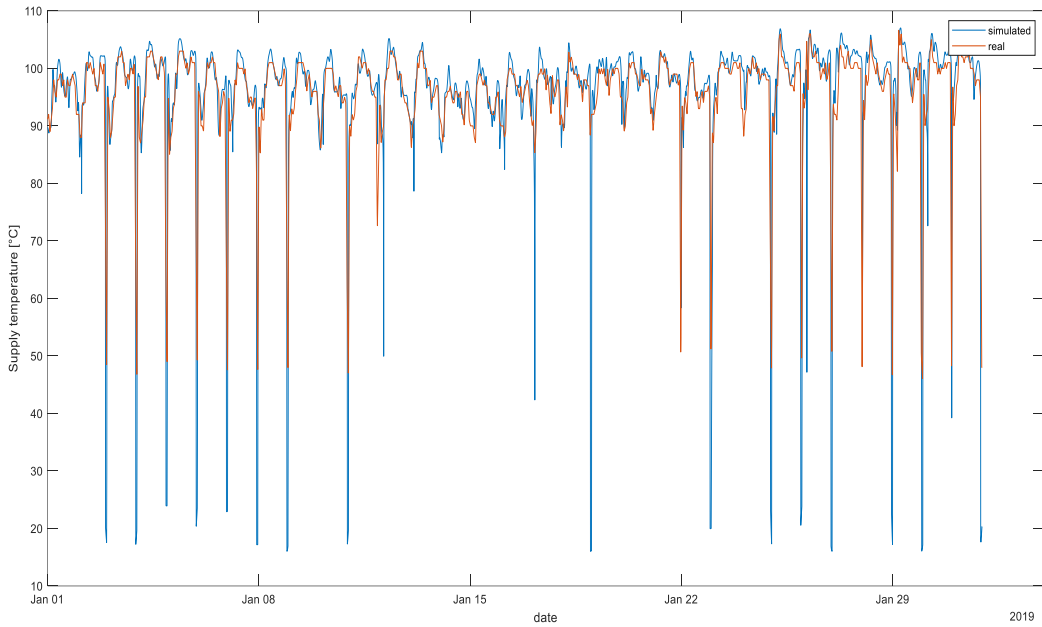


Figure 97 - Data availability for building 10552.

Another aspect to underline concerns a limitation of the model. In fact, the implemented models do not consider the inertial effects at the substation. This is shown in the graph below:



*Figure 98 - Inlet temperature at substation 10551 simulated vs real.*

The figure shows how if the flow rate to the substation is close to zero for several timesteps, the simulated temperature goes to a much lower value than the monitoring data. The inertia effects at the substation keep the temperature at a higher range in those instants.

To solve this problem, a volume of fluid could be concentrated at the outlet node of the pipeline entering the substation (lumped volume strategy). Since the results are reliable when the utilities require heat, the simulation is still considered reliable as well.

## 8. Conclusion

The goal of the thesis is the creation of reliable models in Modelica language for the simulation of district heating networks. In order to achieve the set objectives firstly a data analysis of monitoring data provided by Iren S.p.A. has been developed. The analysis provided useful information on the district heating network under analysis for the subsequent development of the model. In fact, only a few data were available for the users circuit which led to the decision to simulate only the primary circuit of the network. Other useful information concerned the temperatures at the substations in the different seasons and the hourly availability of the different quantities during the monitoring period. The analysis also highlighted the presence of a single pressure measurement point within the portion of the network analyzed.

Once the main operating mechanisms of the district heating network were understood through data analysis and thanks to precious personal communications with a technician of the district heating network, it was decided to proceed with the hydraulic analysis of the network. At this stage a new pipe model has been created. The model is able to evaluate the pressure losses of the network using the Haaland formula for distributed losses and the momentum conservation equation. Using the new pipe model created, through a back modeling technique starting from the known measurement point, it was possible to evaluate the inlet and outlet pressures to the network. Starting from the results obtained and using the measurement point as a benchmark, it was noted that an expression pressure as a function of the flow rate for the boundary conditions led to non-optimal results. It has been shown that these results are mainly caused by the limitation in simulating only a portion of the network.

Substations were then modeled through their characteristic elements (valves and heat exchangers).

Finally, thermal analysis was developed. The model previously created for hydraulic purposes was implemented to manage also the thermal variables. Following several analyzes of different pipe models created and comparing them with the dynamic pipe present in the MSL library, a type of pipe was chosen.

The main equations developed within this pipe model are those at the base of the spatial distribution function implemented in commercial software such as *Dymola* but not yet in *OpenModelica*. The results show the reliability of the model implemented and the significant shorter computation times than the dynamic pipe. Finally, to completely characterize the case study, a video of the evolution of the temperature in the delivery circuit was developed for the entire simulation period (September 2018 - July 2019).

The main limitations of the developed models concern the control of the valve at the substation. Due to lack of data on the secondary circuit, to define the through flow it was necessary to use a simplified statistical approach using interpolation plans based on the variables involved. Furthermore, another limitation of the model concerns the non-consideration of inertia effects at the substation. Finally, a limitation concerning not the model but the case study is the need to assume the flow rate circulating in the network portion equal to the sum of the flow rates required by the users.

While two of the limitations can be easily solved through greater data availability, the limitation concerning the effects of inertia at the substation can be solved by concentrating a volume in the outlet node of the pipe (lumped volume strategy).

In summary, the work led to reliable models for district heating network simulations and with acceptable computation times. The models could be used in other case study to analyze the actual operation of district heating networks and suggests improvement. In addition the models can be further developed through the implementation of other mathematical models such as lumped volume and the availability of data of the secondary circuit.

Finally, for the aggregative structures of the model it is possible to implement other models such as models that simulate the thermal demands of buildings through a study of the dispersions that can be connected with the models presented in the present work.

## ANNEX A

Some of the models implemented are shown below

a) Model for thermal and hydraulic simulation with possibility of flow reversal

```

model Haaland_pipe_pT6_2 "Pipe model"
  extends Modelica.Fluid.Interfaces.PartialTwoPortTransport(dp_start =
dp_nominal, m_flow_small = if system.use_eps_Re then system.eps_m_flow *
m_flow_nominal else system.m_flow_small, m_flow(stateSelect = if
momentumDynamics == Modelica.Fluid.Types.Dynamics.SteadyState then
StateSelect.default else StateSelect.prefer));
  extends Modelica.Fluid.Interfaces.PartialLumpedFlow(final pathLength = 0,
final momentumDynamics = Modelica.Fluid.Types.Dynamics.SteadyState);
  import pi = Modelica.Constants.pi;
  import e = Modelica.Constants.e;
  parameter Modelica.SIunits.Length diameter "Diameter of pipe" annotation(
    Dialog(group = "Pipe data"));
  parameter Modelica.SIunits.Length Length annotation(
    Dialog(group = "Pipe data"));
  parameter Modelica.SIunits.ThermalConductivity cond annotation(
    Dialog(group = "Pipe data"));
  parameter Modelica.SIunits.Temperature Tground annotation(
    Dialog(group = "Ground data"));
  parameter Modelica.SIunits.Length rug(displayUnit = "mm") = 0.00025
"Roughness" annotation(
  Dialog(group = "Pipe data"));
  parameter Modelica.SIunits.MassFlowRate m_flow_nominal = if system.use_eps_Re
then system.m_flow_nominal else 1e2 * system.m_flow_small "Mass flow rate for
dp_nominal" annotation(
  Dialog(group = "Nominal operating point"));
  parameter Modelica.SIunits.Length thickness "thickness of insulation"
annotation(
  Dialog(group = "Pipe data"));
  parameter Modelica.SIunits.Pressure dp_nominal = 1e3 "Nominal pressure drop"
annotation(
  Dialog(group = "Nominal operating point"));
  Medium.Density d = 0.5 * (Medium.density(state_a) + Medium.density(state_b));
  Modelica.SIunits.Pressure dp_fg(start = dp_start) "pressure loss due to
friction and gravity";
  Modelica.SIunits.Area A_mean = Modelica.Constants.pi / 4 * diameter ^ 2 "mean
cross flow area";
  Modelica.Blocks.Interfaces.RealOutput Q_flow(unit = "W");
  Modelica.SIunits.MassFraction Xi_instream[Medium.nXi];
protected
  Modelica.SIunits.SpecificEnthalpy hSet;
  Modelica.SIunits.Time taup = d * 4186 * pi * (diameter / 2) ^ 2 / (2 * cond *
pi * log(diameter / (2 * diameter / 2 + thickness) / (diameter / 2)));
  Modelica.SIunits.Time tau;
  // Variables
equation
// if port_a contains the variables
// p, h, and Xi
if noEvent(port_a.m_flow>0)
  tau =noEvent( floor(Length / ((port_a.m_flow + 0.00001) * 4 / (1000 * pi *
diameter ^ 2))));
```

```

hSet = Medium.specificEnthalpy(Medium.setState_pTX(p = port_b.p, T = Tground
+ (max(delay(port_a_T, tau, 2671200),Tground) - Tground) * e ^ (-Length /
(m_flow / (d * pi * diameter ^ 2 / 4)) / taup)));
Q_flow = m_flow * (hSet - inStream(port_a.h_outflow));
Xi_instream = inStream(port_a.Xi_outflow);
port_a.h_outflow = inStream(port_a.h_outflow);
port_b.h_outflow = hSet;
F_fg = A_mean * dp_fg;
else
    tau = noEvent( floor(Length / ((abs(port_a.m_flow) + 0.00001) * 4 / (d * pi *
diameter ^ 2)));
    hSet = Medium.specificEnthalpy(Medium.setState_pTX(p = port_a.p, T = Tground
+ (max(delay(port_a_T, tau, 2671200),Tground) - Tground) * e ^ (-Length /
(m_flow / (d * pi * diameter ^ 2 / 4)) / taup)));
    Q_flow = m_flow * (hSet - inStream(port_a.h_outflow));
    Xi_instream = inStream(port_a.Xi_outflow);
    port_a.h_outflow = hSet;
    port_b.h_outflow = inStream(port_b.h_outflow);
    F_fg = -A_mean * dp_fg;
end if;
Ib_flow = 0;
F_p = A_mean * (Medium.pressure(state_b) - Medium.pressure(state_a));
dp_fg = 1 / (-1.8 * log10((rug / diameter / 3.7) ^ 1.11 + 6.9 /
Modelica.Fluid.Pipes.BaseClasses.CharacteristicNumbers.ReynoldsNumber(noEvent(ab
s(port_a.m_flow)) / A_mean / d, d, Medium.dynamicViscosity(state_a), diameter)))
^ 2 * Length / diameter * 0.5 * d * (m_flow / A_mean / d) ^ 2;
annotation(
    defaultComponentName = "Pipe",
    Icon(coordinateSystem(preserveAspectRatio = false, initialScale = 0.1),
graphics = {Rectangle(origin = {0, -1}, fillColor = {0, 85, 255}, fillPattern =
FillPattern.HorizontalCylinder, extent = {{-100, 35}, {100, -35}}),
Ellipse(origin = {-3, 62}, fillColor = {0, 255, 255}, fillPattern =
FillPattern.Solid, extent = {{-57, -14}, {57, 14}}, endAngle = 360), Text(origin
= {-3, 63}, extent = {{-49, -13}, {49, 13}}, textString = "Heat loss to the
ground")}),
    uses(Modelica(version = "3.2.3")));
end Haaland_pipe_pT6_2;

```

- b) Pipe model for thermal and hydraulic simulation considering different specific shape factor (that considers also pipe level underground) and no flow reversal.

```

model Haaland_pipe_pT6_22 "Pipe model"
    extends Modelica.Fluid.Interfaces.PartialTwoPortTransport(dp_start =
dp_nominal, m_flow_small = if system.use_eps_Re then system.eps_m_flow *
m_flow_nominal else system.m_flow_small, m_flow(stateSelect = if
momentumDynamics == Modelica.Fluid.Types.Dynamics.SteadyState then
StateSelect.default else StateSelect.prefer));
    extends Modelica.Fluid.Interfaces.PartialLumpedFlow(final pathLength =
0, final momentumDynamics = Modelica.Fluid.Types.Dynamics.SteadyState);
    import pi = Modelica.Constants.pi;
    import e = Modelica.Constants.e;
    parameter Modelica.SIunits.Length diameter "Diameter of pipe"
annotation(
    Dialog(group = "Pipe data"));
    parameter Modelica.SIunits.Length Length annotation(
        Dialog(group = "Pipe data"));

```

```

parameter Modelica.SIunits.ThermalConductivity cond annotation(
  Dialog(group = "Pipe data"));
parameter Modelica.SIunits.Temperature Tground annotation(
  Dialog(group = "Ground data"));
parameter Modelica.SIunits.Length rug(displayUnit = "mm") = 0.00025
"Roughness" annotation(
  Dialog(group = "Pipe data"));
parameter Modelica.SIunits.MassFlowRate m_flow_nominal = if
system.use_eps_Re then system.m_flow_nominal else 1e2 *
system.m_flow_small "Mass flow rate for dp_nominal" annotation(
  Dialog(group = "Nominal operating point"));
parameter Modelica.SIunits.Length thickness "thickness of insulation"
annotation(
  Dialog(group = "Pipe data"));
parameter Modelica.SIunits.Pressure dp_nominal = 1e3 "Nominal pressure
drop" annotation(
  Dialog(group = "Nominal operating point"));
Medium.Density d = 0.5 * (Medium.density(state_a) +
Medium.density(state_b));
Modelica.SIunits.Pressure dp_fg(start = dp_start) "pressure loss due to
friction and gravity";
Modelica.SIunits.Area A_mean = Modelica.Constants.pi / 4 * diameter ^ 2
"mean cross flow area";

Modelica.Blocks.Interfaces.RealOutput Q_flow(unit = "W");
Modelica.SIunits.MassFraction Xi_instream[Medium.nXi];
Modelica.SIunits.Time tau;
protected
  Modelica.SIunits.SpecificEnthalpy hSet;

  Modelica.SIunits.Time
R=1/(2*pi*cond)*log((diameter+2*thickness)/diameter)+1/(2*pi*2.4)*log(2/(
diameter+2*thickness));
  Modelica.SIunits.Time C=pi*diameter^2/4*4186*d;
  // Variables
initial equation
  tau=Length/(m_flow/(pi*diameter^2/4*d));
equation
  der(tau)=1-m_flow/delay(m_flow,tau,2671200);
  hSet = Medium.specificEnthalpy(Medium.setState_pTX(p = port_b.p, T =
Tground + (max(delay(port_a_T, tau, 2671200), Tground) - Tground) * e ^
(-tau / (R*C)) );
  Q_flow = m_flow * (hSet - inStream(port_a.h_outflow));
  Xi_instream = inStream(port_a.Xi_outflow);
  port_a.h_outflow = inStream(port_a.h_outflow);
  port_b.h_outflow = hSet;
  F_fg = A_mean * dp_fg;
  Ib_flow = 0;
  F_p = A_mean * (Medium.pressure(state_b) - Medium.pressure(state_a));
  dp_fg = 1 / (-1.8 * log10((rug / diameter / 3.7) ^ 1.11 + 6.9 /
Modelica.Fluid.Pipes.BaseClasses.CharacteristicNumbers.ReynoldsNumber(noE
vent(abs(port_a.m_flow)) / A_mean / d, d,
Medium.dynamicViscosity(state_a), diameter))) ^ 2 * Length / diameter *
0.5 * d * (m_flow / A_mean / d) ^ 2;
  annotation(
    defaultComponentName = "Pipe",

```

```

Icon(coordinateSystem(preserveAspectRatio = false, initialScale =
0.1), graphics = {Rectangle(origin = {0, -1}, fillColor = {0, 85, 255},
fillPattern = FillPattern.HorizontalCylinder, extent = {{-100, 35}, {100,
-35}}), Ellipse(origin = {-3, 62}, fillColor = {0, 255, 255}, fillPattern
= FillPattern.Solid, extent = {{-57, -14}, {57, 14}}), endAngle = 360),
Text(origin = {-3, 63}, extent = {{-49, -13}, {49, 13}}), textString =
"Heat loss to the ground"))),
uses(Modelica(version = "3.2.3")));
end Haaland_pipe_pT6_22;

```

### c) Heat exchanger

```

model HX "Hx prescribed heat flow rate"
  extends Modelica.Fluid.Interfaces.PartialTwoPortTransport(dp_start =
dp_nominal, m_flow_small = if system.use_eps_Re then system.eps_m_flow *
m_flow_nominal else system.m_flow_small, m_flow(stateSelect = if
momentumDynamics == Modelica.Fluid.Types.Dynamics.SteadyState then
StateSelect.default else StateSelect.prefer));
  extends Modelica.Fluid.Interfaces.PartialLumpedFlow(final pathLength =
0, final momentumDynamics = Modelica.Fluid.Types.Dynamics.SteadyState);
parameter Modelica.SIunits.Pressure dp_nominal = 1e3 "Nominal pressure
drop" annotation(
  Dialog(group = "Nominal operating point"));

  Modelica.SIunits.Pressure dp_fg(start = dp_start) "pressure loss due to
friction and gravity";
  Modelica.SIunits.Area A_mean = 1 "mean cross flow area";

  Modelica.Blocks.Interfaces.RealInput u(unit = "1") "Control input"
annotation(
  Placement(transformation(extent = {{-140, 40}, {-100, 80}}));
  Modelica.SIunits.MassFraction Xi_instream[Medium.nXi];
  Modelica.Blocks.Interfaces.RealOutput Q_flow annotation(
    Placement(visible = true, transformation(origin = {-42, 40}, extent =
{{-10, -10}, {10, 10}}), rotation = 0), iconTransformation(origin = {-42,
40}, extent = {{-10, -10}, {10, 10}}), rotation = 0));
protected
Modelica.SIunits.SpecificEnthalpy hSet;
equation

hSet=Q_flow/(m_flow)+inStream(port_a.h_outflow);

Xi_instream = inStream(port_a.Xi_outflow);
port_a.h_outflow = inStream(port_b.h_outflow);
port_b.h_outflow = hSet;
F_fg = A_mean * dp_fg;
dp_fg=dp_start;
Ib_flow = 0;
F_p = A_mean * (Medium.pressure(state_b) - Medium.pressure(state_a));
connect(u, Q_flow) annotation(
  Line(points = {{-120, 60}, {-80, 60}, {-80, 40}, {-42, 40}, {-42,
40}}, color = {0, 0, 127}));
annotation(

```

```

Icon(coordinateSystem(preserveAspectRatio = false, initialScale =
0.1), graphics = {Rectangle(lineColor = {0, 0, 255}, pattern =
LinePattern.None, fillPattern = FillPattern.Solid, extent = {{-100, 8},
{101, -5}}), Polygon(fillColor = {127, 0, 0}, pattern = LinePattern.None,
fillPattern = FillPattern.Solid, points = {{-70, -60}, {70, 60}, {-70,
60}, {-70, -60}}), Polygon(fillColor = {0, 0, 127}, pattern =
LinePattern.None, fillPattern = FillPattern.Solid, points = {{-70, -60},
{70, 60}, {70, -60}, {-70, -60}}), Rectangle(lineColor = {0, 0, 255},
fillColor = {0, 0, 127}, pattern = LinePattern.None, fillPattern =
FillPattern.Solid, extent = {{70, 60}, {100, 58}}), Text(lineColor =
{255, 255, 255}, extent = {{-56, -12}, {54, -72}}, textString =
"Q=%Q_flow_nominal"), Rectangle(lineColor = {0, 0, 255}, fillColor = {0,
0, 127}, pattern = LinePattern.None, fillPattern = FillPattern.Solid,
extent = {{-100, 60}, {-70, 58}}), Text(lineColor = {0, 0, 127}, extent =
{{-122, 106}, {-78, 78}}, textString = "u"), Text(lineColor = {0, 0,
127}, extent = {{72, 96}, {116, 68}}, textString = "Q_flow")),
defaultComponentName = "hx",
uses(Modelica(version = "3.2.3")));
end HX;

```

## d) Valve

```

model Valve_me4 "Valve"
  extends Modelica.Fluid.Interfaces.PartialTwoPortTransport;
  Modelica.Blocks.Interfaces.RealInput Test annotation(
    Placement(visible = true, transformation(origin = {0, 90}, extent =
{{-20, -20}, {20, 20}}), rotation = 270), iconTransformation(origin = {24,
80}, extent = {{-20, -20}, {20, 20}}), rotation = 270));
  parameter Real coefficient[4] "b1 b2 b3 b4" annotation(
    Dialog(group = "Coefficients"));
  Modelica.Blocks.Interfaces.RealInput Pot annotation(
    Placement(visible = true, transformation(origin = {36, 90}, extent =
{{-20, -20}, {20, 20}}), rotation = 270), iconTransformation(origin = {-
24, 80}, extent = {{-20, -20}, {20, 20}}), rotation = 270));
equation
  m_flow=abs(coefficient[1] + coefficient[2] * Test + coefficient[3] * Pot
+ coefficient[4] * Pot * Test)+0.00003;
  //m_flow=20;

// Isenthalpic state transformation (no storage and no loss of energy)
port_a.h_outflow = inStream(port_b.h_outflow);
port_b.h_outflow = inStream(port_a.h_outflow);
annotation(
  Icon(coordinateSystem(initialScale = 0.1), graphics = {Line(points =
{{0, 50}, {0, 0}}), Rectangle(fillPattern = FillPattern.Solid, extent =
{{-36, 60}, {38, 50}}), Polygon(fillColor = {255, 255, 255}, fillPattern
= FillPattern.Solid, points = {{-100, 50}, {100, -50}, {100, 50}, {0, 0},
{-100, -50}, {-100, 50}}), Polygon(lineColor = {255, 255, 255}, fillColor
= {0, 255, 0}, fillPattern = FillPattern.Solid, points = {{-100, 0},
{100, 0}, {100, 0}, {0, 0}, {-100, 0}, {-100, 0}}), Polygon(points = {{-
100, 50}, {100, -50}, {100, 50}, {0, 0}, {-100, -50}, {-100, 50}})},
uses(Modelica(version = "3.2.3"))));

```

```
end Valve_me4;
```

e) Substation

```
model exc2
```

```

replaceable package Medium = Modelica.Media.Interfaces.PartialMedium
"Medium in the component" annotation(
    choicesAllMatching = true);
Modelica.Blocks.Interfaces.RealInput Test annotation(
    Placement(visible = true, transformation(origin = {20, 110}, extent =
{{-20, -20}, {20, 20}}), rotation = 270), iconTransformation(origin = {24,
80}, extent = {{-20, -20}, {20, 20}}), rotation = 270));
Modelica.Blocks.Interfaces.RealInput Pot annotation(
    Placement(visible = true, transformation(origin = {-16, 106}, extent =
{{-20, -20}, {20, 20}}), rotation = 270), iconTransformation(origin = {-
24, 80}, extent = {{-20, -20}, {20, 20}}), rotation = 270));
parameter Real coefficient[4] "b1 b2 b3 b4" annotation(
    Dialog(group = "Coefficients"));
parameter Modelica.SIunits.MassFlowRate m_flow_nominal annotation(
    Dialog(group = "Exchanger"));
parameter Modelica.SIunits.Pressure dp_nominal annotation(
    Dialog(group = "Exchanger"));
parameter Modelica.SIunits.Temperature T_start annotation(
    Dialog(group = "Exchanger"));
Modelica.Fluid.Interfaces.FluidPort_a Fluid_port_a annotation(
    Placement(visible = true, transformation(origin = {-100, -2}, extent =
{{-10, -10}, {10, 10}}), rotation = 0), iconTransformation(origin = {-
104, -10}, extent = {{-10, -10}, {10, 10}}), rotation = 0));
Modelica.Fluid.Interfaces.FluidPort_b Fluid_port_b annotation(
    Placement(visible = true, transformation(origin = {100, -2}, extent =
{{-10, -10}, {10, 10}}), rotation = 0), iconTransformation(origin = {98, -
8}, extent = {{-10, -10}, {10, 10}}), rotation = 0));
ValveLinear_me4 Valve_me4(redeclare package Medium=Medium, coefficient =
coefficient) annotation(
    Placement(visible = true, transformation(origin = {-24, 0}, extent =
{{-10, -10}, {10, 10}}), rotation = 0));
HeaterSimple1 HX(redeclare package Medium=Medium) annotation(
    Placement(visible = true, transformation(origin = {32, 0}, extent =
{{-10, -10}, {10, 10}}), rotation = 0));
equation
    connect(Valve_me4.port_a, Fluid_port_a) annotation(
        Line(points = {{-34, 0}, {-98, 0}, {-98, -2}, {-100, -2}}, color =
{0, 127, 255}));
    connect(Pot, Valve_me4.Pot) annotation(
        Line(points = {{-16, 106}, {-16, 106}, {-16, 32}, {-28, 32}, {-28,
8}, {-26, 8}}, color = {0, 0, 127}));
    connect(Test, Valve_me4.Test) annotation(
        Line(points = {{20, 110}, {20, 110}, {20, 32}, {-8, 32}, {-8, 16}, {-
22, 16}, {-22, 8}, {-22, 8}}, color = {0, 0, 127}));
    connect(Valve_me4.port_b, HX.port_a) annotation(
        Line(points = {{-14, 0}, {22, 0}, {22, 0}, {22, 0}}, color = {0, 127,
255}));
    connect(HX.port_b, Fluid_port_b) annotation(

```

```
    Line(points = {{42, 0}, {102, 0}, {102, -2}, {100, -2}}, color = {0,  
127, 255});  
    connect(Pot, HX.u) annotation(  
        Line(points = {{-16, 106}, {-16, 106}, {-16, 6}, {20, 6}, {20, 6}},  
color = {0, 0, 127}));  
end exc2;
```

## References

- [1] Danielewicz, J., Śniechowska, B., Sayegh, M.A., Fidorów, N. and Jouhara, H., (2016), *Three-dimensional numerical model of heat losses from district heating network pre-insulated pipes buried in the ground.*
- [2] Sven Werner, *International review of district heating and cooling, Energy, Volume 137, 2017, Pages 617-631.*
- [3] MISE, "Piano energia e clima", implementation of the regulation (EU), 2018/1999.
- [4] E. Parliament, Directive (EU) 2018/2001.
- [5] MINISTRY OF PRODUCTION ACTIVITIES, MINISTER OF THE ENVIRONMENT, Update of the directives for the promotion of electricity produced from renewable sources pursuant to article 11, paragraph 5, of legislative decree no. 79.
- [6] Decree of the President of Republic, Implementation of Directive 2009/28 / EC on the promotion of the use of energy from renewable sources, amending and subsequently repealing Directives 2001/77 / EC and 2003/30 / EC..
- [7] MISE, Definition of the new support scheme for high-efficiency cogeneration..
- [8] Decree of the President of the Republic, *Legislative Decree 102/2014, Implementation of the 2012/27 / EU directive on energy efficiency..*
- [9] EuroHeat&Power with Halmstad University. *Heat Roadmap Europe 2050 - Prestudy.euroheat.org.* 2012.
- [10] Acea energia - Teleriscaldamento-specifica tecnica 13/06/2011.
- [11] Ali Keçebaş, Mehmet Ali Alkan, Mustafa Bayhan, *Thermo-economic analysis of pipe insulation for district heating piping systems, Applied Thermal Engineering, Volume 31, Issues 17–18,, 2011.*
- [12] Nuri Sisman, *Determination of optimum insulation thicknesses of the external walls and roof (ceiling) for Turkey's different degree-day regions, Energy Policy, Volume 35, Issue 10,, 2007.*
- [13] S. Meli, *DEM Working Paper Series, Il Settore del Teleriscaldamento in Italia:Struttura e Assetto Regolatorio,* 2016.
- [14] «[https://www.gse.it/documenti\\_site/Documenti%20GSE/Rapporti%20statistici/Nota%20TLR%202020%20-%20GSE.pdf](https://www.gse.it/documenti_site/Documenti%20GSE/Rapporti%20statistici/Nota%20TLR%202020%20-%20GSE.pdf),» [Online].
- [15] Ralf Starkloff, Falah AlObaid, Karl Karner, Bernd Epple, Martin Schmitz, Felix Boehm, *Development and validation of a dynamic simulation model for a large coal-fired power plant, Applied Thermal Engineering, Volume 91, 2015, Pages 496-506.*
- [16] Lubomir Vasek, *Pulled Plug-flow Model for 4th Generation District Heating, IFAC-PapersOnLine, Volume 52, Issue 4, 2019, Pages 12-17.*

- [17] Gabrielaitiene I, *Application of the finite element method for modelling of district heating networks.* vol. 9. University of Ljubljana: Digital Library of Construction Informatics and Information Technology in Civil Engineering and Construction; 2001..
- [18] V. Stevanovic, *Prediction of thermal transients in district heating systems.* Energy Convers Manage 2009;50:2167–73..
- [19] Grosswindhager S, Voigt A, Kozek M., *Efficient physical modelling of district heating networks.* Model Simul Calgary A 2011..
- [20] Bennonysson A. *Dynamic modelling and operation optimization of district heating systems.* PhD thesis. Denmark: Technical University of Denmark (DTU); 1991..
- [21] J. Pálsson , *Equivalent models of district heating systems for on-line minimization of operational costs of the complete district heating system.* Tech rep 1323. Technical University of Denmark; 1999..
- [22] Velut, Stéphane & Tummescheit, Hubertus. (2011). *Implementation of a transmission line model for fast simulation of fluid flow dynamics..*
- [23] B. van der Heijde, M. Fuchs, *Dynamic equation-based thermo-hydraulic pipe model for district heating and cooling systems,* Energy Conversion and Management, Volume 151, 2017.
- [24] P. Fritzson, *Principles of object-oriented modeling and simulation with MODELICA 3.3.*
- [25] «<https://www.openmodelica.org/>,» [Online].
- [26] M. Association, *Modelica standard library.*
- [27] D. Grattarola, *Produzione e distribuzione di calore mediante reti di teleriscaldamento: modellizzazione e analisi della rete di Rivoli, Grugliasco e Collegno e possibile allacciamento al termovalorizzatore di Gerbido..*
- [28] Vittorio Verda, Sciacovelli Adriano, *Numerical design of thermal systems..*
- [29] Siemens, *Basic documentation for the rvd230 control unit.*
- [30] PREMANT *district heating line technical data sheet.*
- [31] «<https://it.climate-data.org/europa/italia/piemonte/grugliasco-13507/>,» [Online].
- [32] IBSA, *Modelica DisHeatLib library.*
- [33] D. M. M. Tiller, *Modelica by Example.*
- [34] ENEA, *Rapporto ENEA 2014, Analisi e caratterizzazione metrologica dei sistemi di misura delle reti termiche distribuite.*
- [35] «<https://www.openmodelica.org/>,» [Online].
- [36] Soons FFM, Torrens JI, Hensen JLM, Schrevel RAMD. *A Modelica based computational model for evaluating a renewable district heating system.* In: 9th international conference on system simulation in buildings; 2014. p. 1e16..
- [37] GSE, *Diffusioni delle reti ed energia fornita in Italia, nota di approfondimento.,* 2020.
- [38] AIRU, *Data processing Yearbook,* 2015.

- [39] *B. van der Heijde, M. Fuchs, Dynamic equation-based thermo-hydraulic pipe model for district heating and cooling systems, Energy Conversion and Management, Volume 151, 2017.*